Hydraulic Characteristics of Fully Developed Flow in Circular Culverts

by

Nicholas Jon Kehler

A thesis submitted to the Faculty of Graduate Studies in
partial fulfillment of the requirements for the degree of

Master of Science

Department of Civil Engineering
University of Manitoba
Winnipeg, Manitoba, Canada

Abstract

Throughout the world, particularly in water abundant countries such as Canada, water crossings are a significant part of the infrastructure system. For both financial and practical reasons, the majority of small to medium sized streams crossings will be designed with some type of culvert system. Since corrugated metal pipe (CMP) culverts are a reasonably inexpensive choice, as well as hydraulically efficient, they are a very appealing option to designers.

In order to ensure that the natural ecosystem is not adversely affected, culverts must be designed so that throughout the year fish can migrate upstream to feeding and spawning grounds without significant delay. Current design practices and regulations are based on the average velocity within the culvert and by comparing it to the prolonged swimming speed of the fish species present. In order to examine the validity of this approach, a physical modeling study was undertaken using a 0.8 m diameter circular CMP culvert with 68 by 13 mm annular corrugations.

It was found through analysis of the velocity measurements that there is significant cross sectional area below average velocity, and that gravel embedment further increases this area. In addition, through detailed analysis of radial velocity profiles, the distribution of shear stress along the wetted perimeter, and several fitted values, a technique was developed that produced very agreeable streamwise velocity predictions over a two dimensional cross section in the developed region.

Acknowledgements

The assistance and support of many people have been instrumental to the completion of this project. Without their help this undertaking could not have been completed.

I would like to thank my thesis advisor Dr. Shawn Clark for his guidance and mentorship throughout my education. He has given me the opportunity to learn and to develop as an engineer in a thoroughly enjoyable environment through my years as a student.

Many thanks also go to NSERC for generously granting me with a research scholarship that has made dedicating my time to research possible.

I'd like to thank the Department of Fisheries and Oceans, particularly Rob Tkach for both funding of the project as well as his in depth knowledge of fisheries. Many thanks also go to Manitoba Infrastructure and Transportation, particularly Ninel Gonzalez and Ron Richardson for their funding and support. As well I'd like to thank the Corrugated Steel Pipe Institute, particularly Dave Penny, for their donation of the culvert.

Lastly I'd like to thank all those that helped and encouraged me through this project, including Martin Hunt, Jarrod Malenchak, and Scott Toews from the University of Manitoba. Many thanks also go to my family and friends who helped encourage me through my time as a student.

Table of Contents

List of Figures

List of Tables

Nomenclature

Symbol	Units	Description
d_{50}	[m]	grain size diameter with 50% non exceedence probability
d_p	[m]	distance along the wetted perimeter from the centerline
g	[m/s^2]	gravitational constant
h	[m]	flow depth
k_n	[ft$^{1/3}$/m$^{1/3}$]	unit conversion factor for Manning's equation
k	[m]	equivalent roughness height
k^+	[-]	equivalent roughness height normalized by $\underset{\sim}{y}/U_*$
ℓ_r	[m]	representative length for scaling
n	[s/m$^{1/3}$]	Manning's roughness coefficient
n_c	[s/m$^{1/3}$]	composite Manning's roughness coefficient
r	[m]	culvert radius
u	[m/s]	instantaneous streamwise point velocity
u'	[m/s]	streamwise turbulence intensity
v	[m/s]	instantaneous vertical point velocity
v'	[m/s]	vertical turbulence intensity
w	[m/s]	instantaneous spanwise point velocity
w'	[m/s]	spanwise turbulence intensity
y	[m]	elevation above channel bottom
y_d	[m]	elevation of log law deviation
Y^+	[-]	elevation above channel bottom normalized by $\underset{\sim}{y}/U_*$

z	[m]	distance away from the culvert centerline
z_0	[m]	half width of the water surface
A	[m^2]	cross sectional area
A_0	[-]	constant of integration
P	[m]	wetted perimeter
Q	[m^3/s]	discharge
R	[m]	hydraulic radius
S	[m/m]	channel slope
U_{av}	[m/s]	average streamwise velocity
U	[m/s]	streamwise point velocity
U_*	[m/s]	friction velocity
U_{*0}	[m/s]	friction velocity at the culvert centerline
U^+	[-]	streamwise velocity normalized by U_*
V	[m/s]	vertical point velocity
V_r	[m/s]	representative velocity for scaling
W	[m/s]	spanwise point velocity
Δu_m	[m/s]	maximum velocity dip from the log law at the surface
ΔB	[-]	roughness shift
κ	[-]	Karman constant
λ	[-]	Froude length scale
ν	[m^2/s]	kinematic viscosity
τ	[N/m^2]	shear stress
τ_0	[N/m^2]	shear stress at the culvert centerline

CHAPTER 1 *Introduction*

1.1 Background

Throughout the world, particularly in water abundant countries such as Canada, water crossings are a significant part of the infrastructure system. Due to the vast quantity of water ways that need to be crossed, especially in places such as Manitoba, it would be extremely expensive to install bridges that fully span the water course at every location. For this reason the majority of small to medium sized streams that need to be crossed are designed with some type of culvert system.

Since corrugated metal pipe (CMP) culverts are a reasonably inexpensive choice as well as a hydraulically efficient means to convey water, they are a very appealing option to designers. With the benefits, however, come a number of drawbacks as well. Due to the

efficiency of a CMP culvert it is often not necessary to install them across the entire stream width. This reduction in cross sectional area thereby leads to higher velocities within the culvert than are seen in the naturally occurring stream.

Quite often, as is the case in Manitoba and other winter climates, spring yields the largest discharges in rivers and streams as a result of spring snowmelt. Coincidentally, spring is also the time when certain migratory fish travel upstream to instinctual spawning grounds. The time at which fish are traveling upstream through culverts therefore often coincides with the timing of the highest velocities that are seen in the culvert. In addition, many fish species also move up and downstream throughout the year in search of food. Potential velocity barriers at culverts may inhibit fish passage, thereby disrupting the natural movement of fish through the waterways.

For this reason there are guidelines related to the design of culverts to minimize interruptions in fish migration. These guidelines include recommendations such as: all fish must not be delayed for more than 7 consecutive days every 50 years or 3 consecutive days every 10 years (3DQ10); water levels should not be higher than half the culvert diameter; design should maintain the natural slope over the culvert length; and most importantly the design must ensure that the average water velocity within the culvert is lower than the prolonged swimming speed of the fish species within the waterway (Fisheries and Oceans Canada, 1996). These guidelines, as well as several others within the document, have become an important part of culvert designs, and in many cases designing for fish passage can be the limiting criteria. For this reason it has

become important to develop better knowledge of culvert hydraulics, to ensure that both the designs and the guidelines are appropriate.

1.2 Literature Review

There is a significant amount of knowledge that has been developed over time pertaining to the understanding of fluid mechanics. The works completed encompass many topics from simple normal depth calculations described by Manning's equation to two dimensional velocity distributions according to Ead *et al*. (2000). A short review of some of the literature pertinent to the current research is presented in the following sections.

For the sake of consistency the coordinate system used should first be established. For this study the *x*-direction, referred to as streamwise, is defined along the length of the culvert with the positive axis in the direction of flow. The *y*-direction, referred to as vertical, is set with the positive axis upward. Lastly, the *z*-direction, referred to as spanwise, is orientated horizontally perpendicular to the flow with the positive direction defined to the left when looking in the positive *x*-direction.

1.2.1 Manning's Equation

The most commonly used tool for determining uniform flow depth within open channels has and continues to be Manning's equation (Sturm, 2001). The equation, which was developed over an extended period of time and involved many prominent researchers,

started by work of Chezy and was eventually added to by Manning, Flamant, and King (Sturm, 2001). The equation as it is known today began as the Chezy equation (Sturm, 2001). Then, through the work of Manning, Flamant, and King, the form of the equation we commonly use was developed to utilize a roughness parameter known as Manning's n. The final form is written as

$$U_{av} = \frac{k_n}{n} R^{2/3} S^{1/2} \tag{1.1}$$

where U_{av} is the average streamwise velocity [m/s], R is the hydraulic radius [m], S is the channel slope, and k_n is a unit conversion factor. Manning's roughness coefficient is denoted n and the value of k_n is 1 when using metric units and 1.49 when using imperial units to account for unit conversion between [m] and [ft]. A more useful form of using Manning's equation is easily obtained by multiplying both sides by the cross sectional area, resulting in

$$Q = U_{av} A = \frac{k_n}{n} A R^{2/3} S^{1/2} \tag{1.2}$$

which makes it possible to determine open channel normal depth in a culvert by using the discharge, roughness, and slope.

Determining the appropriate value of Manning's n for open channels can be a slightly more complicated matter. There are many different options for choosing a value of n, which can be greatly dependent on the bed surface material. For calculations using

culverts there are two particular areas of concern. Primarily the roughness must be known for the CMP culvert itself, and secondly the roughness of any rock material placed inside the culvert is needed. To estimate *n* for a CMP culvert one can use the tables produced by the CMP culvert industry (Corrugated Steel Pipe Institute, 2007).

When determining the roughness of the bed material within the culvert there are a number of methods available. Generally these methods involve an equation that estimates *n* as a function of some size fraction of the bed material. Although several variations involve lengthy calculations of channel properties, a commonly used and simple equation is that of Strickler (1923).

$$n = \frac{d_{50}^{1/6}}{21.1} \tag{1.3}$$

where d_{50} represents the diameter of the grain size with a 50% non-exceedence probability [m].

Finally, the roughness of the culvert and the roughness of the bed material must be combined to determine the composite roughness of the entire channel. There are again a variety of options which typically involve taking a weighted average as a function of several geometric properties to develop a composite Manning's *n*. One of the more commonly used equations is that of Lotters (1933) where the total discharge is shown as the sum of discharges in each subsection (Chow, 1959). The equation is written as

$$n_c = \frac{PR^{5/3}}{\sum_{i=1}^{N} \frac{P_i R_i^{5/3}}{n_i}} \quad (1.4)$$

where P is the wetted perimeter [m], R is the hydraulic radius [m], and n is the Manning's roughness [s/m$^{1/3}$]. The resulting n_c of this equation represents the compound channel Manning's roughness as distributed by the discharge through the channel. Other methods of determining composite roughness use either the assumption that the total resisting force is equal to the sum of the resisting forces over each segment of the wetted perimeter, or that each section of the channel can be well represented by the average velocity. Due to the nature of culvert flow, the method by Lotters (1933) appears to be an appropriate means of estimating composite roughness for circular culverts and should be used.

1.2.2 Log Law Equations

As with Manning's equation, a considerable amount of research has been conducted in order to develop a detailed understanding of velocity profiles, and in particular, developing equations that can reliably reproduce the vertical variation of streamwise velocity in a wide channel (Sturm, 2001).

Experimental observations, such as those made by Magura (2007), Abs *et al.* (2007), and Ead *et al.* (2000) have shown that the velocity profile in the near boundary region typically follows a universal velocity distribution known as the log law, which represents

a large portion of the law of the wall (Nezu and Nakagawa, 1993). The log law in its general form for smooth walls can be written as

$$U^+ = \frac{1}{\kappa}\ln(y^+) + A_0 \tag{1.5}$$

where U^+ and Y^+ are the streamwise point velocity (U [m/s]) and the vertical point location (y [m]) normalized by the inner variables U_* [m/s] and ν/U_* [m], respectively. The Karman constant κ and the integration constant A_0 need to be determined according the experimental data.

The applicability of the log law is typically valid in the wall region only, where *y/h* is less than 0.2 and Y^+ is greater than 26 (Nezu and Nakagawa, 1993). The region where Y^+ is less than 26 includes the viscous sub layer and the buffer layer, where the log law is not valid. Although the dimensionless constants of κ and A_0 are to be determined through experimental data, past work by other researchers have yielded typical values pertaining to certain conditions. Coles (1968) and Brederode and Bradshaw (1974) have both developed acceptable constants for boundary layers, and Nezu and Rodi (1986) developed typical values for open-channel flows.

$\kappa = 0.41\ and\ A_0 = 5.0$ Coles (1968)

$\kappa = 0.41\ and\ A_0 = 5.2$ Brederode and Bradshaw (1974)

$\kappa = 0.41\ and\ A_0 = 5.29$ Nezu and Rodi (1986)

Through review of several texts including that of Nezu and Nakagawa (1993) and Pope (2000) it appears to be commonly accepted that the choice of parameters should be that of Coles (1968) as they provide a better fit to many velocity profiles.

An additional term needs to be added to Equation 1.5 in order to account for the effect of a rough boundary. The added term is known as the roughness shift and causes the values of U^+ to shift downward on the vertical axis. The roughness shift term acts as a general reduction in velocity resulting from the increased resistance of the boundary. The log law equation for flow over rough surfaces is

$$U^+ = \frac{1}{\kappa}\ln(y^+) + A_0 - \Delta B \tag{1.6}$$

where the roughness shift term is represented by

$$\Delta B = \frac{1}{\kappa}\ln(k^+) \tag{1.7}$$

and k^+ is the equivalent roughness height (k [m]) normalized by $\underset{\sim}{y}/U_*$ [m], and κ is the Karman constant. It is important to note that the value of ΔB is not a unique function of k because it varies significantly with the shape, orientation, and density of the roughness element on the bed surface (Pope, 2000). This variation is not captured in Equation 1.7 but shows up as result of the fitting the log law to the data set. For a given value of roughness height (k), there can be a variety of different values of roughness shift (ΔB).

1.2.3 Turbulence Quantities

As previously noted, the amount of energy dissipation can be represented by the amount of turbulence within the water column. Turbulence intensity is defined as the root mean square of the fluctuating component of velocity (Nezu and Nakagawa, 1993), calculated as

$$u' = \sqrt{\overline{(u - U)^2}} \tag{1.8}$$

where *u'* is the streamwise turbulence intensity, *u* is the instantaneous streamwise point velocity, and *U* is the streamwise point velocity found by averaging the instantaneous samples. This equation applies in the same form for *v'* and *w'* as well, using the vertical (*v*) and spanwise (*w*) instantaneous point velocities.

As with the predictive equations used to describe the streamwise velocity, there are a set of empirically based equations that have been developed by Nezu and Nakagawa (1993) to describe the three dimensional turbulence intensities along a vertical profile of a wide open channel.

$$u'/U_* = 2.30\exp\left(-y/h\right) \quad \text{(Nezu and Nakagawa, 1993)} \tag{1.9}$$

$$v'/U_* = 1.27\exp\left(-y/h\right) \quad \text{(Nezu and Nakagawa, 1993)} \tag{1.10}$$

$$w'/U_* = 1.63\exp\left(-y/h\right) \quad \text{(Nezu and Nakagawa, 1993)} \tag{1.11}$$

where *u'*, *v'*, and *w'* are the *x*, *y*, and *z*-direction turbulence intensities, respectively (Nezu and Nakagawa, 1993). From these equations it can be seen that the level of turbulence intensity exponentially decays with the distance from the boundary. This makes sense because the turbulence is a result of the shear stress at the boundary, which is dissipated into the water column.

1.2.4 Previous Culvert Research

Over the past decade there has been an increase in studies focusing on more specific details of culvert systems. Several of these studies have similar attributes to those seen in this project, which provides the opportunity to both verify and build upon research already published. A select list of recent studies relating to culvert hydraulics is reviewed in the following sections.

1.2.4.1 Knight and Sterling (2000) and Sterling and Knight (2000)

The studies, completed by both Knight and Sterling, were focused on the velocity profiles, overall resistance, and the boundary shear of circular pipes. The two papers, although separate, were based on similar tests performed by both researchers. For their project a 0.244 m diameter smooth plastic pipe with a total length of 19 m was constructed to flow partially full, both with and without a flat bed. Experiments were conducted using culvert slopes ranging between 0.1% and 0.9%, bed depth to culvert diameter ratios between 0.0 and 0.664, and a wide range of discharges.

The first conclusion of their study was that the Manning's n value was completely independent of stage within the culvert. It is important to note that they used a bed consisting of the same material as the pipe walls. Secondly, by collecting velocity profiles near the outlet of the pipe, it could be seen by the depressed location of maximum velocity from the surface and the high level of distortion near the boundary that secondary circulation may have been present. Since they used a Pitot tube to measure water velocity, they could not verify this hypothesis with measurements of secondary circulation. Lastly, it could be seen that the location of highest shear stress was along the centerline, and the shear stress then decreased along the wetted perimeter until the surface was reached. Higher flow rates yielded a more uniform distribution of boundary shear stress. When the flat bed was utilized and the geometry of the flow area changed, the variation of shear stress became more pronounced and a sharp dip was noted at the 'corner' between the flat bed and the pipe walls. This means that there could be an area of reduced velocity in the 'corner' where the shear stress is lesser than along the bed and the sidewalls.

1.2.4.2 Ead *et al.* (2000)

In another culvert study that was conducted by Ead *et al.* (2000), empirically based equations of the variation of streamwise velocity across the entire circular cross section of the culvert were developed. This study involved the use of a 0.62 m diameter circular CMP culvert with 68 mm by 12 mm annular corrugations. Their testing procedure consisted of several tests using slopes of 0.55%, 1.14%, and 2.55%, over a range of discharges from 0.030 m^3/s to 0.200 m^3/s. They used a Pitot tube to measure streamwise

velocity and were able to obtain centerline velocity profiles at 14 stations along the length of the culvert system. Additionally they collected a series of velocity profiles at one station for a range of non-centerline spanwise locations. By using all the non-centerline profiles together they were able to create a complete representation of the variation in streamwise velocity at a cross section within a CMP culvert.

Using this data they were able to draw several conclusions. The equivalent roughness height was determined for each test by fitting the experimental data to the ideal log law. It was found that each test yielded a k value of 12 mm, equal to the height of the corrugations. This same observation was also noted when the same method was used on the data from Katopodis *et al*. (1978). The next observation was that the velocity profile could perhaps fit a modified log law equation outside of the boundary layer. This was noted because of the observed consistency with which the measured velocity deviated from the log law near the surface. In order to account for this in the log law equation, as well as to attempt to make the log law applicable at non-centerline profiles within the culvert, Eat *et al*. (2000) developed the following set of equations to describe the streamwise velocity over the entire cross section of the culvert.

$$\frac{U}{U_{av}} = \left[\left(\frac{2.3}{\kappa}\right)\log\left(\frac{y}{k}\right) + 8.5\right]\sqrt{f_3\left(\frac{z}{z_o}\right)}\left(\frac{J\sqrt{g}n}{R^{1/6}}\right)$$

for $y/k < y_d/k$ (1.12)

$$\frac{U}{U_{av}} = \left[\left(\frac{2.3}{\kappa}\right)\log\left(\frac{y}{k}\right) + 8.5 - \frac{\left(\frac{y}{k}\right) - f_1\left(\frac{z}{z_o}\right)}{\left(\frac{h}{k}\right) - f_1\left(\frac{z}{z_o}\right)} f_2\left(\frac{z}{z_o}\right)\right]\sqrt{f_3\left(\frac{z}{z_o}\right)}\left(\frac{J\sqrt{g}n}{R^{1/6}}\right)$$

for $y/k \geq y_d/k$ (1.13)

where

$$f_1\left(\frac{z}{z_0}\right) = \frac{y_d}{k} = -6.91\left(\frac{z}{z_0}\right)^2 - 2.05\left(\frac{z}{z_0}\right) + 9$$

$$f_2\left(\frac{z}{z_0}\right) = \frac{\Delta u_m}{U_*} = 5.58\left(\frac{z}{z_0}\right) + 0.9$$

$$f_3\left(\frac{z}{z_0}\right) = \frac{\tau}{\tau_0} = -20\left(\frac{z}{z_0} - 0.6\right)^3 + 2.75\left(\frac{z}{z_0} - 0.6\right)^2 - 0.4\left(\frac{z}{z_0} - 0.6\right) + 1$$

$$J = \frac{U_{*_0}}{\sqrt{gRS}}$$

The three modification equations developed by Ead *et al*. (2000) are all a function of the relative distance from the centerline, where z [m] is the horizontal distance from the centerline and z_0 [m] is the half width of the water surface. Other parameters include the elevation of log law deviation (y_d [m]), the maximum velocity dip from the log law at the water surface (ΔU_m [m/s]), the shear stress at any plane (τ [N/m^2]), the shear stress at the centerline (τ_0 [N/m^2]), and the friction velocity at the centerline (U_{*0} [m/s]). The development of equations to describe a two dimensional flow distribution is a significant achievement as they could be a useful tool in culvert design.

1.2.4.3 Abbs *et al*. (2007)

Another culvert study conducted by Abbs *et al.* was performed to quantify the effect that a backwater condition would have on the velocity distribution within a CMP culvert. In their experiments they used an 8 m long, 0.5 m diameter culvert with 68 mm by 13 mm annular corrugations. Using an Acoustic Doppler Velocimeter (ADV) they collected

velocity measurements at a developed cross section for both uniform flow conditions, as well as for backwater conditions. The tests they performed were operated with a slope of 0.72% and with discharges of 0.050 m^3/s and 0.070 m^3/s. For each case a full cross section of data was collected for uniform flow conditions, as well as two backwater conditions set to 44 mm and 64 mm above normal depth.

From the test data Abbs *et al*. (2007) were able to conclude that while operating at uniform flow there was approximately one third of the flow area with a velocity of less than average velocity. The velocity data was presented this way so that comparisons could be made to the regulation stating the average velocity in the culvert should be less than the prolonged swimming speed of a given fish species. Secondly, the results from the backwater conditions indicated that with the tailwater level raised, the amount of flow area with velocity less than average velocity significantly increased. These tests also showed an increase in turbulence intensity around the boundaries. These observations are important because most low slope culverts will operate with a backwater condition, yielding a more favorable environment for fish passage than uniform flow.

1.2.4.4 Magura (2007)

Another recent culvert study performed by Magura made use of a 0.62 m diameter circular CMP culvert, also with 68 mm by 13 mm annular corrugations. In similar fashion to the other previously mentioned projects, this study was once again aimed at culvert hydraulics as they relate to fish passage issues. The model was operated at slopes of 0%, 0.5%, and 1.0%, using discharges ranging between 0.064 m^3/s and 0.254 m^3/s. Testing

procedures involved the use of an ADV in order to collect point velocity measurements in two-dimensional cross sections. The data was then analyzed to determine the effect of various parameters on the velocity structure (Magura, 2007).

Magura (2007) observed that there was substantial flow area with velocity lower than average, created as a result of the rough boundaries. As well he noted that the velocity gradient due to the culvert walls was greater than that of the rock bed, which resulted in a wider area along the rock bed that had low velocity (Magura, 2007). This result would indicate that there is a variation of shear stress along the wetted perimeter that changes significantly at the interface of the rock bed and the culvert walls. Additionally, the observations showed that with higher discharges the low velocity region along the bed was reduced.

As opposed to the velocity distributions produced by Ead *et al.* (2000) that indicated the maximum velocity at the water surface, Magura (2007) showed that the maximum velocity occurred below the surface. The significant difference in overall profile shape causes concern over the applicability of the two-dimensional velocity equations produced by Ead *et al.* (2000). Through fitting the data to the log law equation, Magura also made observations that the value of equivalent roughness height became equal to the culvert corrugation height. One of the most significant differences between the experiments of Magura (2007) and Ead *et al*. (2000) is the culvert slope, which may have an effect on the location of maximum velocity.

1.3 Objectives

This thesis provides the details of a physical model study on the hydraulic properties of flow through a circular CMP culvert. The tests, performed over a variety of slopes, discharges, and gravel embedment depths will provide the data necessary to reach the following objectives to:

- determine the effect of slope, discharge, and gravel embedment on the development length;
- provide observations of the vertical and spanwise velocities, as well as the three components of turbulence;
- provide evidence of secondary circulation if it exists in the culvert;
- evaluate the two-dimensional log law equations presented by Ead *et al*. (2000) and provide any improvements; and
- provide data for use in future numerical models and recommendations for future research topics.

CHAPTER 2 *Experimental Setup*

2.1 Physical Model

The experimental setup for this project is located within the Hydraulics Research and Testing Facility at the University of Manitoba. The space allocated to the project consisted of an open area on the basement level, approximately 3.65 m wide, 27 m long, and 2.5 m high.

2.1.1 Model Requirements

The project required a physical culvert model to be built that was capable of operating over a range of conditions typical to Manitoba water crossings. This meant that the setup should be capable of testing at slopes ranging between horizontal and at least one percent.

It also needed to be of sufficient diameter and length to encompass the testing plan proposed. As previously stated, other research projects have already been conducted to test various aspects of culvert hydraulics using smaller diameter pipes. Therefore to reduce questions of scaling effects, a larger diameter culvert was chosen. It was also ensured that the capacity of the laboratory's water supply system exceeded the demands of all test scenarios.

2.1.1.1 Scaling

Since culvert flow is dominated by gravitational forces rather than inertial forces, and since all test conditions were conducted at high Reynolds numbers, Froude model scaling was chosen when designing the experiment. According to this type of model scaling the Froude number of the model must be equal to the Froude number of the prototype (Sturm, 2001), such that,

$$\left(\frac{V_r}{\sqrt{g\ell_r}}\right)_m = \left(\frac{V_r}{\sqrt{g\ell_r}}\right)_p \tag{2.1}$$

which leads to

$$\frac{(V_r)_m}{(V_r)_p} = \sqrt{\frac{(\ell_r)_m}{(\ell_r)_p}} = \sqrt{\lambda} \tag{2.2}$$

where V_r is a representative velocity [m/s], ℓ_r is a representative length [m], and λ is the length scale of the culvert model. By solving for various other parameters using the same

technique, Table 2.1 was produced, and with the use of $\lambda = 3$ as an example, representative values can be seen. Although the results of this study will not be scaled-up within the conclusion of this report, the scaling technique outlined here could be used to determine specific values for other size culverts. It is important to note these scaling factors when expanding the results of this study to different diameter culverts.

Table 2.1 - Froude Scaling

Parameter	Units	Scaling Factor	Scaling Factor Value
Length	[m]	λ	3.00
Area	[m^2]	λ^2	9.00
Velocity	[m/s]	$\lambda^{1/2}$	1.73
Discharge	[m^3/s]	$\lambda^{5/2}$	15.59
Manning's n	[$s/m^{1/3}$]	$\lambda^{1/6}$	1.20

2.1.2 Laboratory Survey

In order to gain a detailed understanding of the potential space within the laboratory the first step was to undertake a survey of the space. The rudimentary survey consisted of plan view orientations of all potential obstructions as well as the vertical component of any overhead limitations. The survey data was then input into AutoCAD, creating a three dimensional map of the lab space allocated to this project. With this map as a tool it made deciding on the orientation of various sections of the apparatus much simpler. This ensured that the entire experimental setup would fit within the allocated space and have enough room to properly operate all the tests. Figure 2.1 shows the drawing of the lab including the final model design in AutoCAD.

2.1.3 CMP Culvert

The culvert for this setup was chosen to be a 0.8 m diameter circular corrugated metal pipe culvert. The corrugations were 13 mm in amplitude and 68 mm in wavelength. The size of culvert was chosen because it was of sufficiently large diameter to provide assurance that scaling effects would be minimal. The chosen culvert diameter was also near the maximum size permissible in the allocated lab space while ensuring sufficient length and measurability.

Typically full-scale large diameter culverts are constructed with helical corrugations, however, due to their large diameter the angle of the corrugations is extremely small. Using helical corrugations in a small diameter culvert would introduce flow circulation along the culvert. This would also result in a reduced resistance to flow thereby creating a lower Manning's roughness than was desired, which would affect the ability of the results to be scaled-up. Therefore the corrugations of the model culvert had an annular orientation rather than helical

The culvert itself consists of five 4.27 m long sections of 0.8 m diameter corrugated metal pipe. Each of the five sections was joined together using culvert couplers, creating an adequately rigid connection and building a total culvert length of 21.35 m. The style of culvert coupler used can be seen in Figure 2.2. Since the culvert being used for the laboratory study was constructed the same as a culvert for field use, significant work needed to be done to reduce leakage. Each section of culvert was manufactured with metal rivets, resulting in countless leaks at both the rivets and at the seams. In order to

sufficiently reduce the leaks to an amount well below having any effect on the results, the rivets and seams were sealed inside and outside with an industrial polyurethane waterproofing sealant. The rate of water leaking from the culvert during any particular test was visually estimated to be no more than one or two liters per minute, which is an insignificant amount compared to the total discharge, less than a fraction of a percent.

2.1.4 Support System

The entire culvert was held up by 18 cradle supports as seen in Figure 2.3. Each support was built with two pieces of ¾ inch plywood laminated together and cut to fit into the outside ridges of the culvert. The laminated plywood was then mounted on joist hangers attached to the support posts. The support posts consisted of a threaded rod drilled through a four inch by four inch timber post. A metal plate was attached to the bottom of the timber post and held up on the threaded rod with a nut. The threaded rod was counter sunk six inches into the concrete floor for lateral stability and to provide a firm location to support the culvert. The slope of the culvert could then be adjusted by moving the supports up or down on the threaded rod. This technique was created so that one or two people could change the slope within two hours. The maximum attainable slope within the laboratory setup is 1.5%, and the minimum slope is completely horizontal.

2.1.5 Headwater Box

A headwater box was constructed at the upstream end of the culvert with sufficient length and width to properly model natural entrance conditions. Based on these design criteria it

was chosen that the headwater box should have at least one culvert diameter of space on either side of the culvert. Therefore the headwater box was built with a total internal width of 2.73 m, resulting in just over 1.2 culvert diameters of channel width on either side of the culvert. The headwater box, as seen in Figure 2.4, was constructed as a wood frame structure lined with high density overlay (HDO) plywood. The seams and screw holes were once again sealed with polyurethane sealant to bring leakage to a minimum.

The length of the headwater box was chosen such that there was sufficient space to include the inlet pipe, a flow straightener, and ample distance for the flow to stabilize and enter the culvert naturally. The inlet pipe, seen at the top left hand side of Figure 2.4 discharged straight down onto the floor of the headwater box where it hit a deflector that pushed the water against the back wall to dissipate energy. The water then flowed through the flow straightener, which was composed of a wall of 0.3 m long PVC tubing oriented in the preferred direction of flow. Lastly, a horsehair filter was set to drag along the water surface to eliminate any surface disturbances. After the inclusion of these features the final internal length of the headwater box was 4.56 m. The implementation of the flow straightener and the drag filter provided satisfactory inlet flow conditions.

2.1.6 Inlet Configuration

The inlet chosen for the laboratory setup was an elevated projecting inlet, which has the culvert bottom elevated off the bed and the culvert protruding into the headwater box. The distance that the culvert projected into the headwater box was chosen to be 1.22 m, decided upon by the limitations of the space in the laboratory and the headwater box

dimensions. The chosen distance proved to be ample after having observed the culvert inlet under multiple discharges. This type of inlet, seen in Figure 2.5, also provided the most convenient method of adjusting the slope, since the setup allowed for the culvert end to change height without requiring any extra modification. The drawback of this was that for different slopes the culvert inlet had a slightly different elevation above the headwater box. At the minimum slope of 0.028% the invert elevation was 0.204 m and at the maximum slope of 0.488% the invert elevation was 0.253 m. The difference between the two elevations could potentially have a small effect on the development length but the difference is relatively small and is not expected to have any significant effects.

2.1.7 Tailwater Box

The tailwater box was constructed using the same construction technique as the headwater box. The design of the tailwater box required that there be sufficient length and orientation to allow the water to exit the culvert as naturally as possible. There also needed to be a method of controlling the tailwater level in order to model anything from free outfall conditions to high tailwater conditions. Due to the location of the water collection channel in the laboratory, the tailwater box needed to turn the flow 180 degrees and return the water from the model to the lab system. Therefore the tailwater box was designed to be 3.34 m long and 1.75 m wide with well-rounded corners to direct the flow into the return channel. The 0.91 m wide return channel allowed the flow to move back to the lab system. Within the return channel a radial gate was installed to provide control of the tailwater conditions as seen in Figure 2.6.

2.1.8 Culvert/Tank Connection

Due to the scale of this project it was not possible to have the headwater and tailwater box rise and drop with the culvert. In order to facilitate the changing slope of the culvert there needed to be a non-rigid connection between the culvert and the headwater box. As a result of the culvert length there was a significant vertical range of motion at both the culvert ends and at the support rods. For these reasons it was decided that when changing the slope of the culvert, the supports would be adjusted in a manner that would pivot the culvert about its center. This resulted in the minimum height movement at both ends. By knowing the total movement at the culvert-headwater box connection a non-rigid connection could be designed to accommodate.

The connection consisted of a rubber sheet sealed between two pieces of HDO plywood. One piece of plywood was the portion of the headwater box wall where the culvert went through. Then a sheet of rubber was fit over the culvert and sealed tightly to the culvert using large hose clamps. A second piece of plywood, cut to the same shape as the first was placed over the rubber. Eight bolts were then placed through all three layers as close to the culvert as possible to ensure a tight seal. The connection can be seen fairly well in Figure 2.4 as well.

2.1.9 Gravel Embedment

For tests involving gravel embedment a selection of limestone was used to model the infill material. The material was run through a sieve analysis to determine the value of

d_{50}. The sieve analysis resulted in a d_{50} of 2.76 cm and a reasonably uniform gradation. The material was manually unloaded into the culvert and leveled by hand. After an initial setup of the gravel embedment a survey was done to verify a consistent gravel depth over the length of the culvert. In the case that certain areas were too deep or too shallow, additional material would be added or removed. Once a satisfactory depth was achieved a final survey was done in order to produce a reliable measure of the gravel depth for calculation of the flow area.

2.2 Sampling Equipment

2.2.1 Discharge Measurement

In order to have a consistently reliable form of discharge measurement that did not interfere with other testing within the lab, an independent measurement system needed to be installed. Therefore a MSR Magnum Standard Magmeter was used to provide discharge measurement for the culvert model. As seen in Figure 2.7, the Magmeter was installed on the inlet pipe along the longest straight section of pipe to reduce any random variation that would result by being located directly next to a bend. There was one tee on the water supply line, slightly after the Magmeter, but since it was closed there were no noticeable problems.

To collect data from the Magmeter the display unit was connected via serial port to a computer located nearby. Then a LabVIEW program was written to receive samples for a specified amount of time and output the averaged value. The front panel of the LabVIEW

program can be seen in Figure 2.8. Since the Magmeter output a nonzero value when no flow was present a correction value was needed. By taking multiple readings of the Magmeter at zero discharge an average value was recorded and then subtracted from subsequent discharge measurements.

2.2.2 Water Surface Profiles

In order to gain a meaningful understanding of the flow conditions within the culvert it was important to be able to clearly define the water surface profile along the entire culvert. To do this, 28 clear tube manometers were installed into the bottom of the culvert. The tubes were then collected together into three groups, to reduce tube length, and displayed against a printed scale on a mounting board. The manometers, shown in Figure 2.9, provided the water surface elevations in relation to a set datum within the lab, and a survey of the culvert bottom provided the culvert bed elevations. Outputs of survey data and manometer data were then stored together in an EXCEL file for each setup.

2.2.3 Velocity Measurement

Three different Acoustic Doppler Velocimeters (ADVs) were used to collect point velocity measurements. The instruments chosen were an upward and a downward looking SonTek 16 MHz MicroADV, as well as a side looking SonTek 10 MHz ADV. SonTek was chosen because of past experience and therefore a better understanding of the equipment.

The ADVs were capable of measuring the three components of velocity, which was an important feature since one objective was to provide evidence of secondary flow within the culvert. Additionally, the 16 MHz MicroADVs were chosen over the 10 MHz ADVs because of the reduced sampling volume size (0.09 cc for the 16MHz MicroADV vs. 0.25 cc for the 10 MHz ADV) and the increased sampling rate (50 samples/second for the 16 MHz MicroADV vs. 25 samples/second for the 10 MHz ADV). By having a smaller sampling volume it would allow for measurements closer to the boundary, and the increased sampling rate would make obtaining turbulence quantities less time consuming. Both versions of the ADVs have a sampling resolution of 0.01 cm/s and an accuracy of 1% of the measured velocity. One fault of the MicroADV was that it typically has a much lower signal to noise ratio (SNR). This was found to be true, but the SNR was still high enough to not cause concern, 40 dB when 15 was needed. The ADV principles of operation are explained in the SonTek technical documentation (SonTek, 2001). A check was performed on the ADVs to confirm that each measured the same velocity. The ADVs were set to measure the identical location, and one after the other collected a set of samples. The results were well within 1% of each other.

Special care needed to be taken when setting up the orientation of the instruments to ensure that the data points would match when placing data from two different instruments together in a plot. This was achieved by adding a thin rubber sheet around the top of the ADV conditioning module where it attached to the traversing mechanism. The rubber sheet held lines and ridges that made consistent attachment simple. It also served very well for creating a snug connection.

2.2.4 Traversing Mechanism

In order to vastly reduce the time required to take samples it was decided that an automated traversing mechanism should be built to handle this task. The traversing mechanism needed to be built in such a manner that it could move the ADVs to a specified location within a cross section and remain there for a given amount of time. The mechanism also needed to be able to be moved from one location along the culvert to another for the sake of determining the development length. For simplicity this was done manually. Lastly, the mechanism needed to be able to perform all these operations with any one of the three ADVs.

Taking these design criteria into account the traversing mechanism was designed in AutoCAD. Figure 2.10 shows the design of the traversing mechanism, and Figure 2.11 shows the final result along with the associated computer control system. Although the process of designing and building this mechanism was very time consuming it has proven to be very beneficial and will continue to be for future projects.

In order to provide an accurate means of placing the traversing mechanism at different locations along the length of the culvert, access holes were cut into the obvert as shown in Figure 2.2. These holes were cut in such a manner that both a leveling device and the traversing mechanism could be placed within the cut out. Due to the fact that each access hole was not cut perfectly level, the leveling platform was adjusted and placed in the access hole. Once it was leveled the traversing mechanism itself could be placed on top,

already properly leveled in all directions. It was important to keep the traversing mechanism level to ensure vertical profiles were indeed vertical. Finally, the entire system was held tight using a ratcheting strap to reduce vibrations. The locations of the access holes are shown in Table 2.2.

Table 2.2 – Access hole locations

Access Hole	Downstream Distance	Access Hole	Downstream Distance
-	[m]	-	[m]
H01	0.197	H12	9.690
H02	0.800	H13	11.303
H03	1.607	H14	12.109
H04	3.226	H15	13.729
H05	3.962	H16	14.535
H06	4.769	H17	16.154
H07	5.709	H18	16.897
H08	6.452	H19	17.704
H09	7.195	H20	18.644
H10	8.141	H21	19.387
H11	8.884	H22	20.130

Once fully assembled at a given location, the ADVs were used to measure the location of the culvert bottom and the water surface using the 'BOUNDARY' command. This procedure determined the orientation of the traversing mechanism within the culvert, so that measurement points would be properly located. Therefore each different location could be directly compared since each was referenced to the culvert bottom for a particular setup of the traversing mechanism.

The computer control system was once again constructed using LabVIEW, the front panel of which can be seen in Figure 2.12. The basic function of the control program was

to perform the repetitious operations associated with stopping the ADV, moving to a subsequent point, and starting the ADV. Inputs into the control system were the number of samples, the water temperature, and the locations of points to sample. The file setup required a large amount of work to create a standard system to organize the files. This was important so that the computer control system would have a consistent organization to work with. The details of the control files used for performing tests will be further outlined in Chapter 3.

The system used for controlling the traversing mechanism was centered on a Galil DMC4020 two axis controller. The digital motion controller was powered by a 12 volt power supply also purchased through Galil. Communication to the controller was done through serial connection. Attached to the controller were two Galil brushless servo motors. One was fixed at the top of the traversing mechanism mast and the other was attached to the horizontal track of the traversing mechanism. Both of the motors, the controller, and the power supply can be seen mounted on the traversing mechanism in Figure 2.11.

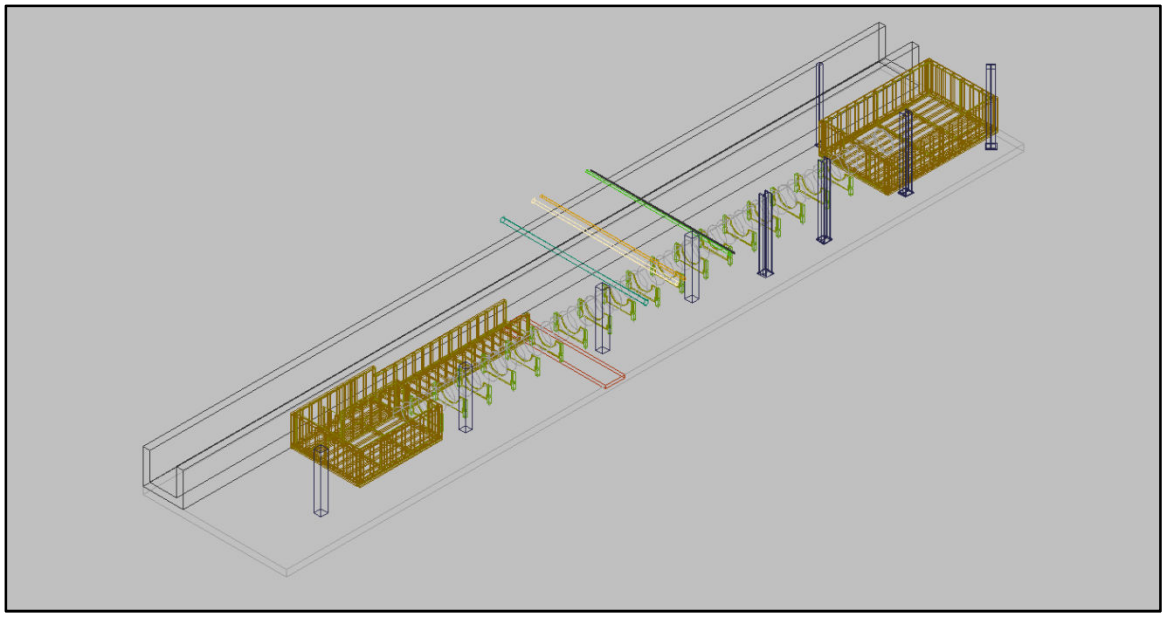

Figure 2.1 AutoCAD drawing of lab with layout of final model design

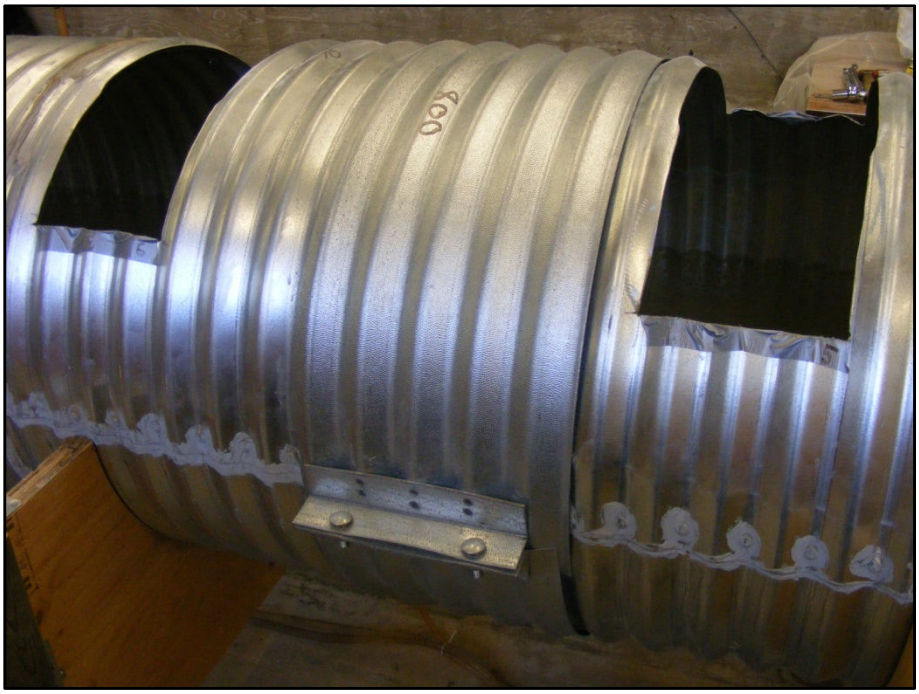

Figure 2.2 Culvert coupler connection and instrumentation access holes

Figure 2.3 Culvert support post

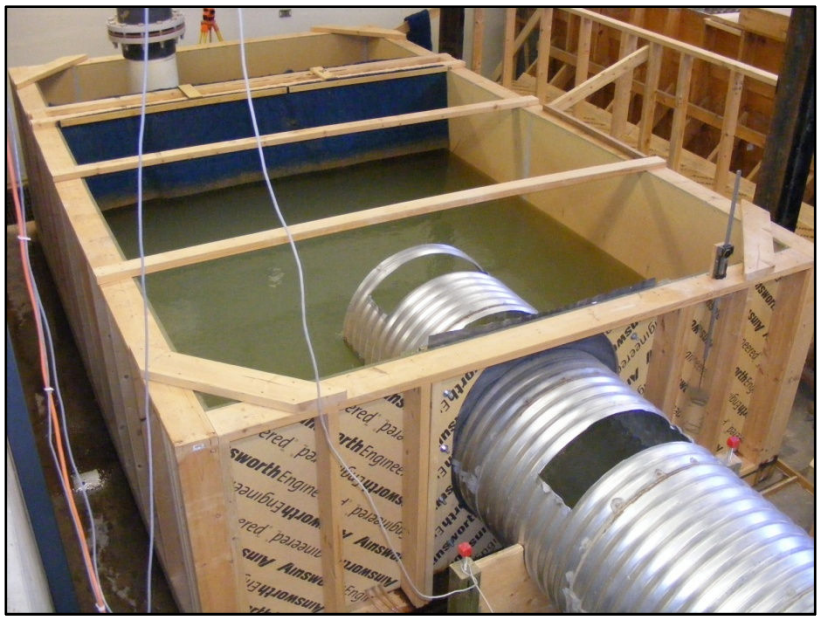

Figure 2.4 Culvert model headwater box

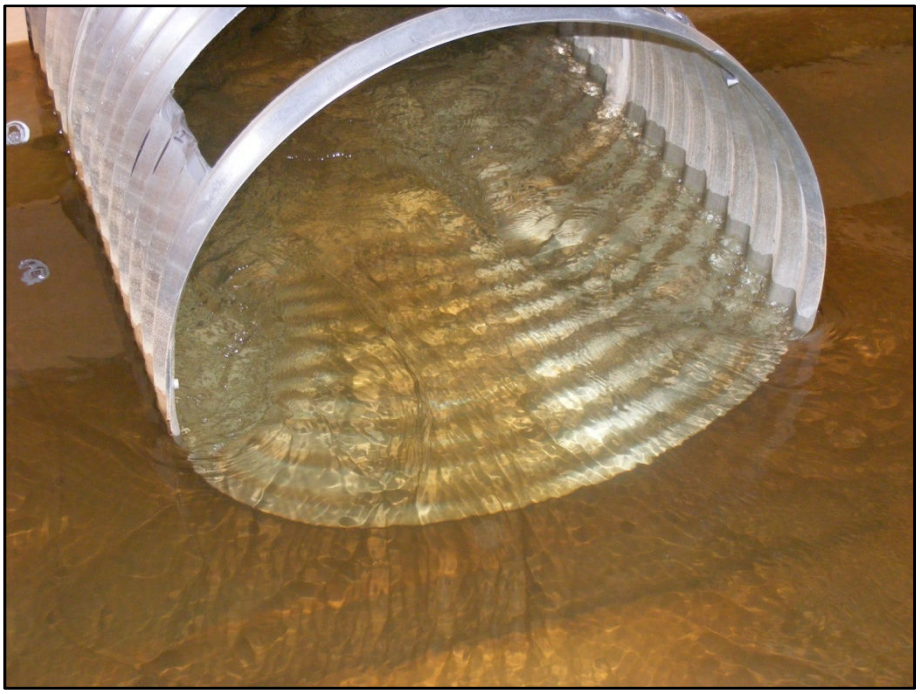

Figure 2.5 Elevated projecting inlet

Figure 2.6 Radial gate controlling tailwater levels

Figure 2.7 Magmeter installed on water supply line

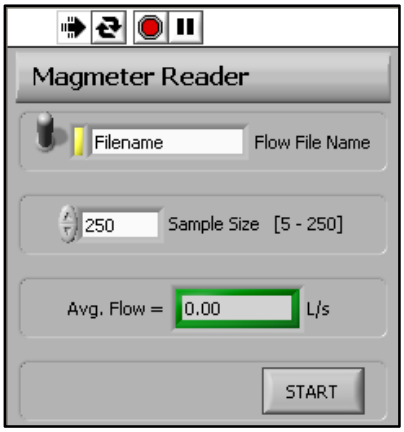

Figure 2.8 Front panel of LabVIEW program to read Magmeter

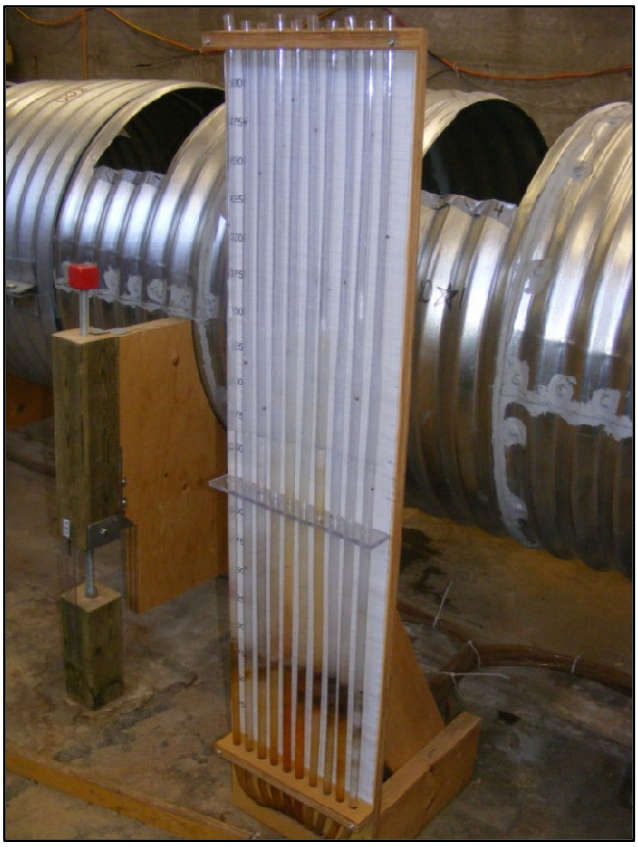

Figure 2.9 Manometer board #1 displaying water levels

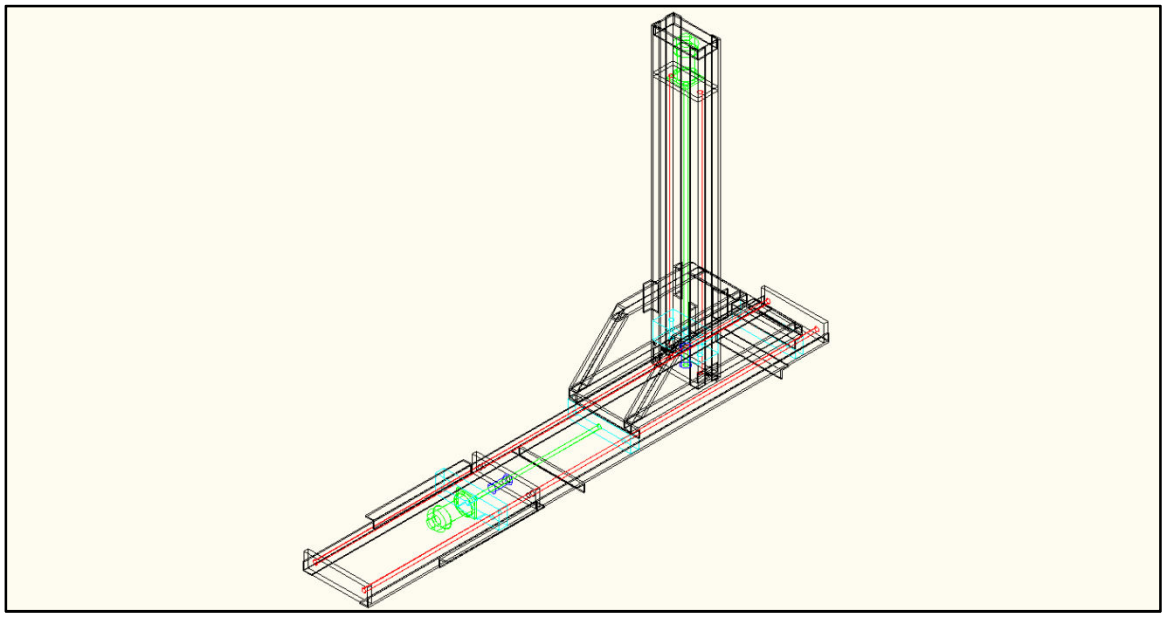

Figure 2.10 AutoCAD drawing of traversing mechanism design

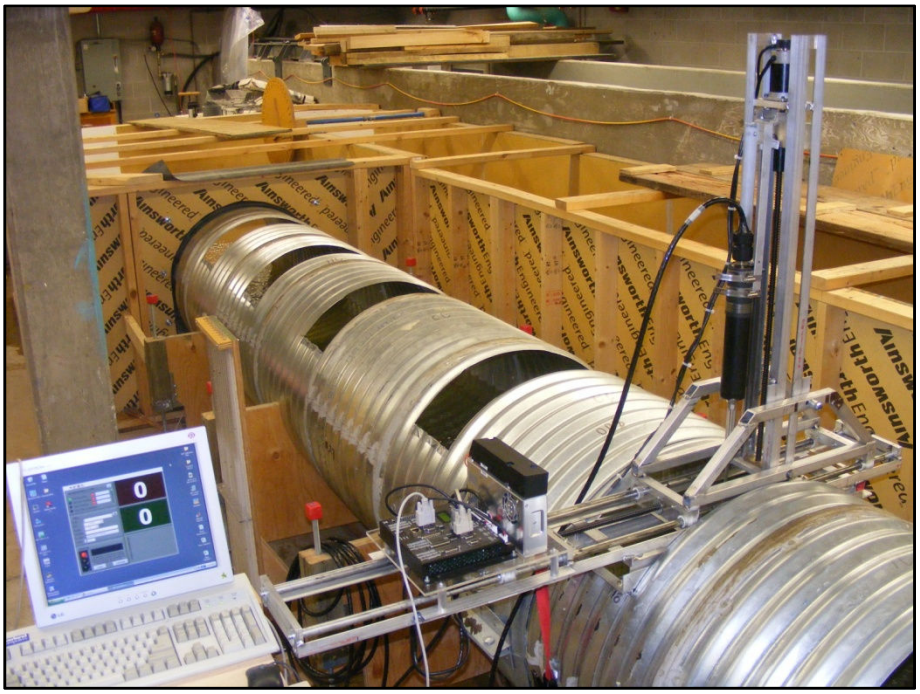

Figure 2.11 Traversing mechanism along with computer control setup

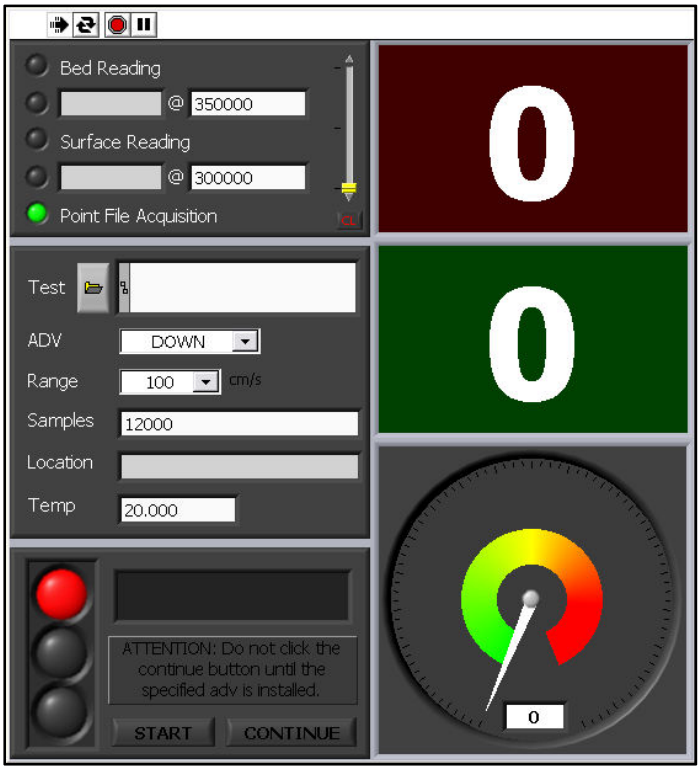

Figure 2.12 Front panel of LabVIEW program to control traversing mechanism

CHAPTER 3 *Testing Procedure*

3.1 Experimental Plan

The outline of experiments was chosen such that there would be sufficient data to accomplish all project objectives. Tests outside of the normal operating conditions as put forth by the current guidelines were conducted in order to assist with assessing the adequacy of these guidelines. The conditions tested in our experimental setup included a total of four different slopes (0.028%, 0.110%, 0.270%, and 0.488%) that are representative of most slopes that would be found in a typical prairie setting. This represents one significant difference from the work of Ead *et al.* (2000), which involved much higher slopes. The large difference in slope could have a substantial effect on the nature of flow observed. Through discussion with local culvert designers, it was stated that most culverts are designed with a slope only slightly above horizontal, around

0.025%. Since setting up such small slopes was difficult, 0.028% was considered to be representative of the lower slopes.

For the four different slopes chosen there were several different flow rates tested. The choice of flow rates was made such that each slope would have at least one discharge that would be comparable to another test at a different slope. There were a total of three different discharges used (0.086 m^3/s, 0.130 m^3/s, and 0.175 m^3/s) through the testing phase. Not every slope was tested with each flow rate. Since the chosen operating conditions were to set up each situation at normal depth, the slope of the culvert limited the discharge. It was decided to operate at normal depth because of the number of variables already chosen. Normal depth also allows for a single water depth condition for a particular test. By having a M1 or M2 profile there is an infinite number of water depths along the length of the culvert for a given slope and discharge. In order to achieve normal depth for each setup the radial gate was used to raise and lower the tail water level to the appropriate point.

Three different gravel embedment depths were tested to explore the effects of the guideline recommending 30 cm of gravel infill or 10% of the culvert diameter (Fisheries and Oceans Canada, 1996). The three levels of gravel embedment used were 9.7%, 18.4%, and 27.9%. Each gravel depth was only tested on one slope with one discharge to keep the amount of experiments to a manageable size. This resulted in a total of 11 test scenarios, allowing for comparison between slopes, flow rates, and gravel embedment depths. The testing matrix is shown in Table 3.1.

Table 3.1 - Testing Scheme

Slope (%)	Discharge (m^3/s)	Embedment (%)	Test Name
0.028	0.0858	0	S00028_Q086
0.110	0.0864	0	S00110_Q086
0.110	0.1759	0	S00110_Q175
0.270	0.0852	0	S00270_Q086
0.270	0.1762	0	S00270_Q175
0.270	0.0857	9.71	S00270_Q086_R10
0.270	0.0868	18.38	S00270_Q086_R18
0.270	0.0844	27.85	S00270_Q086_R28
0.488	0.0855	0	S00488_Q086
0.488	0.1287	0	S00488_Q130
0.488	0.1751	0	S00488_Q175

3.2 Data Collection

3.2.1 Water Surface Profiles

The first step when running an experiment was to set the water surface profile and record the final setup. In order to determine when normal depth was achieved, the culvert bottom was surveyed using a surveying level and the water surface elevations were recorded using the manometer boards. The water levels in the headwater and tailwater boxes were recorded as well. The difference between the measured bed elevation and the water surface elevation gave the water depth. Interpolation between points was required since each survey location did not correspond to each manometer point. When the water depth was plotted in EXCEL it could be seen whether the flow was operating as either a M1 or M2 profile. The radial gate was then adjusted to raise or lower the tailwater level to approach normal depth.

After normal depth was achieved the final readings from the manometer boards and the survey data were input into an EXCEL template that displayed the water surface profiles. The profiles, as seen in Appendix C, provided details of the head drop through the culvert, the culvert slope, the water depth, and the rock embedment depth.

3.2.2 Velocity Data Collection

There were two separate portions of the velocity data collection that needed to be done for each experiment, the first of which pertained to the study of the development length. In order to determine the downstream location where the flow profile became fully developed, centerline streamwise velocity profiles were measured. Therefore, each experimental setup required that a centerline streamwise velocity profile should be taken at a sufficient number of downstream locations to accurately determine the development length. Rather than testing at a set number of locations, each test used a different set of locations depending on where the onset of fully developed flow occurred. The specific downstream locations used will be outlined in Chapter 4.

The second portion of detailed velocity data collection was to obtain data points over a two-dimensional plane at one location within the fully developed region. This collection of data would then be used to depict the full cross sectional flow distribution, as well as to compare to the equations created by Ead *et al*. (2000). Since the time required to acquire these data points was extensive, the velocity distribution inside the culvert was assumed to be symmetric about the centerline. For the sake of creating full section plots,

the data from one side of the culvert was simply mirrored to the other side, which Magura (2000) found to be a valid assumption. This assumption would likely not be valid for a situation where the inflow to the culvert approached at an angle.

Before each experiment was conducted the ADV boundary function was used to measure the location of the culvert bottom and the water surface. These two measurements were then used to create a reference system for locating the exact location of the subsequent measurement locations. A MATLAB script was developed to select data point locations that were orientated perpendicular to the culvert, and that were distributed with a higher resolution near the boundary where the high velocity gradient was present.

The sampling duration was set to ensure that accurate velocity statistics were obtained. Magura (2007) collected a total of 1,000 samples and Abbs *et al*. (2007) collected a total of 15,000 samples. Magura (2007) did not find it necessary to sample for such an extended period of time since he chose not to determine turbulence quantities. For this study, due to the need for turbulence information, a total of 12,000 samples were collected for each point location. This was determined by collecting 30,000 points at a representative location 4 cm from the boundary and observing the change in turbulence intensity with sample size. Turbulence intensities within 2% of the long term mean were obtained within 12,000 samples as can be seen in Figure 3.1, which shows the three components of turbulence intensity. Accurate values of mean velocity were obtained well within the 12,000 sample total.

3.3 Data Processing

3.3.1 Organization

The data from each experiment was contained within a unique folder, labeled by the slope, discharge, rock depth if applicable, access hole number, profile angle, and the date. For example, a vertical profile test in access hole 18 on January 02/09 using a slope of 0.27%, operated at a discharge of 0.086 m^3/s, with a gravel depth of 9.7% would be labeled, S00270_Q086_R10_H18_A0000_020109. As can be seen, several values within the test name were approximate values rather than the exact values. Within each experiment folder three separate folders were made to hold velocity data files from the three different orientations of ADV. Alongside the three folders were three text files containing the locations of the points for each of the three different orientations of ADV. The locations in these text files were used to communicate to the motion control system. Lastly, one more text file containing various setup data was created for processing purposes.

After the sampling was completed, each of the three folders allocated to hold the data points were filled with a text file from each point location. Within the text file was the output of the ADV and a single line containing the exact location of the ADV according to the traversing mechanism. Each of these text files was labeled according to their order of sampling, P1, P2, P3, etc. The output of the ADV contained ten values for each sample that was taken. The first value of the set of 10 is simply the sample number. The next three values were the *x*, *y*, and *z*-components of velocity, where the three dimensions are

defined in SonTek technical documentation (SonTek, 2001). The second set of three values is the amplitude, again in the *x*, *y*, and *z*-directions. Lastly, the third set of three values is the correlation in the *x*, *y*, and *z*-directions.

3.3.2 Data Clean Up

After sampling was completed the data was contained within the folder structure as previously stated. In order to get the data into a more user-friendly, accessible format one of two MATLAB scripts was run. Either the program datacleanupEMPTY.m or datacleanupROCK.m was used to achieve this task, for tests without gravel embedment and for tests with gravel embedment, respectively. The process undertaken within these scripts used the data files to calculate the mean velocity, turbulence intensity, second order turbulence quantities, signal to noise ratio (SNR), correlation score (COR), and several other basic geometric properties of the flow field.

SNR is an indication of the signal strength being record by each of the three ADV receivers. It is a function of the amount of particulate matter within the water, which causes the acoustic reflections that the ADV needs for measurements. A lower value of SNR indicates a poor signal. It is recommended in the SonTek technical documentation that for high resolution measurements the SNR should be at least 15 dB (SonTek, 2001). COR is an indication of data quality, where a lower correlation score represents poor data quality. The COR can be a function of the environment of the testing location, such as highly turbulent regions. It is recommended that the correlation score should be above 70%, but for mean flow calculations anything above 30% is acceptable. For these

experiments any data point with a SNR of less than 15 dB or a COR of less than 50% was excluded. The choice of the limit on COR was made to keep as many points as possible for mean velocity data, but to limit the data points with very poor quality for turbulence data. The above calculations resulted in all of the data for one experiment being organized into a single .mat file.

Following data cleanup, the calculated values were input into EXCEL. Here the streamwise velocity data was manually fitted to the ideal log law, (Equation 1.6). By visually choosing the most appropriate values to create a good fit, the parameters of U_*, k, and ΔB were obtained. Since data processing is much more convenient in MATLAB, the newly found log law parameters were exported back into the experimental .mat file for later use through the script modlogvalues.m.

Lastly, a final set of MATLAB scripts named tecplot1Dfile.m as well as either the empty culvert script tecplot2DfileEMPTY.m or tecplot2DfileROCK.m for tests with gravel embedment were used. These scripts simply converted the experimental data from the .mat file into a format acceptable to TecPlot 360, which was used to plot the final results. Discussions of these results are presented in the following chapters.

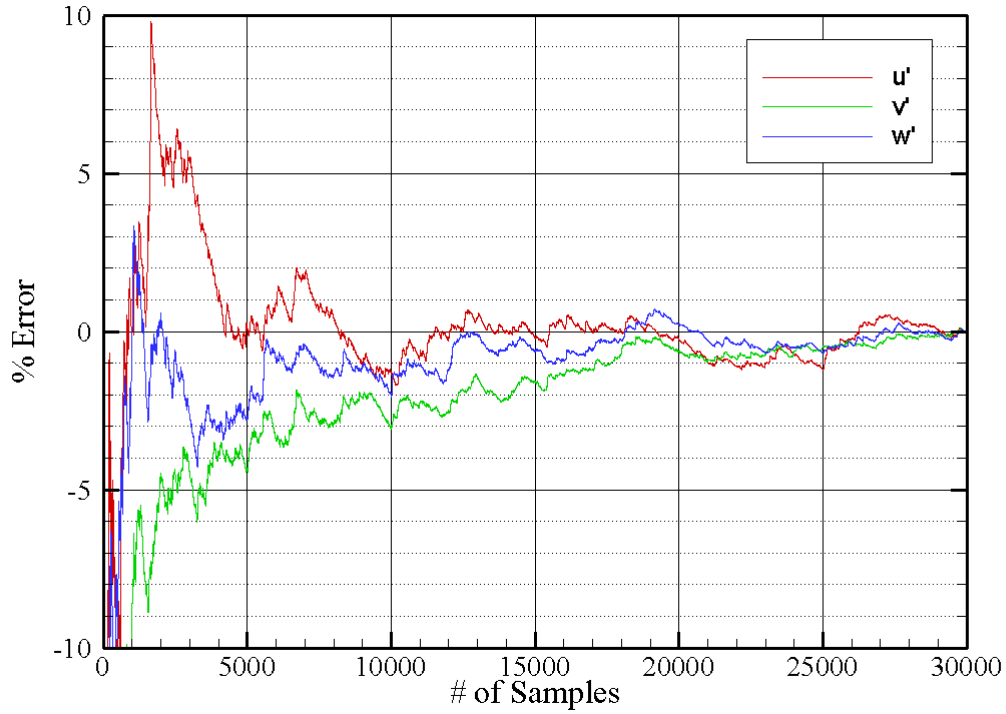

Figure 3.1 Percent error of a certain sample size from a long term average

CHAPTER 4 *Results and Analysis*

4.1 Introduction

The following pages outline the final analysis of the data and the corresponding results. The data, after having been collected and organized, was run through a set of standard plots in order to properly extract and display the information. Within each of the plots the variables were displayed non-dimensionally so that the results from different tests can be compared to each other. Each of the tests, as previously outline in Table 3.1, were plotted by themselves, and comparisons are drawn between them. Certain points of interest are also extracted from the plots and the analysis and clearly displayed within tables in the text. Table 4.1 outlines the various parameters describing the flow conditions that occurred during the set of tests.

Table 4.1 - Hydraulic parameters

Test Name	U_{av}	d	A	P	R	Re	F
[-]	[m/s]	[m]	[m^2]	[m]	[m]	[-]	[-]
S00028_Q086	0.265	0.491	0.324	1.440	0.225	98375	0.132
S00110_Q086	0.402	0.354	0.215	1.165	0.184	97072	0.247
S00110_Q175	0.506	0.522	0.348	1.505	0.231	206138	0.239
S00270_Q086	0.557	0.275	0.153	1.002	0.153	100154	0.397
S00270_Q175	0.693	0.404	0.254	1.264	0.201	196696	0.393
S00270_Q086_R10	0.553	0.233	0.155	1.042	0.149	98104	0.396
S00270_Q086_R18	0.552	0.215	0.157	1.090	0.144	97280	0.397
S00270_Q086_R28	0.557	0.195	0.151	1.120	0.135	94268	0.409
S00488_Q086	0.757	0.221	0.113	0.885	0.128	106751	0.609
S00488_Q130	0.830	0.278	0.155	1.008	0.154	150869	0.588
S00488_Q175	0.914	0.325	0.192	1.106	0.173	198944	0.591

4.2 Manning's Roughness

Since one of the first steps in the testing procedure was to determine water surface profiles and to ensure that everything was operating at normal depth, it seems intuitive to calculate the Manning's roughness for the culvert. By using the depth of flow and the rock depth available in the survey sheets, Appendix C, Manning's equation could be solved to determine *n*. Table 4.2 outlines the results of these calculations.

As can be seen in Table 4.2, the global average from all of the test conditions was 0.0250, slightly higher than 0.0240 as was obtained from the Corrugated Steel Pipe Institute (2007). This difference could be attributed to the choice of when the flow was at normal depth. This was done by plotting the water depth and visually deciding when the water level was constant. For the more horizontal slopes, a M1 or M2 profile is very gradual and choosing the correct water depth is subjective. Nevertheless, the amount of variation is small and the value of Manning's *n* found was satisfactory.

Table 4.2 – Manning's Roughness for each test condition

Test Name	Manning's *n*
S00028_Q086	0.0233
S00110_Q086	0.0267
S00110_Q175	0.0247
S00270_Q086	0.0266
S00270_Q175	0.0257
S00270_Q086_R10	0.0264
S00270_Q086_R18	0.0259
S00270_Q086_R28	0.0245
S00488_Q086	0.0234
S00488_Q130	0.0241
S00488_Q175	0.0238
AVERAGE	**0.0250**

4.3 One Dimensional Velocity Profiles

4.3.1 Streamwise Velocity

As previously stated, the streamwise velocity is defined as the velocity along the length of the culvert, with the positive axis in the direction of flow. The three components of velocity are collected and plotted together in Appendix A. The streamwise velocity data can be seen in Figure A.1(a) through A.11(a). In order to remove the small variation from one access hole to another, the streamwise velocity was normalized by the average velocity. Since the ADVs measured the culvert bottom and the water surface for each test, there was an individual water depth and therefore flow area for each access hole. The area, as measured by the ADVs, was then used to determine the average velocity. The data was normalized using average velocity rather than the friction velocity because of the applicability to the fish passage regulations and current design techniques. In

similar fashion, the water depth (h) measured by the ADVs was used to normalize the elevation data. For all tests the origin (y = 0) was defined at the peak of the culvert corrugations. There was one exception for test S00270_Q086 where the measured water depth from the ADV was clearly not reliable. The problem was found and each test was checked to be sure the error did not occur anywhere else. Therefore this one test used the water depth from the manometers for normalization.

By observing the set of profiles taken for each test there are several noticeable patterns that arise. First off, and most noticeable, is the shape of the streamwise velocity profile near the inlet of the culvert. Since the culvert inlet was not the main focus of the study not every test setup had profiles near to the inlet, nonetheless the same pattern is somewhat apparent in each test. Since the inlet condition was a projecting inlet there was no boundary layer development at the point of entry into the culvert. This meant that the velocity profile at the entrance of the culvert was essentially uniform. By observing the streamwise velocity profiles this is apparent in the development of the profile. Early access hole locations are noticeably uniform in shape, then develop primarily from the bottom surface. In addition, but to a lesser degree, the velocity profile develops from the water surface downward. As can be seen in each of the 11 tests, the velocity profile reaches the developed profile at the top and bottom first, and the location of maximum velocity reaches the developed profile last.

The properties of the velocity profiles in the developing region give an indication of the differences between the developed region and the undeveloped region. It can be seen that

in the developed region there is a significant portion of the profile that is less than average velocity, which could be useful for fish passage. In the undeveloped region, with an elevated projecting inlet, the velocity distribution appears to be better represented by the average velocity, which may also have implications for fish passage.

When comparing the streamwise velocity profile to the ideal log law outlined in Equation 1.6, the three log parameters can be obtained. The process of fitting the data to the log law is a somewhat subjective process because the three parameters, U_*, d_0, and ΔB, can be adjusted to within a range of values that all produced similar results. Although not explicitly stated in Equation 1.6, d_0 is a slight shift in the location of the origin. By adjusting the location of the origin a better fit to the log law can be obtained. As a result of attempting to fit all three parameters, U_* fell between 1.03 and 1.23 times the average friction velocity, centered around 1.1. In order to assist in obtaining a more consistent means of determining the three values, it was chosen to set the friction velocity of the centerline to be equal to 1.1 times the average friction velocity for simplicity, as shown in Equation 4.1.

$$U_{*0} = 1.1 * U_{*av} = 1.1 * \sqrt{gRS} \tag{4.1}$$

where U_{*0} [m/s] is the centerline friction velocity. The solver function in EXCEL was then used to optimize d_0 and ΔB, which resulted in very good fit to the data with appropriate values. The streamwise velocity profile can be seen in semi-log scale in Figure A.1(b) to Figure A.11(b). Within each plot only the profiles within the developed

region are plotted, because undeveloped velocity profiles were not fitted to the log law. The following table shows the resulting average value of each of the three log law parameters. Additionally, the value of k is solved for from the fitted value of ΔB according to Equation 1.7. The results of the fitting can be seen in Table 4.3.

Table 4.3 – Fitted Log Law Parameters

Test Name	U_{*0}	d_0	ΔB	k
-	**[m/s]**	**[m]**	**[-]**	**[m]**
S00028_Q086	0.027	-0.005	12.61	0.007
S00110_Q086	0.049	0.000	15.76	0.015
S00110_Q175	0.055	0.003	16.17	0.016
S00270_Q086	0.074	0.006	16.94	0.016
S00270_Q175	0.080	0.008	17.41	0.018
S00270_Q086_R10	0.070	-0.011	16.25	0.013
S00270_Q086_R18	0.069	-0.003	16.11	0.012
S00270_Q086_R28	0.068	-0.015	15.60	0.010
S00488_Q086	0.087	0.000	15.80	0.008
S00488_Q130	0.095	0.001	16.25	0.009
S00488_Q175	0.100	0.002	16.58	0.010

From this it can be seen that the values of equivalent roughness height vary a significant amount. Although the equivalent roughness height does change a fair bit, for tests without gravel embedment the values average to 0.0123 m, which is similar to the corrugation height (0.013 m). The value of d_0, which acts as an adjustment to the location of $y = 0$, is an insignificant term, it is possibly a result of small errors in defining the culvert boundary. Relationships between these values and the test conditions will be discussed further in chapter 5.

4.3.2 Vertical and Spanwise Velocity

Both the vertical and spanwise velocity components were again plotted normalized by the average streamwise velocity. It was chosen to use the streamwise velocity so that the magnitudes of the three components could be compared. One point of small error became apparent when observing the vertical and spanwise velocity. The error was a result of not installing the ADVs in exactly the same orientation for each test. When an ADV is installed even slightly rotated, the total measured velocity magnitude is redistributed amongst the three components of velocity. The resulting offset can be seen in several of the profiles and must be noted.

By observing the vertical velocity plots in Figure A.1(c) through A.11(c) there are several trends that can be seen. Initially, it becomes apparent that the majority of the data points are negative. This indicates that there is a consistent downward velocity along the centerline of the culvert, which would suggest that there is secondary circulation within the two dimensional cross section. It is also seen that there is greater variability higher in the water column, which is possibly an effect of the higher velocities in this region.

When looking at the spanwise velocity as seen in Figure A.1(d) through A.11(d) the slight error in the orientation of the ADV becomes clear. In order to ignore this error it should be assumed that the top five points are incorrect, and the remaining bottom points are correct. Given that the profiles are along the center, it would make sense to say that if symmetry is present there should be no spanwise velocity. Within all of the plots it is clear that there is minimal spanwise velocity, but also that any spanwise velocity present

generally varies near linearly with depth. Initially this could indicate that there is a large circulation pattern within the cross section, where water moves in the positive *z*-direction along the bed and in the negative *z*-direction at the surface. Alternatively, since the pattern is not consistent among all of the tests, where several are reversed and others are centered on zero, this could suggest that the orientation of the ADV was slightly off vertical. For this reason, and because of the scale of both the vertical and spanwise velocity, the results should be taken with a word of caution.

4.4 Development Length

One of the key objectives of this study was to determine the development length for a variety of test conditions and to determine a relationship between them. In order to determine the development length, the streamwise velocity profiles were compared along the culvert length. Since the profiles each contained some amount of variation, the development length for each test condition was determined by visual comparison of one profile to another. For several of the test conditions where the water depth was lower it was slightly easier to choose a certain location as the development length, but for other tests it was not so easy. For deeper and slower moving tests, such as those in Figures 4.1 and 4.3, the undeveloped profiles simply appeared more uniform relative to developed profiles. For shallower tests, such as those in Figures 4.2 and 4.9, the undeveloped profiles appear to have not yet reached of maximum velocity only. For each test, one profile before and two profiles after the chosen development length are plotted in Figure 4.1 through 4.11.

Additionally, for tests with gravel embedment there was a difficulty in obtaining consistent parameters for normalization because it was not easy for the ADV to measure the bed level of the gravel. Depending on the location, it could read the top of a rock, resulting in the water depth appearing shallower, or it could read a gap between rocks, resulting in the water depth appearing deeper. For this reason the vertical location of the data points was shifted upwards or downwards by the difference in depth readings from the manometers and from the ADV. This technique helped the profiles to collapse together and make comparisons possible. Table 4.4 outlines the development lengths associated with each test.

Table 4.4 – Development Lengths

Test Name	**Development Length**
-	**[m]**
S00028_Q086	9.69
S00110_Q086	8.88
S00110_Q175	8.88
S00270_Q086	8.88
S00270_Q175	8.88
S00270_Q086_R10	13.73
S00270_Q086_R18	13.73
S00270_Q086_R28	12.11
S00488_Q086	4.77
S00488_Q130	6.45
S00488_Q175	5.71

The chosen development length was measured as the distance along the length of the culvert from the inlet to the first access hole that exhibited developed flow. This is why several tests have the exact same development length as others. Since the profiles were

measured at discrete locations, the exact development length was likely between access holes. It is clear by observing Table 4.4 that for tests without gravel embedment the development length is longer for mild slopes. In addition, it can be seen that gravel embedment generally results in longer development lengths, but due to the variable nature of the gravel bed, this would be expected.

4.5 Turbulence Intensity

As stated earlier in the objectives of this report, it is important to gain an understanding of the turbulence quantities within the culvert because of their potential importance to where the fish may choose to swim. According to past open channel flow data, the vertical distribution of turbulence intensity in all three dimensions can be approximated by Equation 1.9 through 1.11. For comparison these equations have been plotted on their respective plots with the data (Figure 4.12 through 4.22). Since the vertical location y is normalized by the depth, and the turbulence intensity is normalized by the friction velocity, these predictive equations are generally valid for all wide open channels.

As can be seen in Figure 4.12 through 4.22, the distribution of turbulence intensity does not follow that of the predictive equations. The data shows that the turbulence intensity decreases much faster than the predictive equations away from the boundary, and then increases toward the surface. This pattern would be expected, since the shape of the culvert causes a significant standing wave along the surface, which also affects the shape of the streamwise velocity profiles. This is expected since the change in streamwise

velocity with depth (dU/dy) results in turbulence production. Additional support of this idea is evident in Figure 4.17 through 4.19, which are the three tests with gravel embedment. It's clear that as the depth of gravel embedment increases the distribution of turbulence intensity moves closer to the predictive Equations 1.9, 1.10, and 1.11. This would be expected because with increased gravel embedment the cross section becomes more rectangular in shape, causing the turbulence intensity distribution to be closer to that of a wide open channel. Additionally, plots of turbulent kinetic energy (TKE) and Reynolds stress (-uv) can be seen in Appendix B.

4.6 Two Dimensional Cross Sections

Data was collected over the entire flow area for each test at access hole 18 in order to determine the entire two dimensional flow structure within the developed region. With the data collected at a given two dimensional section it leaves the possibility to develop a set of equations that could provide approximations of the streamwise velocity in more than just the centerline. An attempt has been made by Ead *et al.* (2000), but their results do not properly represent the data, this will be further discussed in chapter 5.

The normalized streamwise velocity and their associated point sample locations can be seen for several of the tests in Figures 4.23 to 4.38 for access hole 18. In order to save time, velocity points were only taken on one half of the cross section and the other half was assumed to be a reflection. This also explains the apparent symmetry for each of the cross sections. All two dimensional tests were performed at access hole 18.

By observing the plots of average velocity for each of the two dimensional tests there are several observations that can be made. First, it can be seen in each test that the location of maximum velocity is below the water surface. This observation was also seen in the centerline velocity profiles discussed. It is important to note because of the discrepancy with that of Ead *et al.* (2000), where it was found that the maximum streamwise velocity was at the water surface. Rather, the data from this project better resemble the distributions found by Abbs *et al.* (2007) and Magura (2007). Second, for the tests without gravel embedment (Figure 4.23, 4.25, 4.27, 4.29, and 4.31) the maximum velocity region is somewhat circular, whereas when gravel embedment is present (Figure 4.33, 4.35, and 4.37) the maximum velocity region becomes more elongated in the spanwise direction. This shape thereby creates an area in the corner where the gravel meets the culvert with a reduced velocity. The corner region may provide an area better suited to fish passage than a similar culvert without gravel embedment.

By calculating the area weighted average of an un-normalized cross section plot of streamwise velocity it is possible to obtain the average velocity as represented by the data. This process was done in order to compare the discharge as determined by the Magmeter to the integrated discharge of the velocity measurements. In order to calculate the integrated discharge, the measured average velocity at a point was multiplied by the flow area represented by this point measurement. The total cross sectional flow area was calculated using the measured water level from the manometers. Table 4.5 shows the resulting average velocities, Magmeter discharge, and the resulting integrated discharge.

Table 4.5 – Average velocity and integrated discharge

Test Name	Average Velocity	Magmeter Discharge	Integrated Discharge	Difference
-	m/s	m^3/s	m^3/s	%
S00028_Q086	0.253	0.0858	0.0817	4.8
S00110_Q086	0.393	0.0864	0.0843	2.4
S00110_Q175	0.463	0.1759	0.1609	8.5
S00270_Q086	0.516	0.0852	0.0790	7.3
S00270_Q175	0.630	0.1762	0.1603	9.0
S00270_Q086_R10	0.478	0.0857	0.0740	13.6
S00270_Q086_R18	0.475	0.0868	0.0746	14.0
S00270_Q086_R28	0.482	0.0844	0.0730	13.5

From Table 4.5 it becomes apparent that there is a significant difference between the integrated discharge and the discharge from the Magmeter. It is difficult to say if this is a problem or not because there was only data for one half of the cross section. The difference in discharge could easily be counteracted on the other side of the cross section, if complete symmetry was not present. Secondly, there is a definite increase in error for the tests with gravel embedment. This strongly indicates that there is a significant amount of flow moving through the gravel bed. The flow moving through the gravel bed would be expected in nature, provided the void space in the gravel has not been filled with sediments or vegetation.

By using built in TecPlot functions it was possible to blank out areas of the cross section based on the velocity. Since fish passage criteria are based on average velocity, knowing the amount of area with a velocity lower than average velocity would be useful. Table 4.6 outlines the percentage of the area where the velocity is less than average velocity, and where it is less than 75% of average velocity.

Table 4.6 – Flow area less than average velocity

Test Name	Flow Area	Area < U_{av}	Area < 0.75U_{av}
-	m^2	%	%
S00028_Q086	0.3235	46.1	19.1
S00110_Q086	0.2147	38.5	20.1
S00110_Q175	0.3475	48.3	19.8
S00270_Q086	0.1530	44.6	25.4
S00270_Q175	0.2543	49.5	19.5
S00270_Q086_R10	0.1550	49.3	28.4
S00270_Q086_R18	0.1572	54.8	28.9
S00270_Q086_R28	0.1514	49.7	32.0

One very important note on Table 4.6 is that the average velocity was taken as the area weighted average velocity of the data found in Table 4.5. This was done because it was unknown how much flow was moving through the gravel bed. If the average velocity as determined by the Magmeter discharge divided by the area had been used all of the values would increase slightly, but those with gravel would increase drastically. From the results in Table 4.6, it is clear that there is considerably more area less than 0.75 U_{av} when gravel embedment is used. This gives a good indication that by placing gravel in the culvert it significantly alters the flow structure in a manner that will likely facilitate fish passage.

4.7 Shear Stress Distribution

By using the two dimensional cross section velocity measurements at hole 18, each individual profile was analyzed to determine the shear stress distribution over the entire wetted perimeter. In order to collect the necessary data points for fitting a value of shear

stress the data was extracted from the contour plots in TecPlot. This was done because the sampled points were not always directly inline with the radials. Therefore data was extracted from the TecPlot contour plots along the same radials as they were sampled, this produced as many points as were desired along the specified radial. The one exception to this rule was with the gravel embedment tests, where the data was extracted as vertically profiles along the gravel bed and as radials along the culvert boundary.

First the centerline profile was fitted to the log law, and the shear stress was determined. Then to provide a consistent means of fitting the other profiles without forcing the shear stress, the equivalent roughness height was set to the value obtained while fitting the centerline profile. The assumption was that for a given test, the equivalent roughness height would not change for different values of shear stress. Therefore the only value to fit to each of the other profiles was the shear stress. Plots of the shear stress distributions can be seen in Figures 4.39 and 4.40.

From this is it apparent that there is a general trend that the centerline shear stress is typically around 1.1 times the average shear stress, as previously stated. Then the shear stress ratio decreases along the wetted perimeter toward the water surface. For the three tests with gravel embedment there is a relatively constant shear stress along the gravel bed, then a sharp drop at the corner between the gravel and the culvert. This was expected according to the results of Magura (2007). Assessing the trend in the shear stress distribution will be further discussed in Chapter 5.

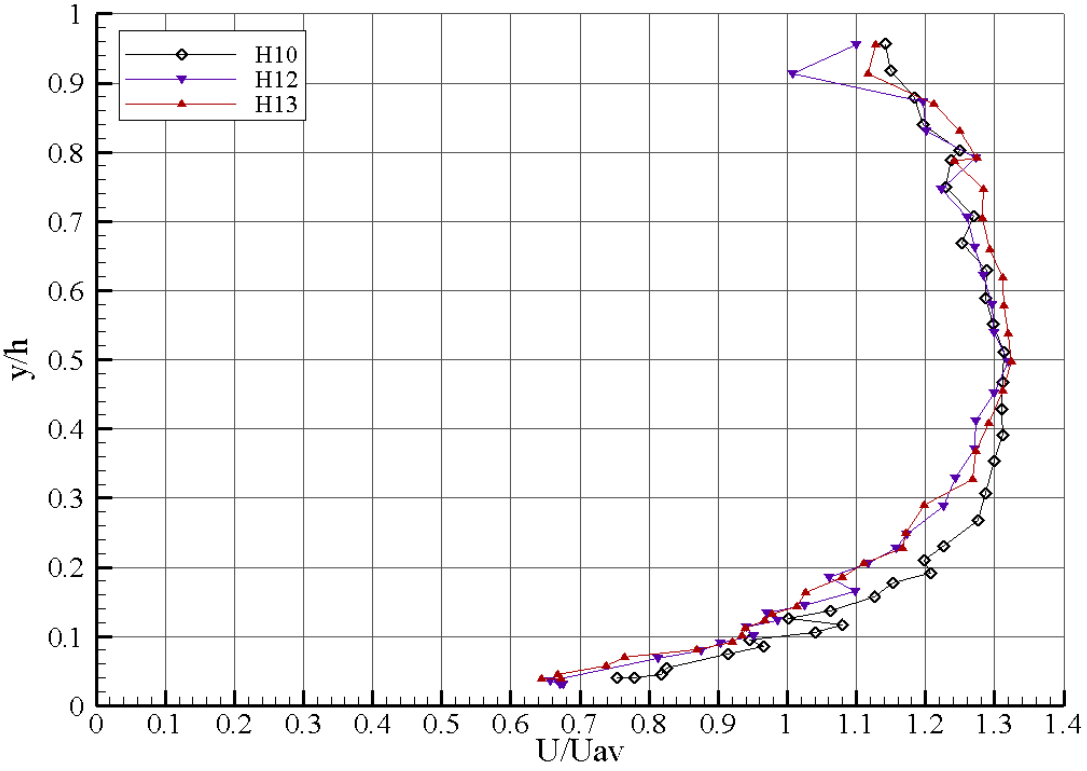

Figure 4.1 Transitional streamwise velocity profiles for test S00028_Q086

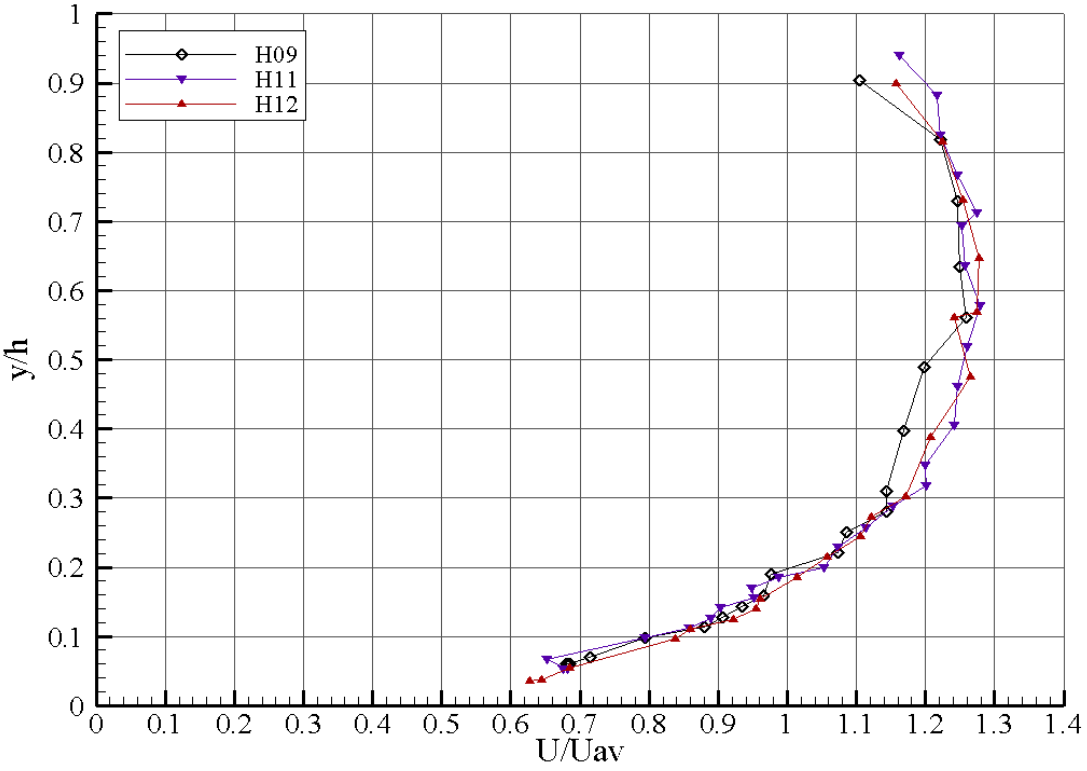

Figure 4.2 Transitional streamwise velocity profiles for test S00110_Q086

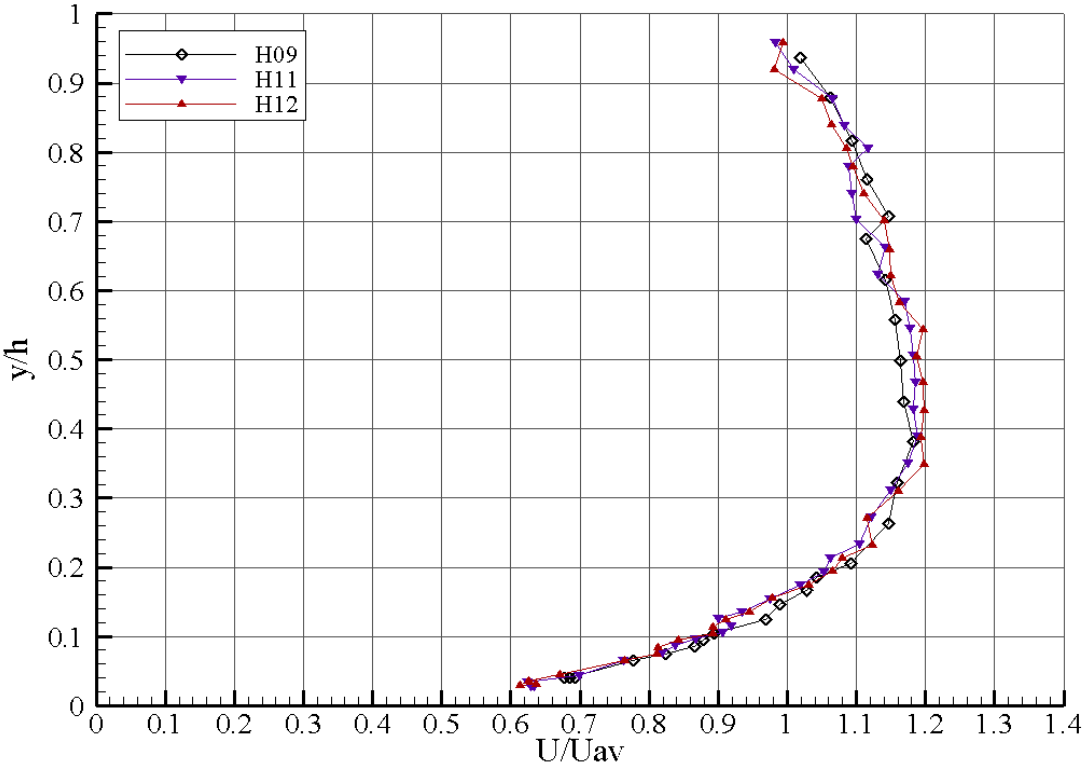

Figure 4.3 Transitional streamwise velocity profiles for test S00110_Q175

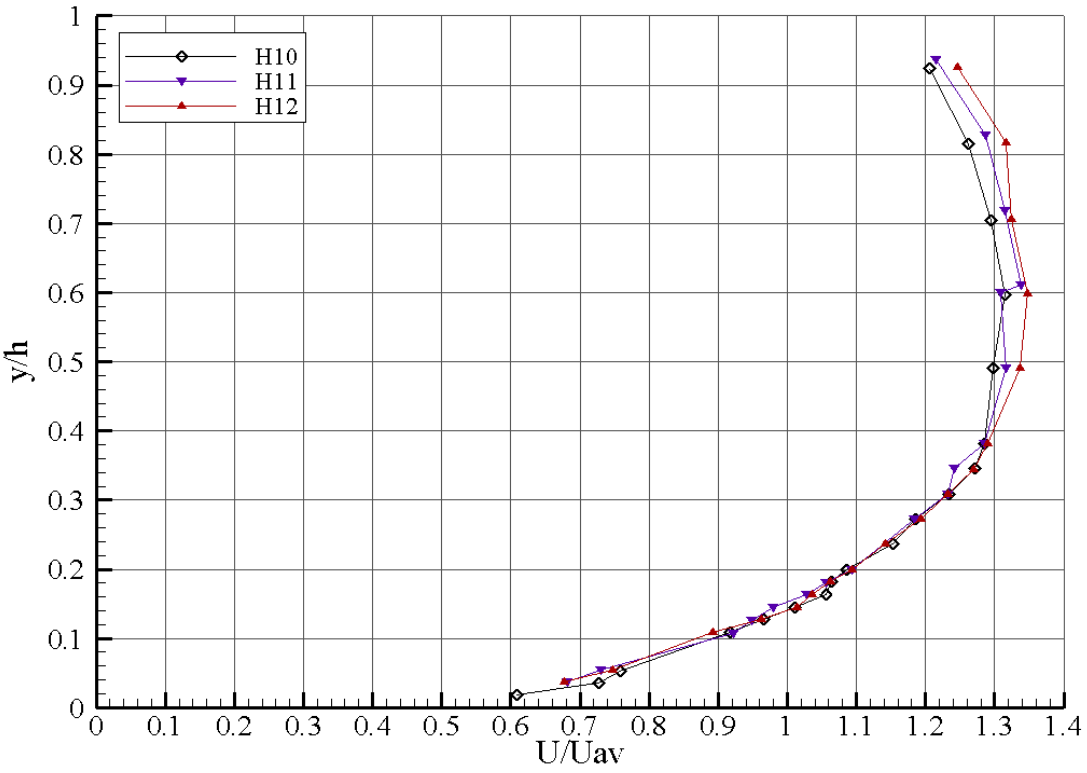

Figure 4.4 Transitional streamwise velocity profiles for test S00270_Q086

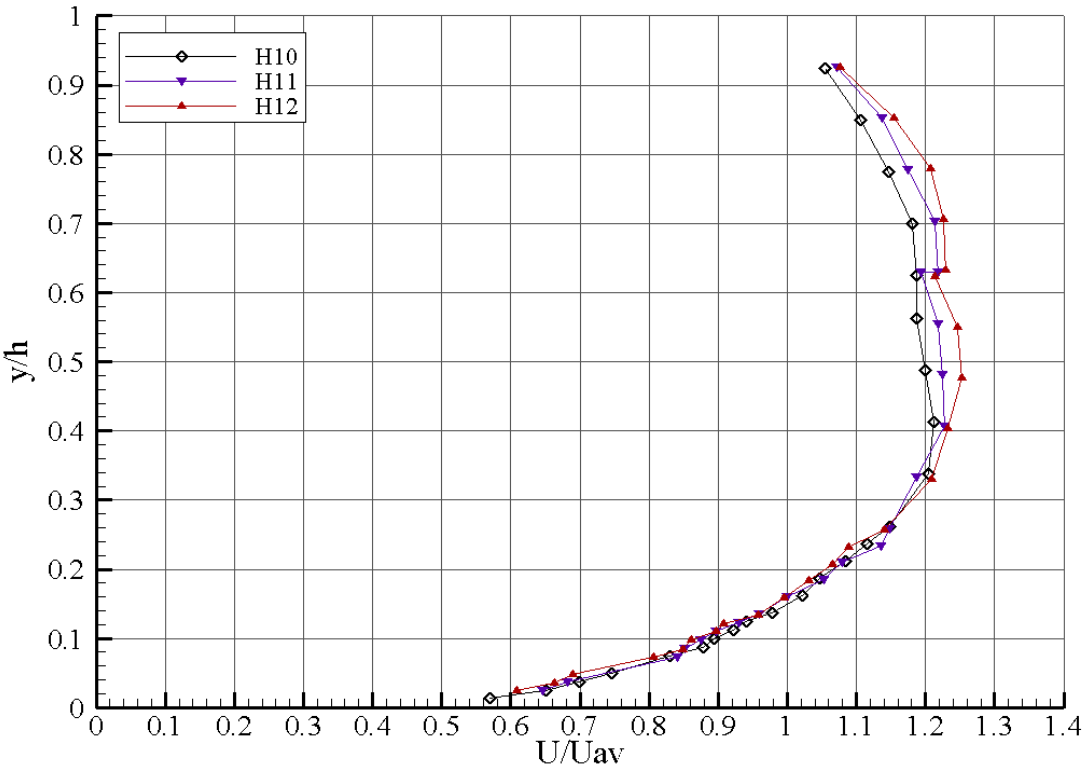

Figure 4.5 Transitional streamwise velocity profiles for test S00270_Q175

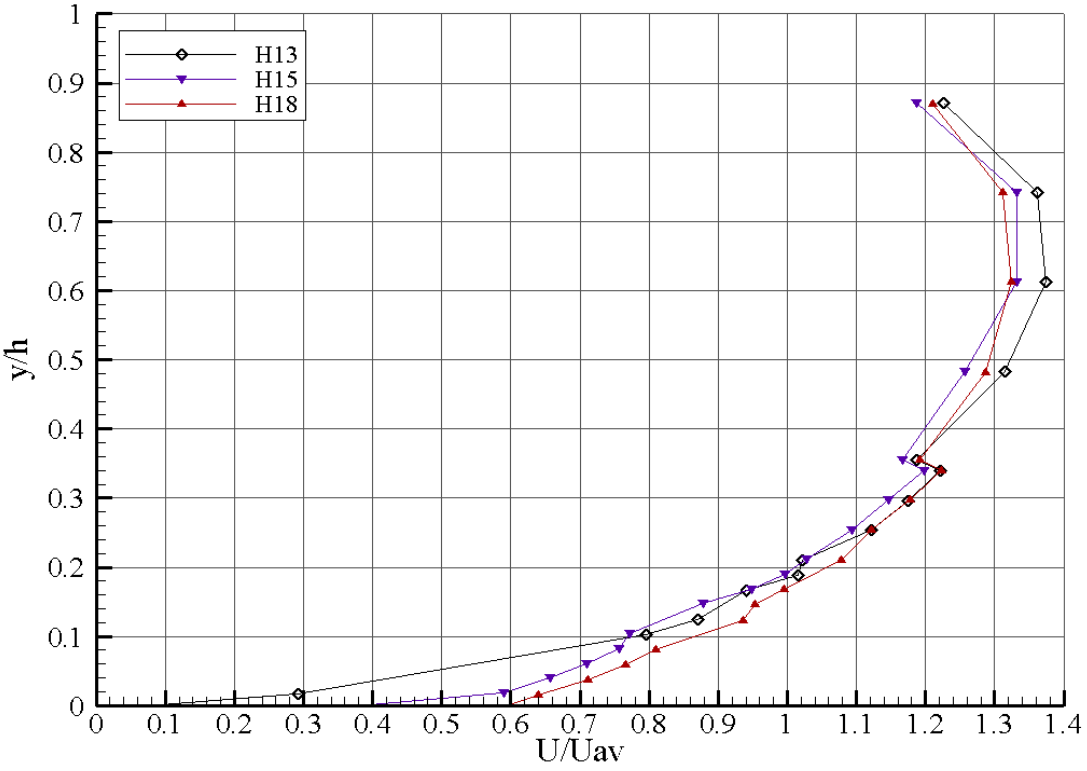

Figure 4.6 Transitional streamwise velocity profiles for test S00270_Q086_R10

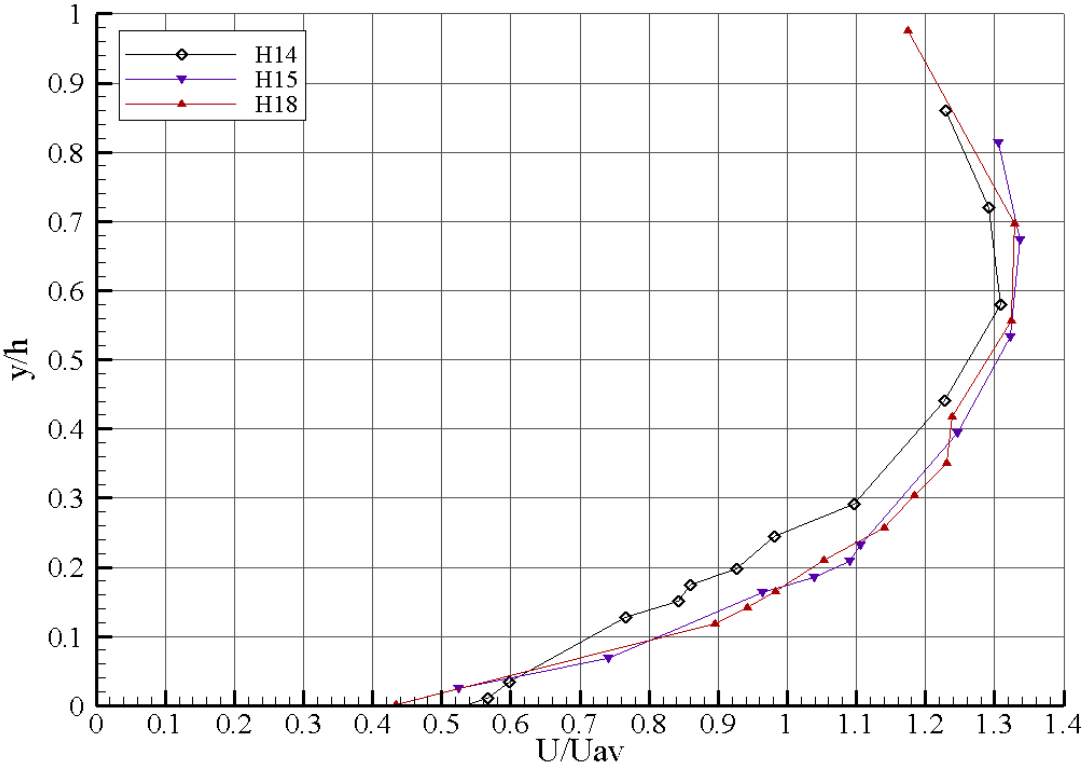

Figure 4.7 Transitional streamwise velocity profiles for test S00270_Q086_R18

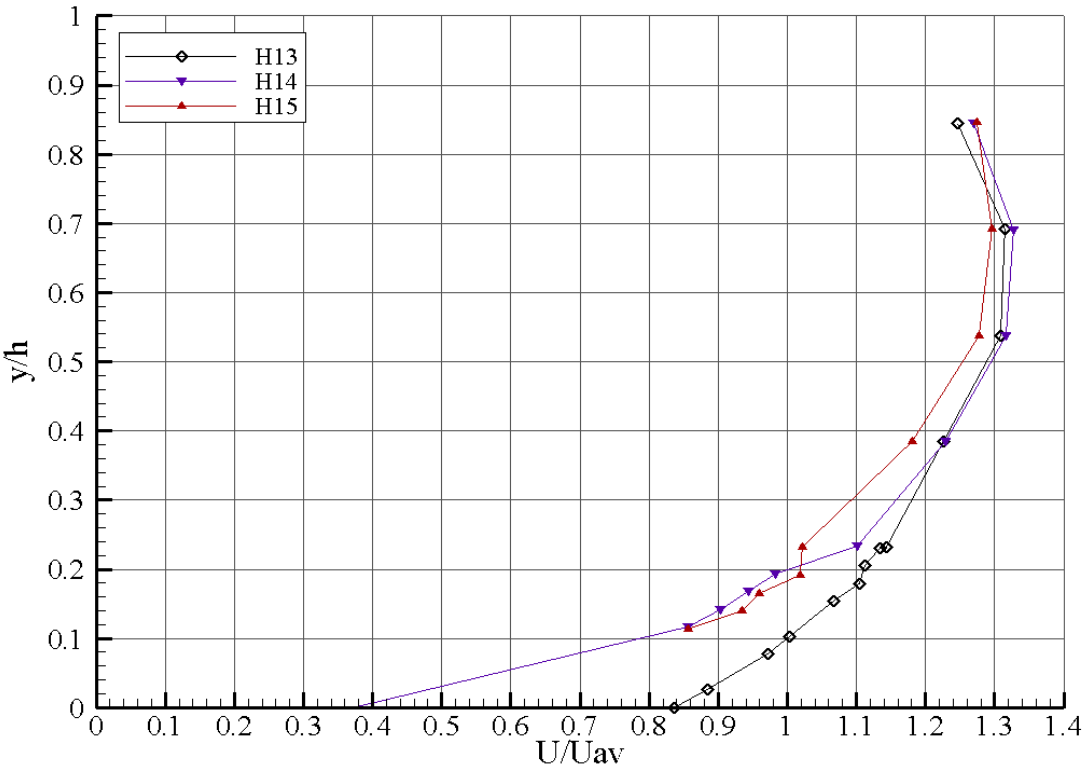

Figure 4.8 Transitional streamwise velocity profiles for test S00270_Q086_R28

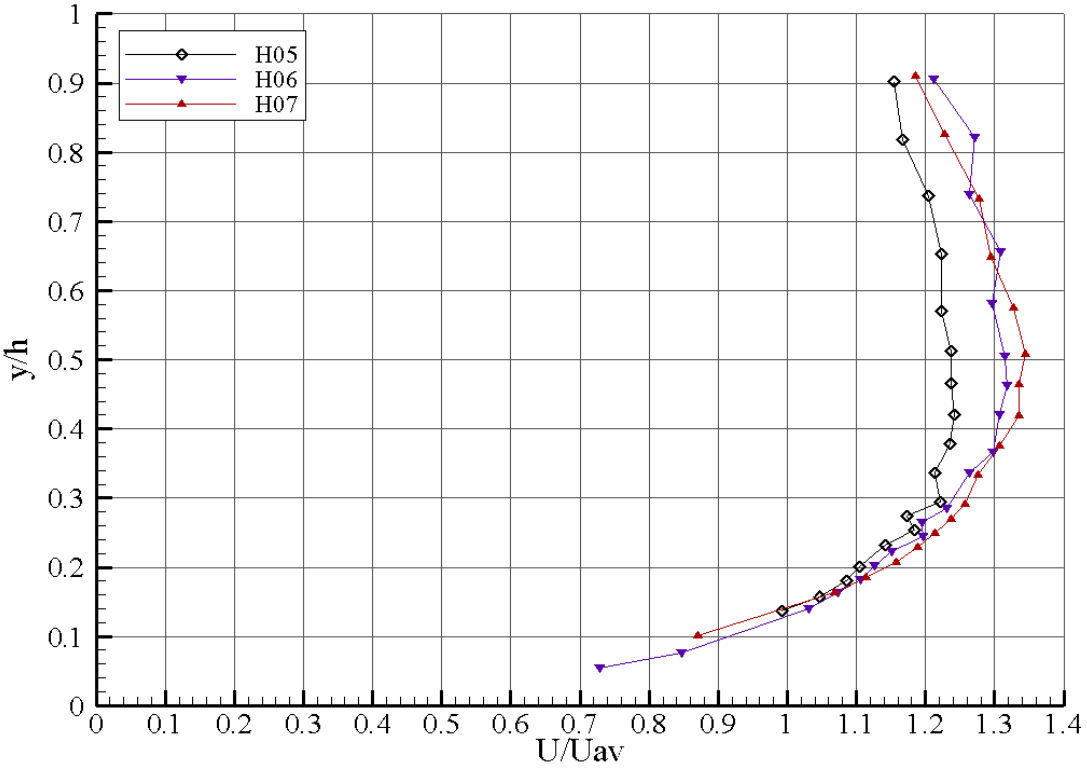

Figure 4.9 Transitional streamwise velocity profiles for test S00488_Q086

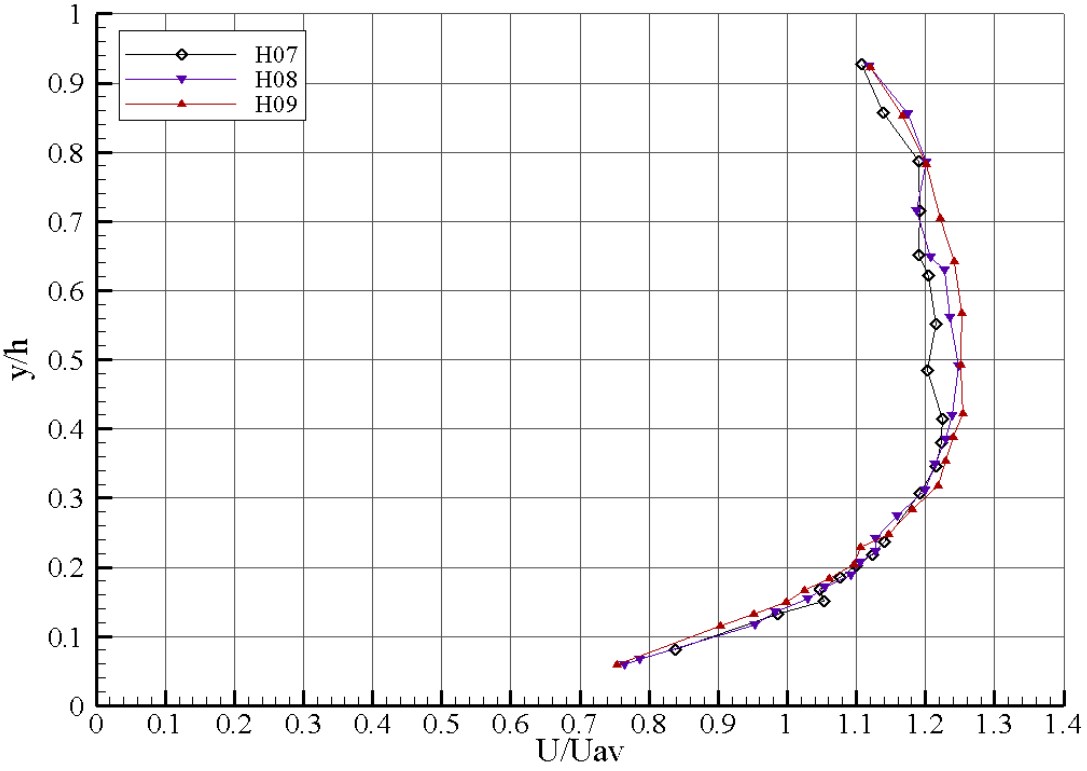

Figure 4.10 Transitional streamwise velocity profiles for test S00488_Q130

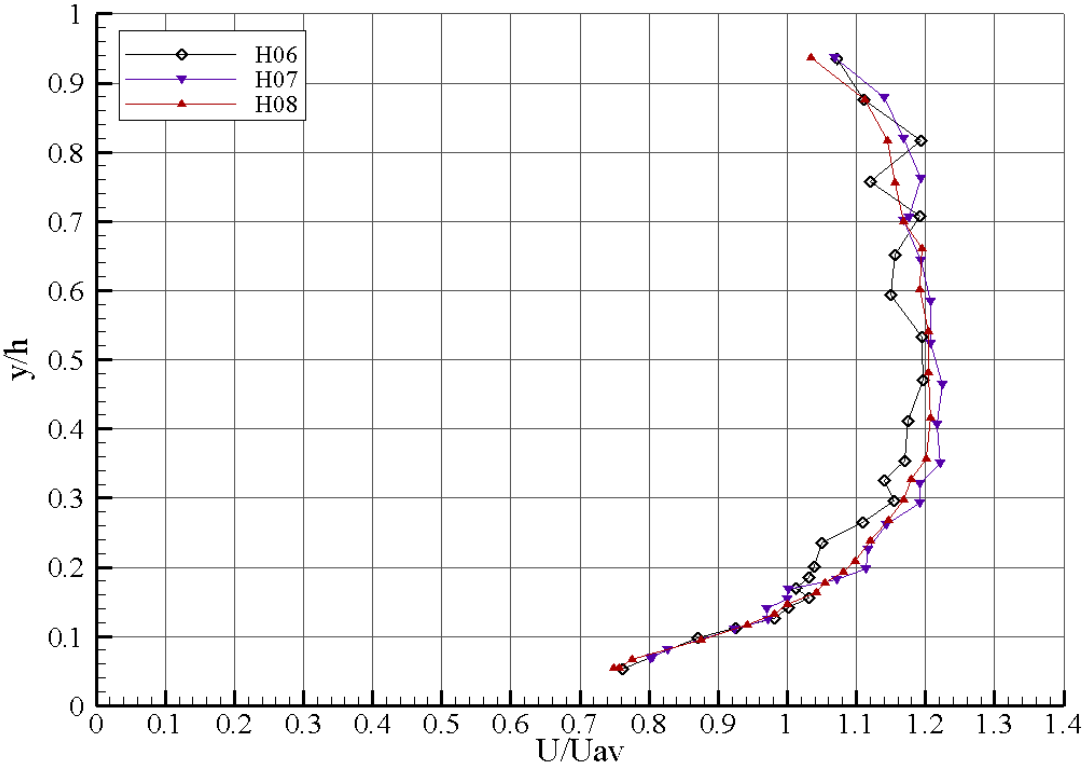

Figure 4.11 Transitional streamwise velocity profiles for test S00488_Q175

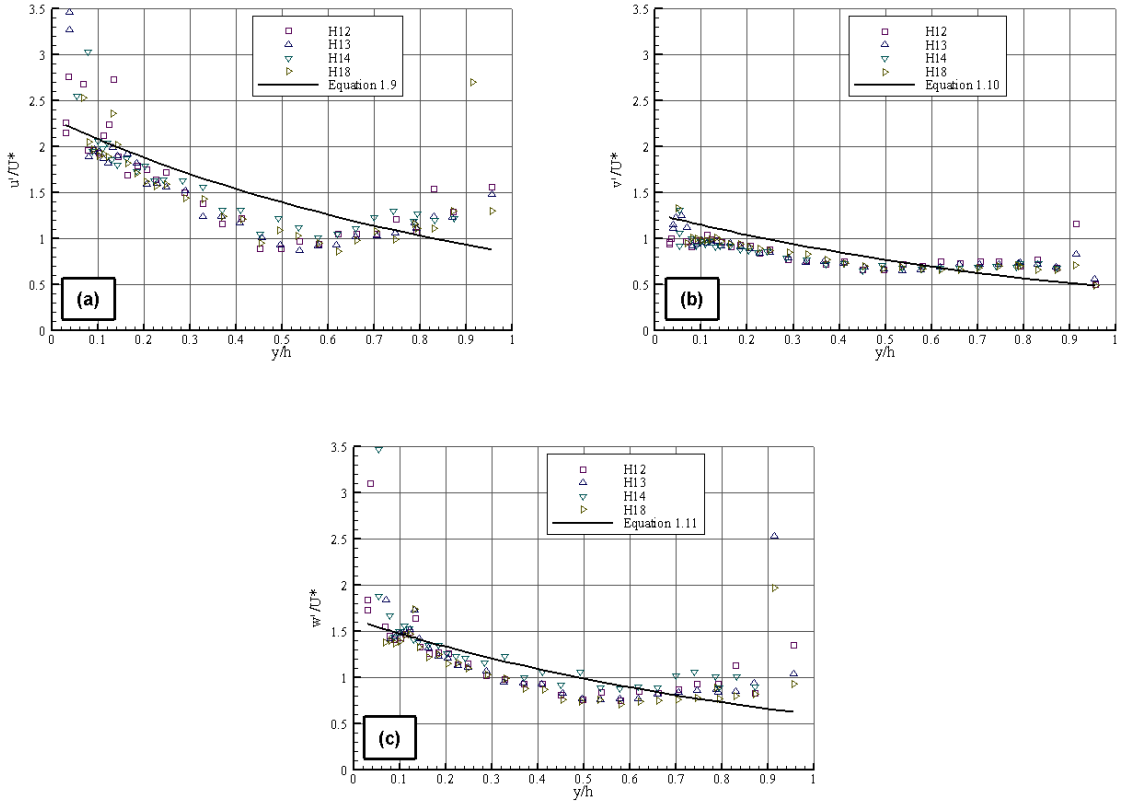

Figure 4.12 (a) Streamwise, (b) vertical and (c) spanwise turbulence intensities for test S00028_Q086

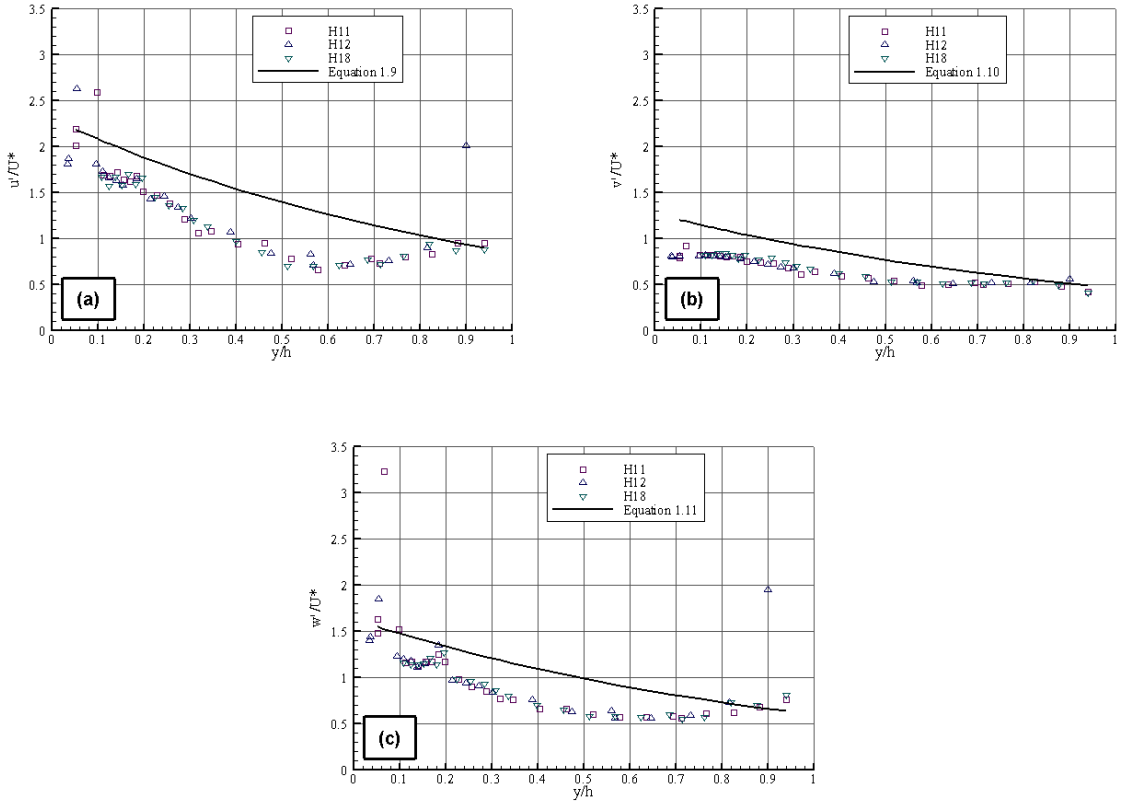

Figure 4.13 (a) Streamwise, (b) vertical and (c) spanwise turbulence intensities for test S00110_Q086

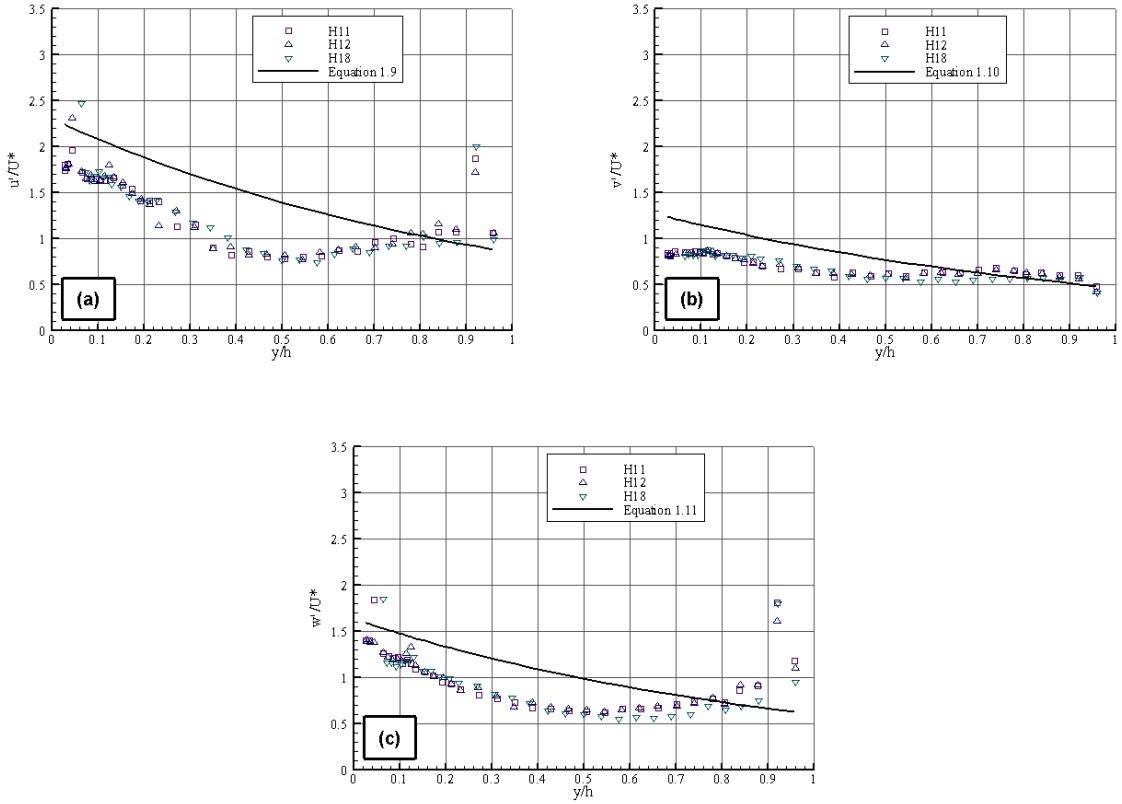

Figure 4.14 (a) Streamwise, (b) vertical and (c) spanwise turbulence intensities for test S00110_Q175

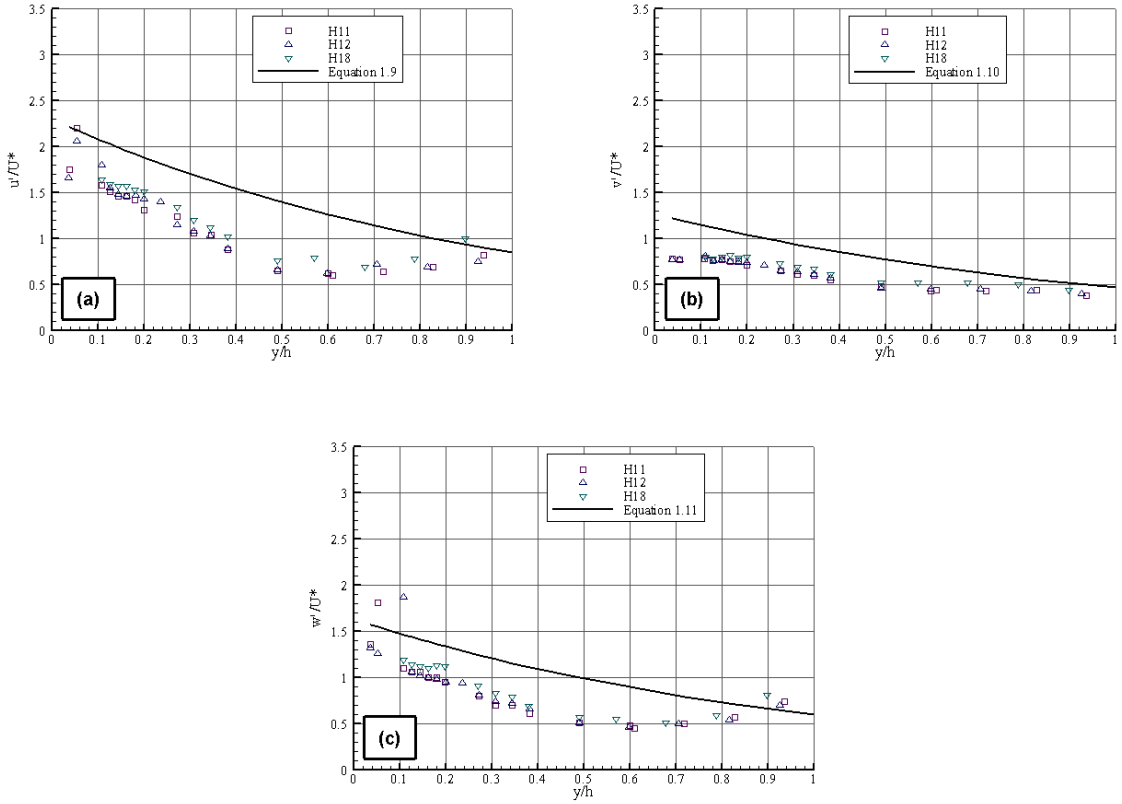

Figure 4.15 (a) Streamwise, (b) vertical and (c) spanwise turbulence intensities for test S00270_Q086

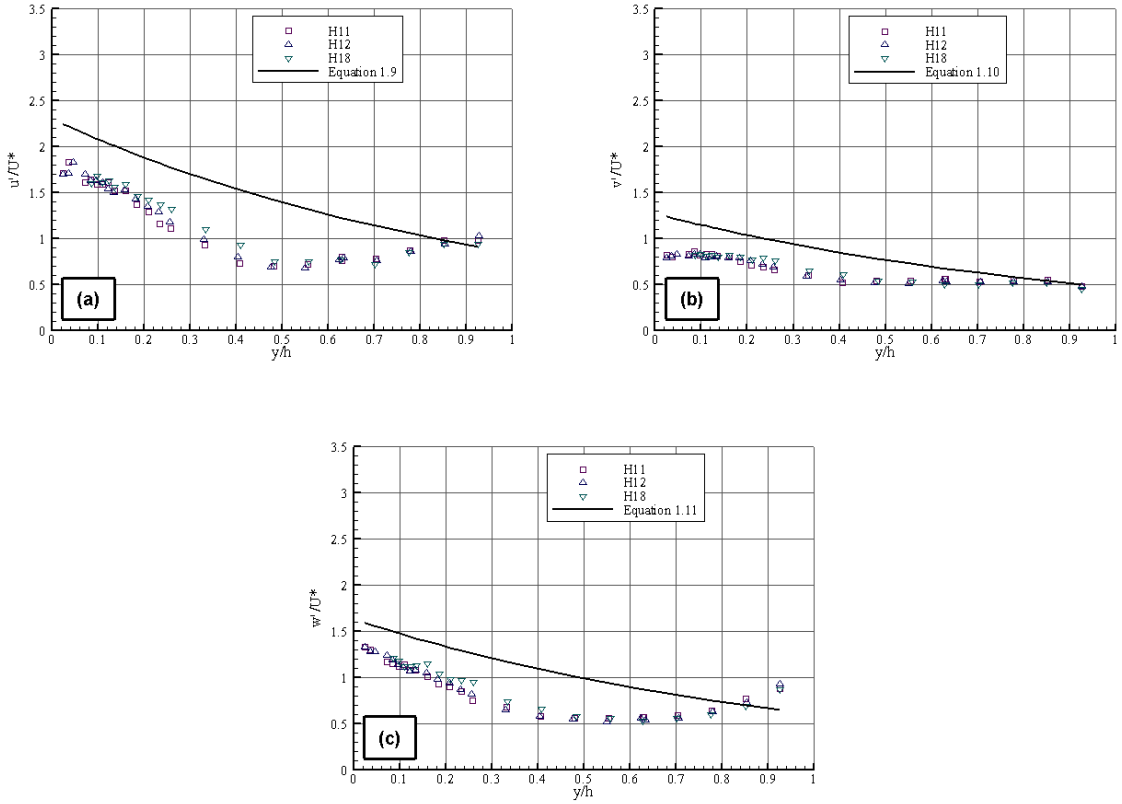

Figure 4.16 (a) Streamwise, (b) vertical and (c) spanwise turbulence intensities for test S00270_Q175

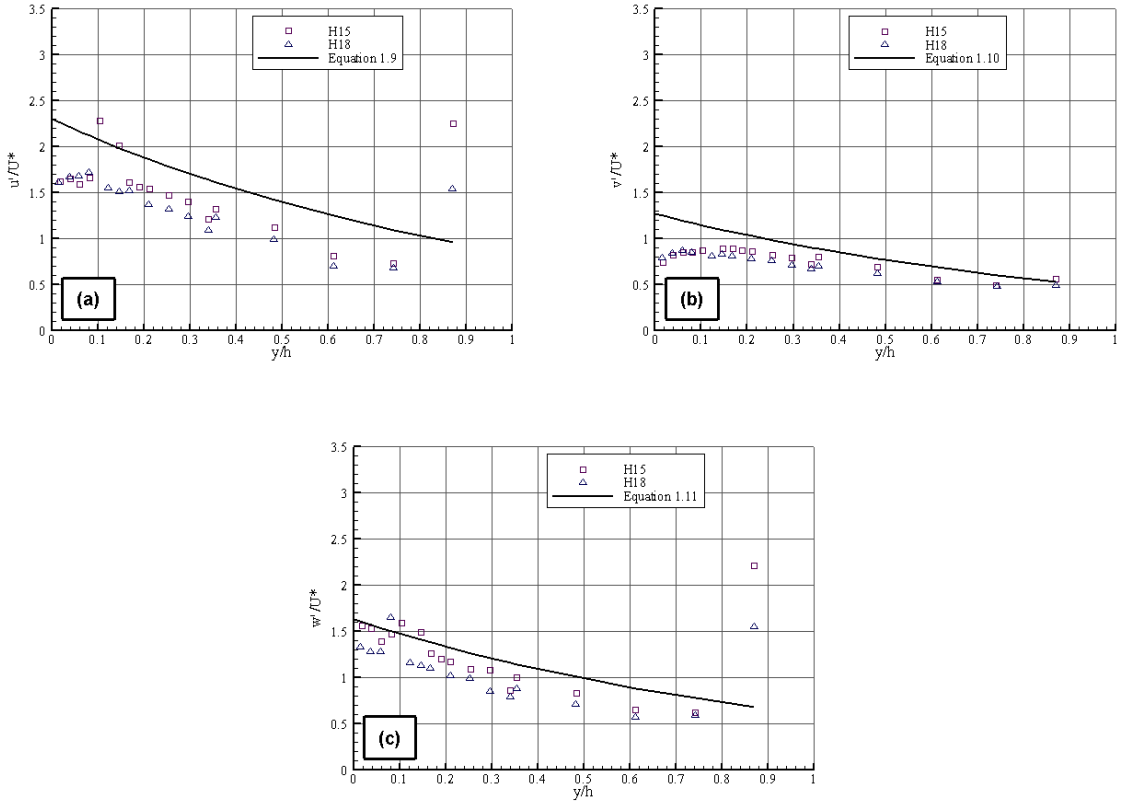

Figure 4.17 (a) Streamwise, (b) vertical and (c) spanwise turbulence intensities for test S00270_Q086_R10

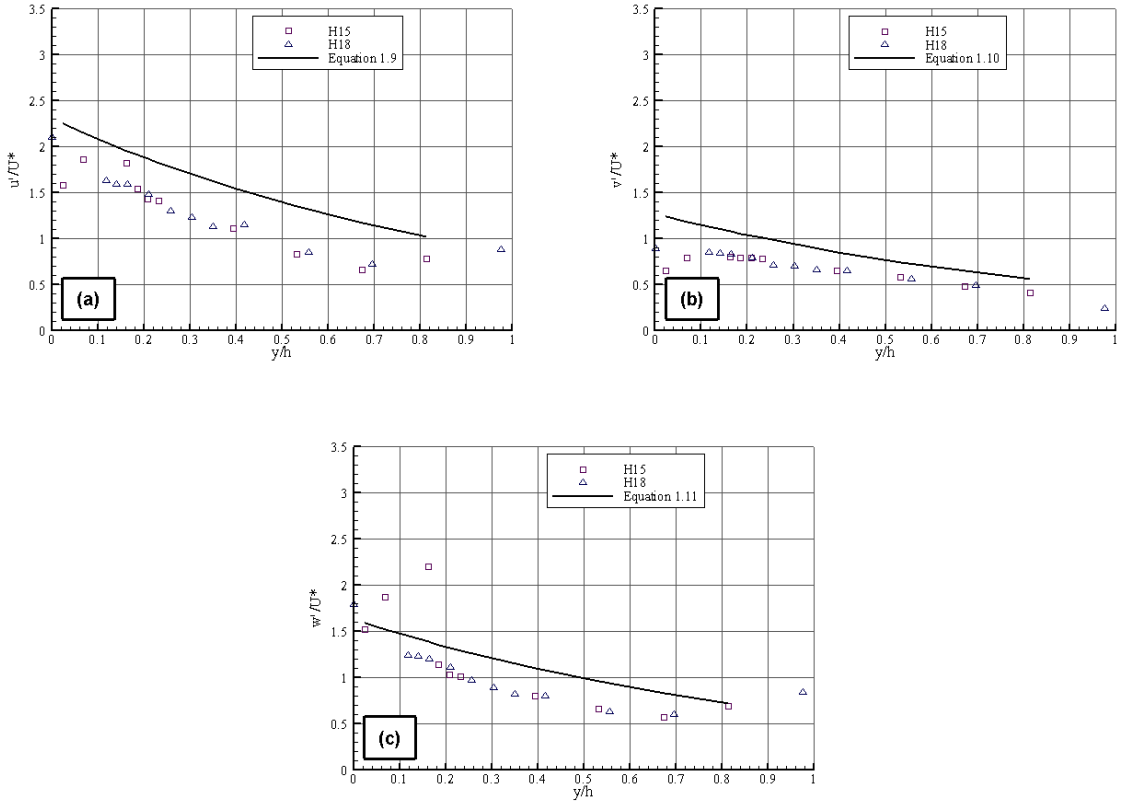

Figure 4.18 (a) Streamwise, (b) vertical and (c) spanwise turbulence intensities for test S00270_Q086_R18

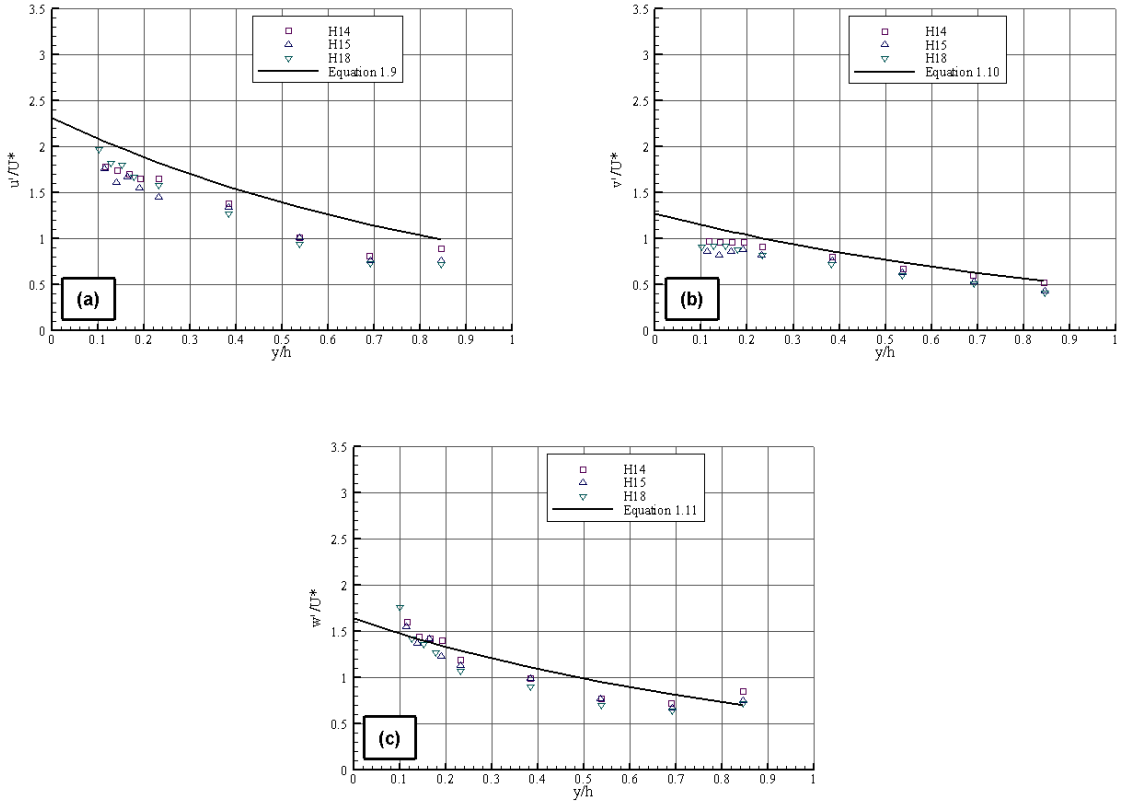

Figure 4.19 (a) Streamwise, (b) vertical and (c) spanwise turbulence intensities for test S00270_Q086_R28

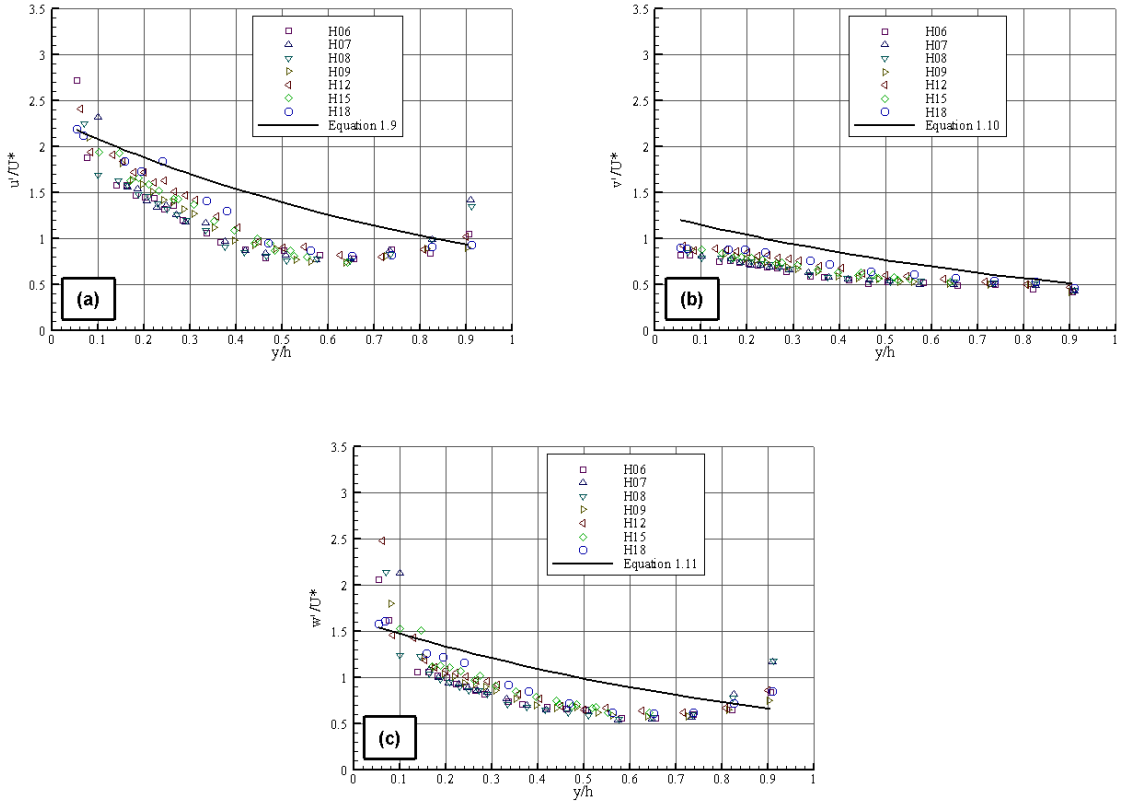

Figure 4.20 (a) Streamwise, (b) vertical and (c) spanwise turbulence intensities for test S00488_Q086

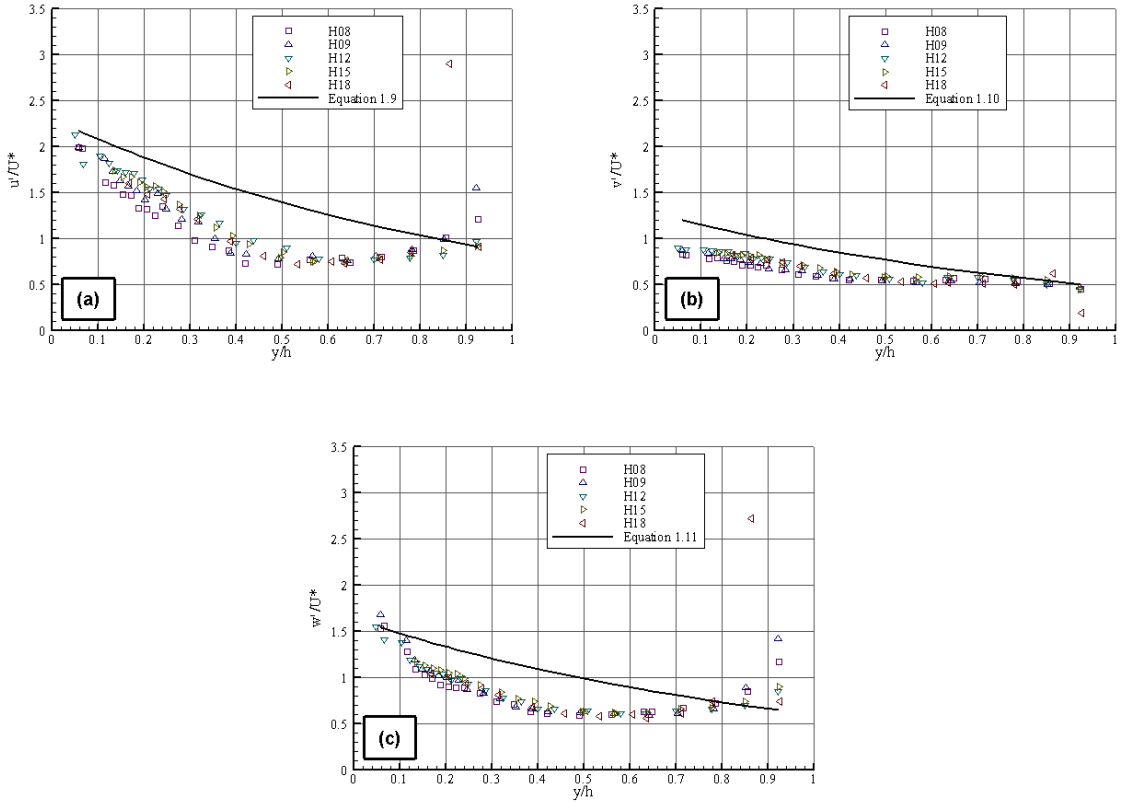

Figure 4.21 (a) Streamwise, (b) vertical and (c) spanwise turbulence intensities for test S00488_Q130

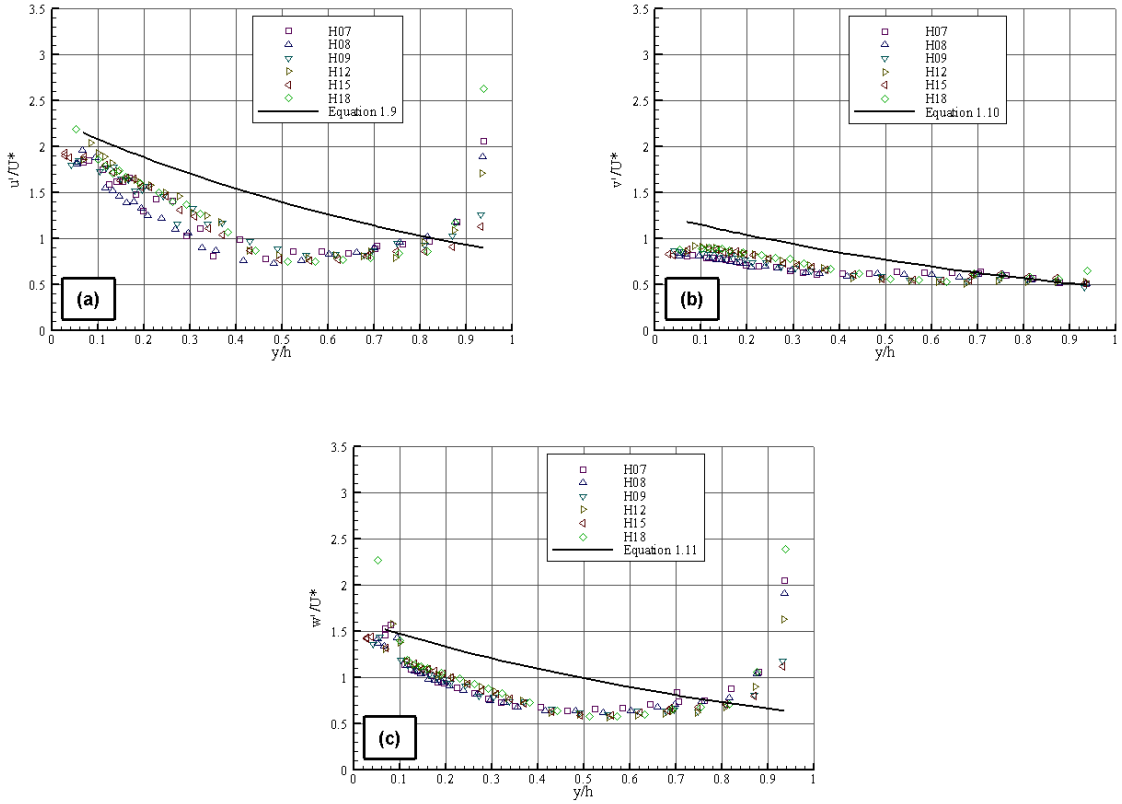

Figure 4.22 (a) Streamwise, (b) vertical and (c) spanwise turbulence intensities for test S00488_Q175

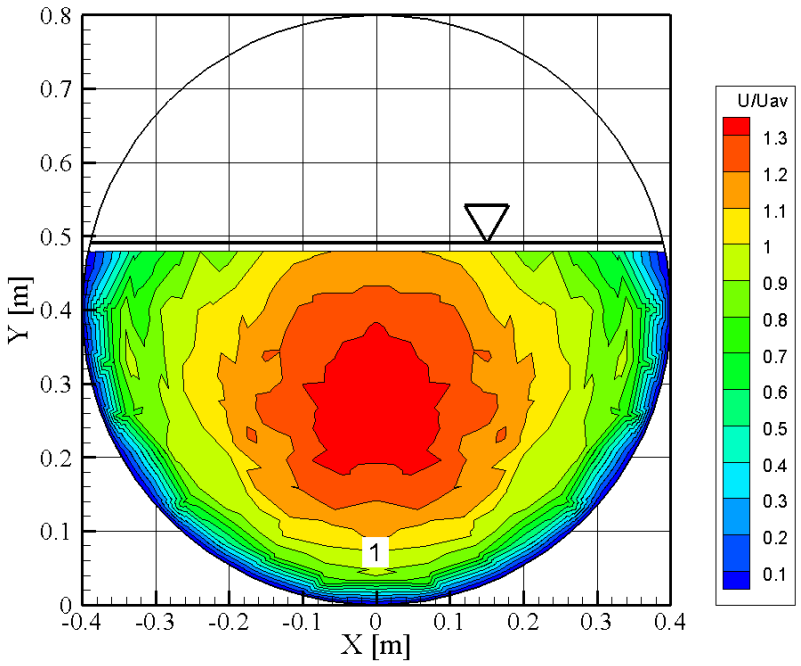

Figure 4.23 Normalized 2D velocity distribution for test S00028_Q086_H18

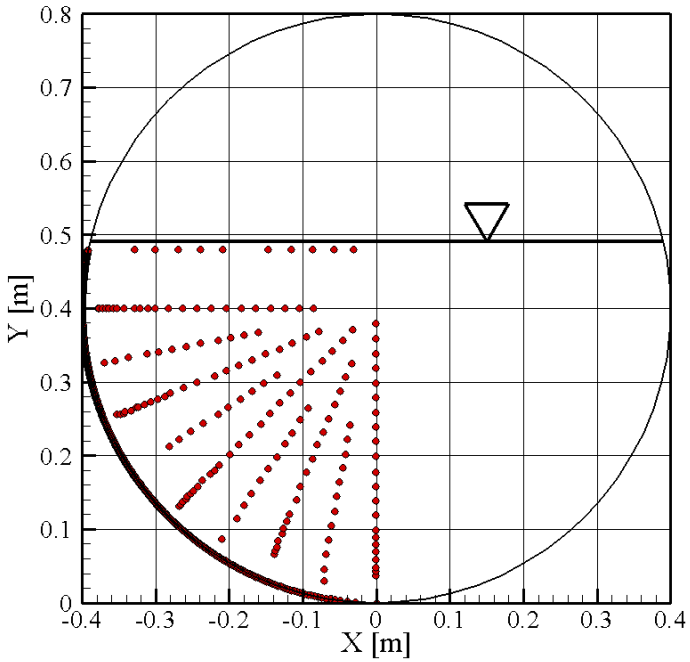

Figure 4.24 2D point velocity locations for test S00028_Q086_H18

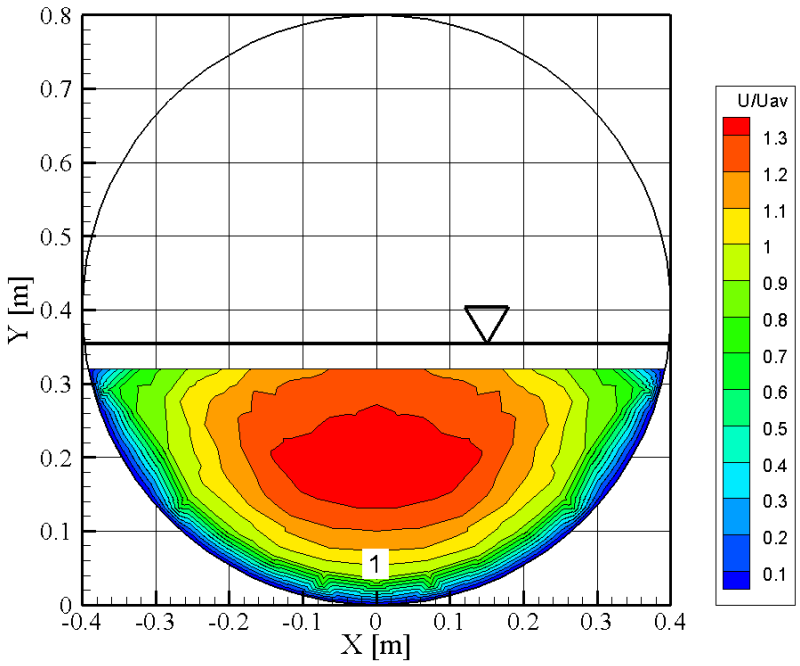

Figure 4.25 Normalized 2D velocity distribution for test S00110_Q086_H18

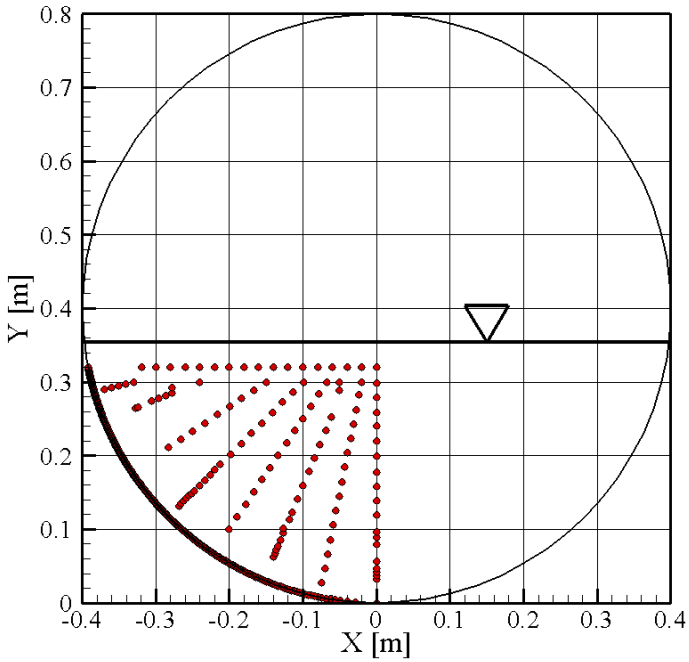

Figure 4.26 2D point velocity locations for test S00110_Q086_H18

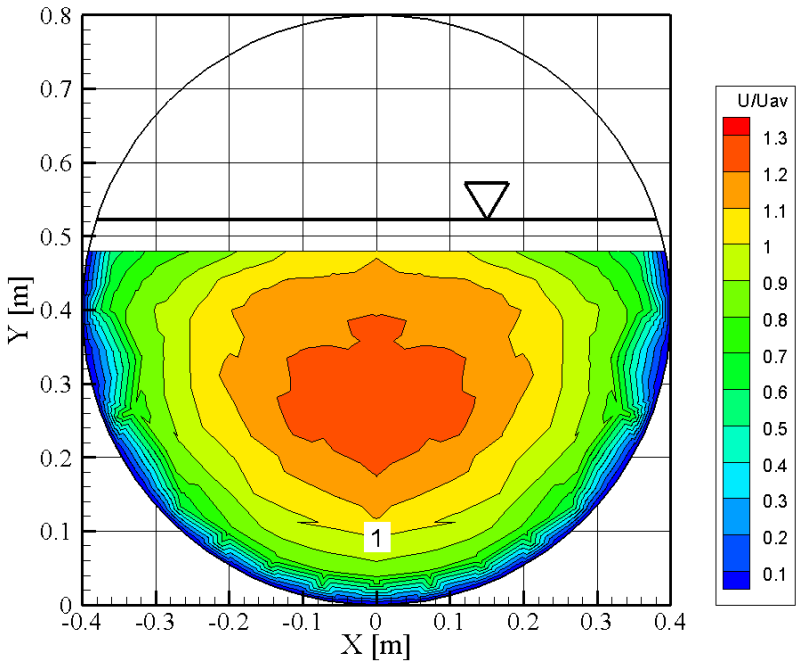

Figure 4.27 Normalized 2D velocity distribution for test S00110_Q175_H18

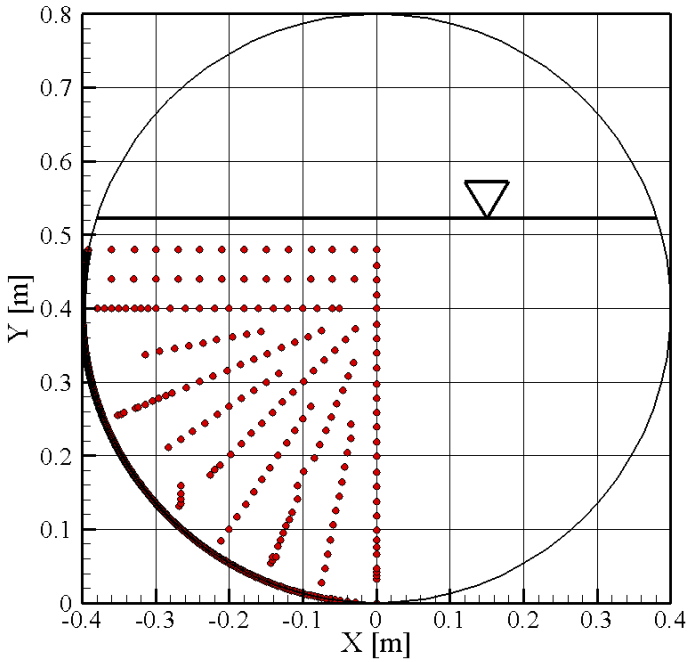

Figure 4.28 2D point velocity locations for test S00110_Q175_H18

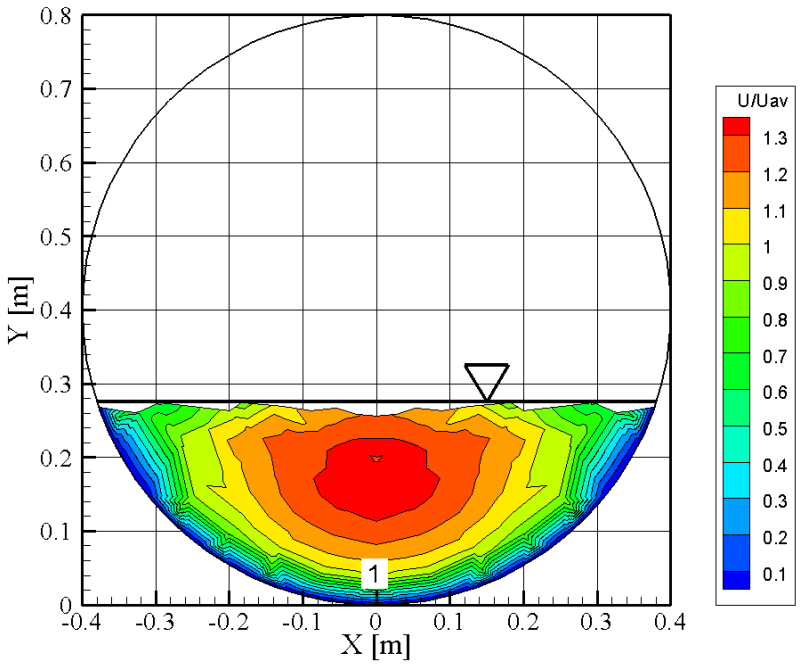

Figure 4.29 Normalized 2D velocity distribution for test S00270_Q086_H18

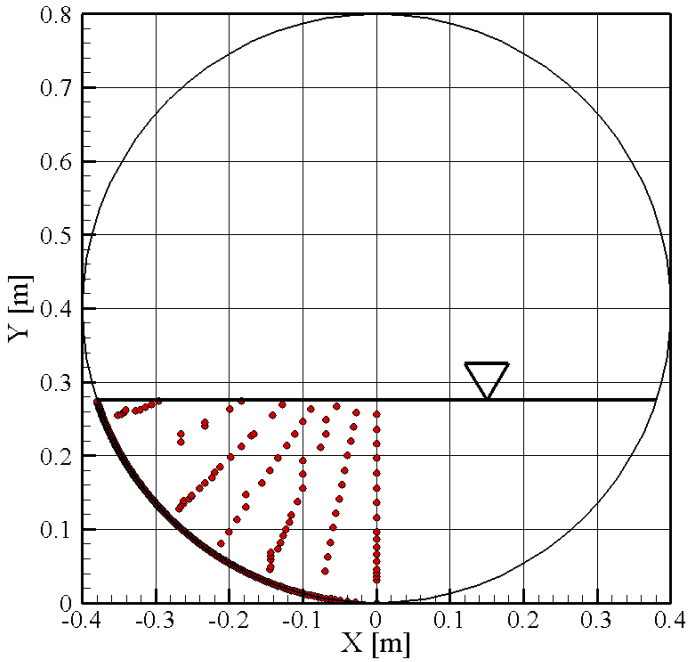

Figure 4.30 2D point velocity locations for test S00270_Q086_H18

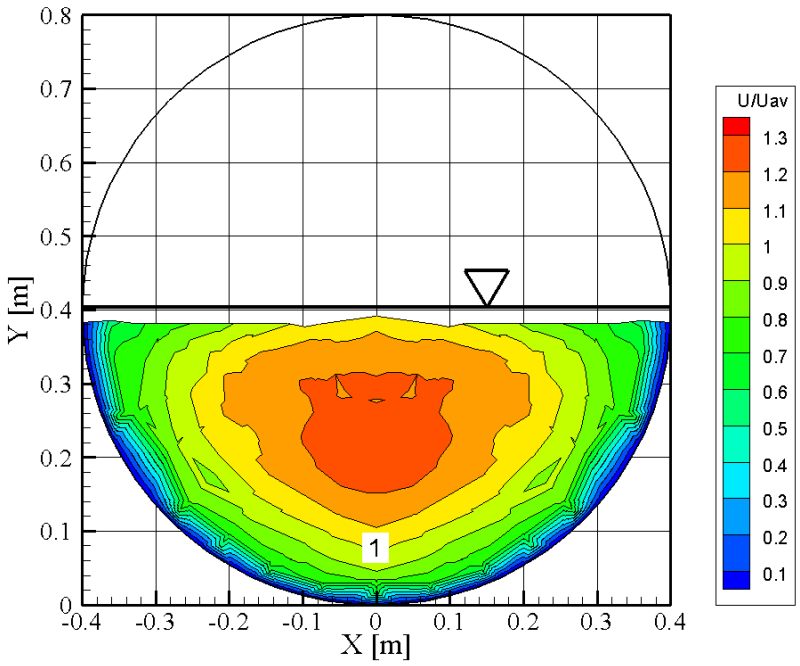

Figure 4.31 Normalized 2D velocity distribution for test S00270_Q175_H18

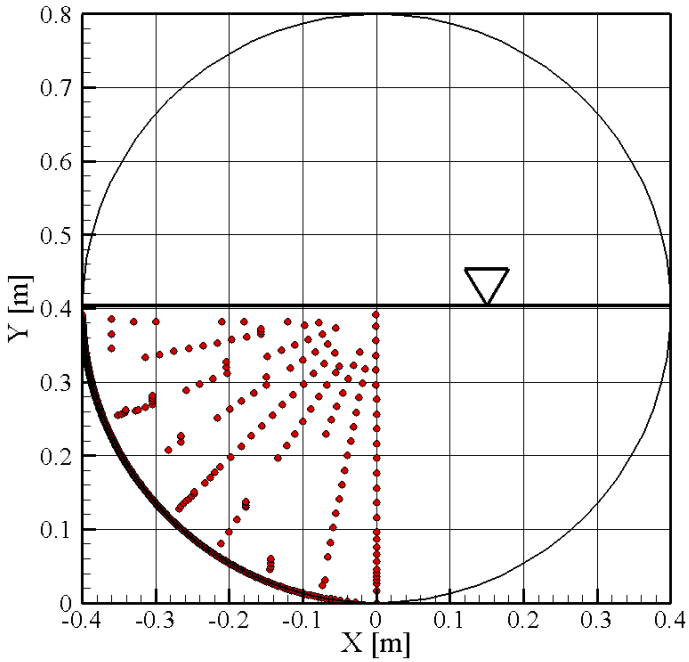

Figure 4.32 2D point velocity locations for test S00270_Q175_H18

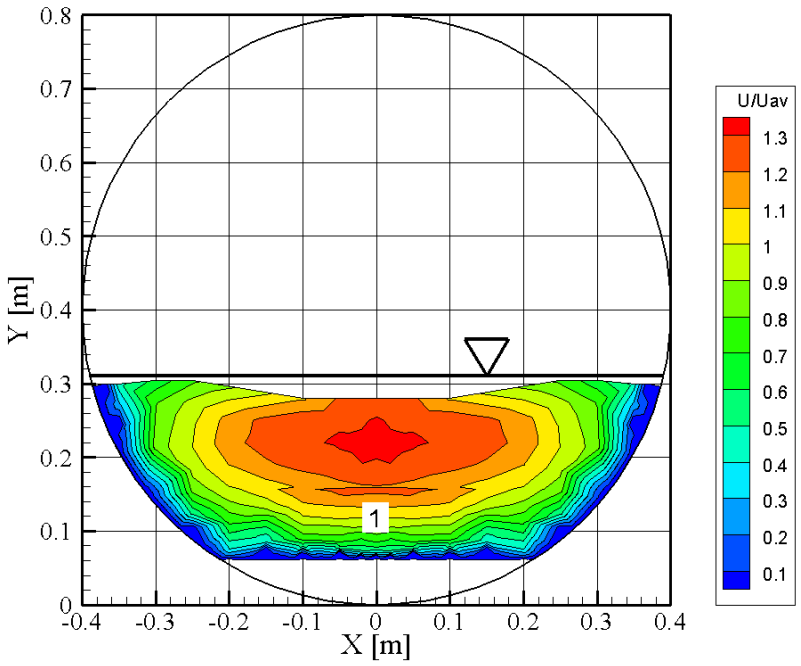

Figure 4.33 Normalized 2D velocity distribution for test S00270_Q086_R10_H18

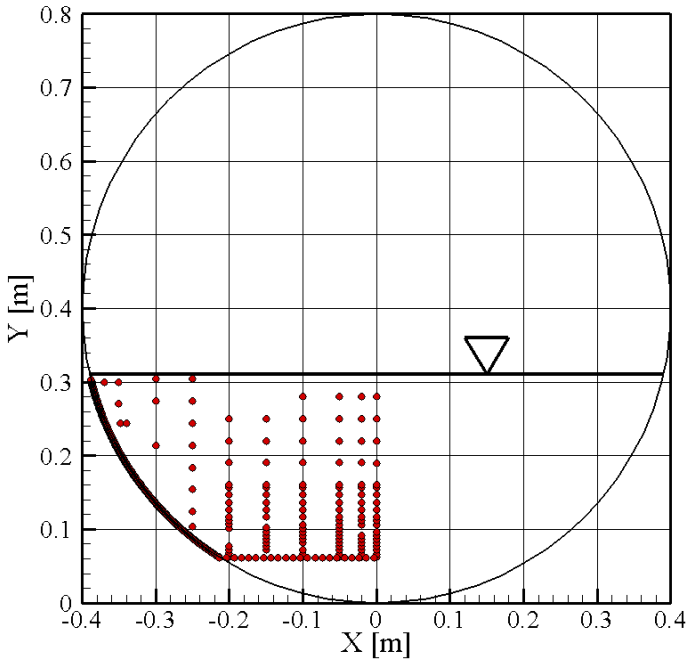

Figure 4.34 2D point velocity locations for test S00270_Q086_R10_H18

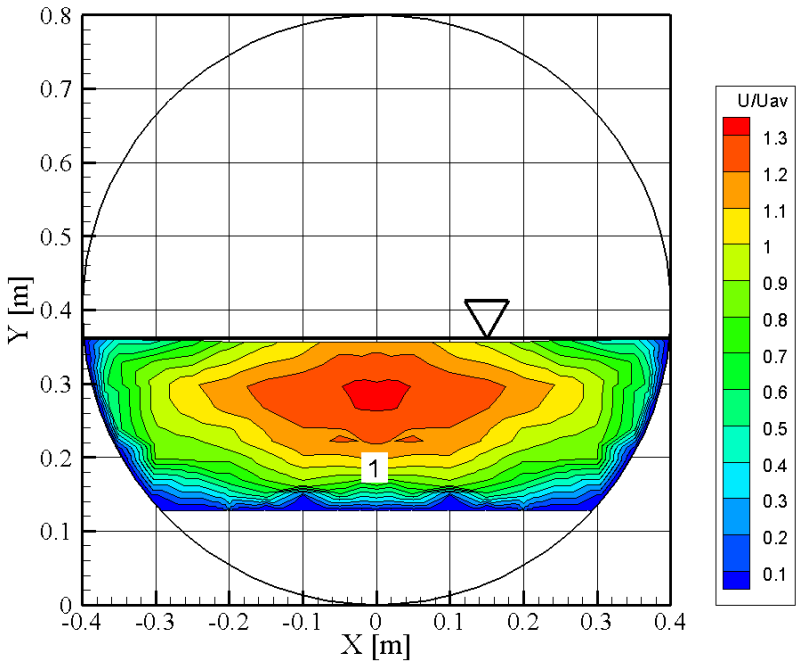

Figure 4.35 Normalized 2D velocity distribution for test S00270_Q086_R18_H18

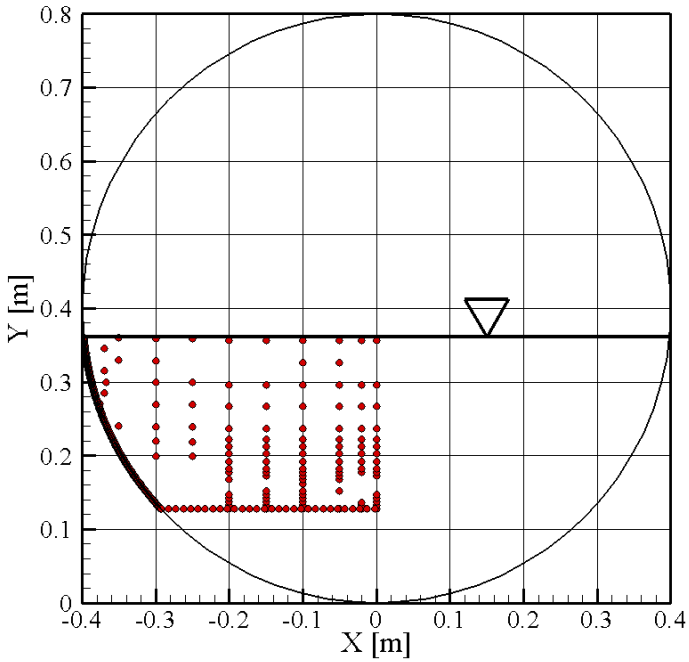

Figure 4.36 2D point velocity locations for test S00270_Q086_R18_H18

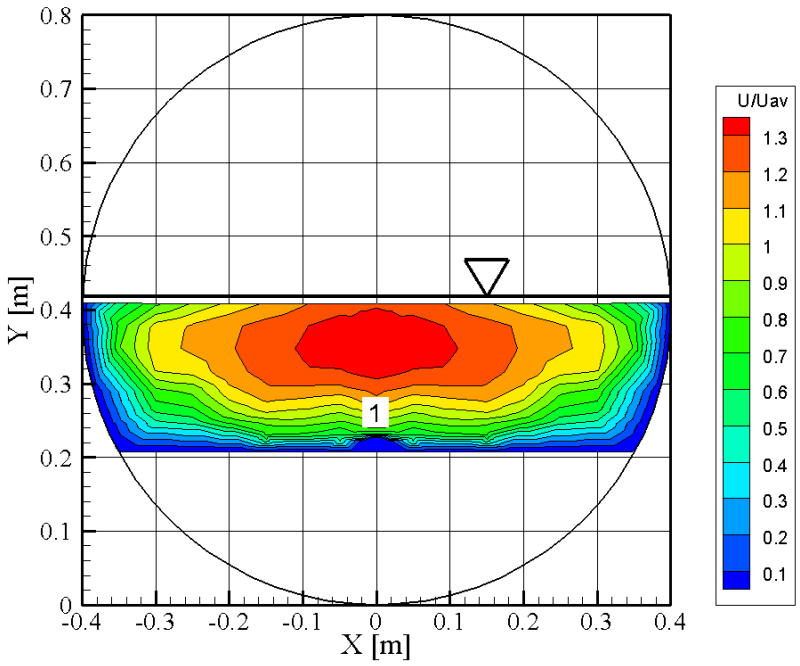

Figure 4.37 Normalized 2D velocity distribution for test S00270_Q086_R28_H18

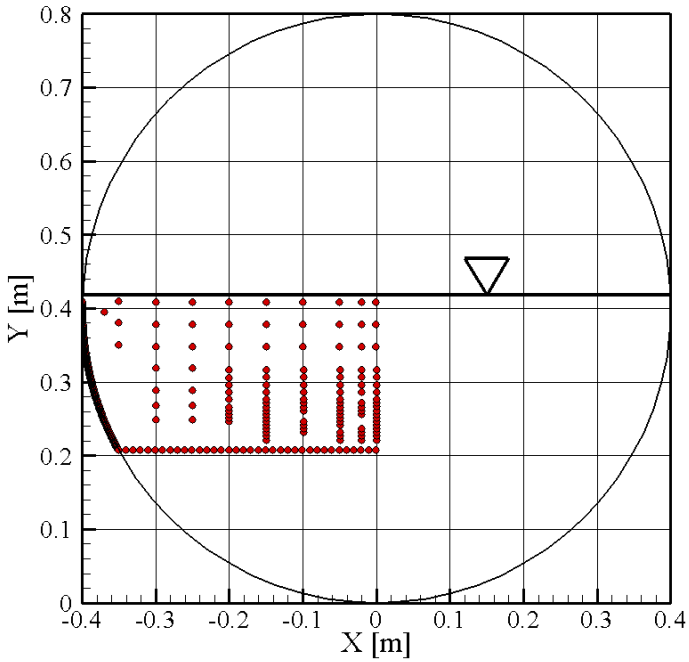

Figure 4.38 2D point velocity locations for test S00270_Q086_R28_H18

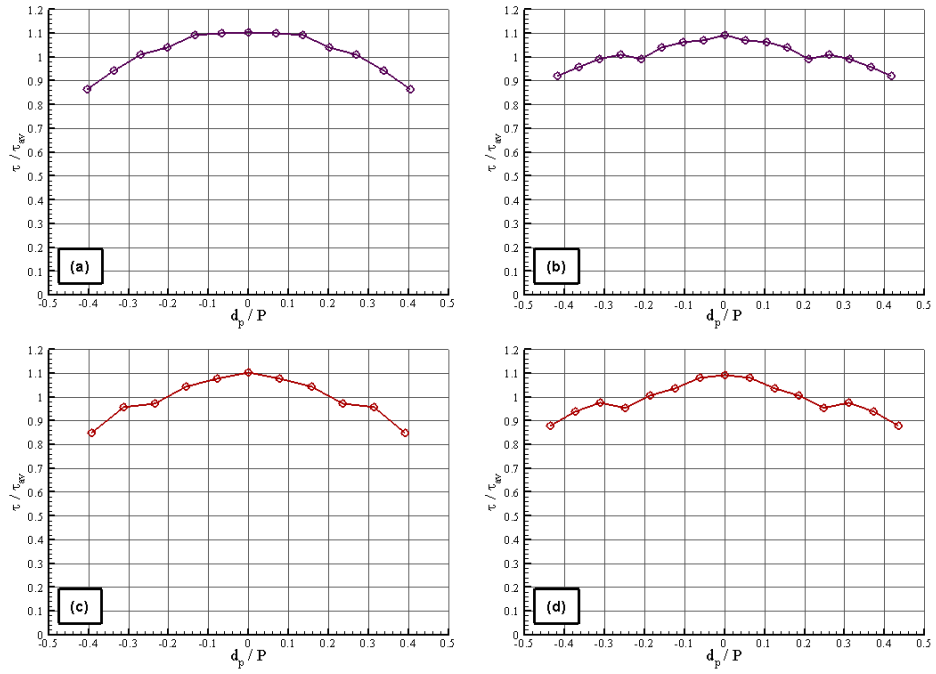

Figure 4.39 Shear distribution for tests (a) S00110_Q086, (b) S00110_Q175, (c) S00270_Q086, and (d) S00270_Q175

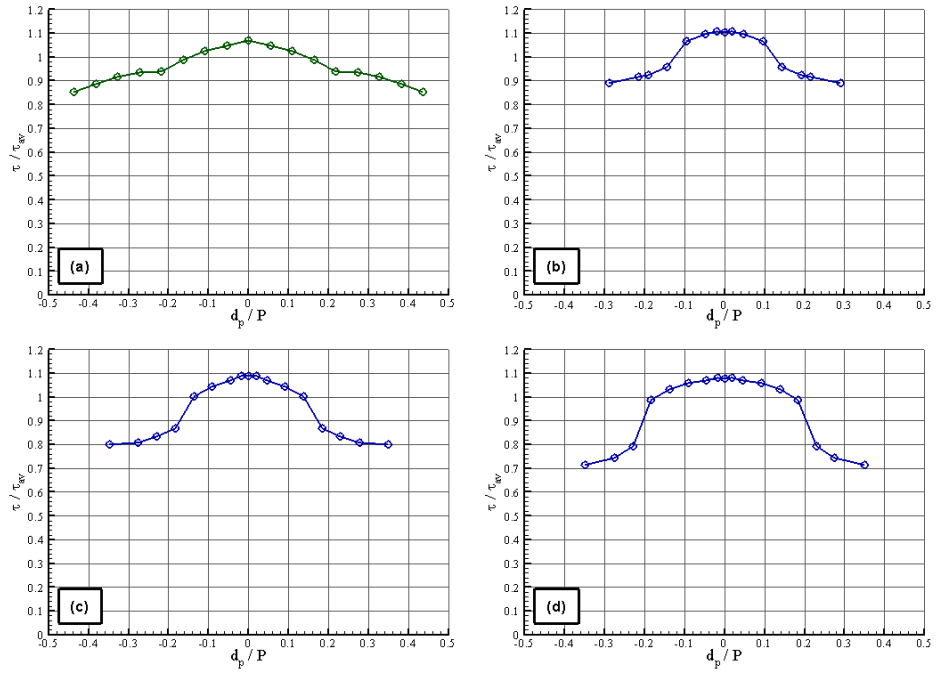

Figure 4.40 Shear distribution for tests (a) S00028_Q086, (b) S00270_Q086_R10, (c) S00270_Q086_R18, and (d) S00270_Q086_R28

CHAPTER 5 *Empirical Equations*

5.1 Turbulence Intensity

Since the culvert data exhibited a very consistent distribution from one test to another it is clear that within circular pipes the vertical distribution of turbulence intensity follows a different distribution than wide open channels. In order to evaluate this, data from the developed region of each test without gravel embedment was gathered together. Several different best fit equations were applied to the data. Since the turbulence intensity increased as it approaches the surface, it was not likely that the distribution follows an exponential decay for circular geometry as it does for a rectangular geometry. The only type of curve that presented a reasonable approximation was a second order polynomial. Since the data included multiple outliers which would skew the result, they were removed prior to fitting a curve. As a result the following equations were produced.

$$u'/_{U_*} = 3.74\left(y/_h\right)^2 - 4.70\left(y/_h\right) + 2.30 \quad (5.1)$$

$$v'/_{U_*} = 0.53\left(y/_h\right)^2 - 0.93\left(y/_h\right) + 0.95 \quad (5.2)$$

$$w'/_{U_*} = 2.93\left(y/_h\right)^2 - 3.44\left(y/_h\right) + 1.63 \quad (5.3)$$

A point of note on the above mentioned equations is that for Equations 5.1 and 5.3 the *y*-intercept was found to be similar to that of Equations 1.9 and 1.11 and was therefore set to be equal. In addition, since the turbulence intensity should be equal to zero directly at the boundary, these equations are not valid all the way to the wall. Equations 5.1 to 5.3 are a statistically best-fit to the data with a set *y*-intercept. The three equations provided a satisfactory representation, with R^2 values of 0.86, 0.75, and 0.82 respectively. The compilation of all developed-region turbulence intensity measurements and the fitted curves can be seen in Figure 5.1. More work should be done to verify that these approximates are applicable for other circular cross sections.

These equations show that above the inflection points, as the turbulence intensity increases toward the surface, there should be a decrease in water velocity. This completely agrees with the observed streamwise velocity plots where the velocity is seen to decrease toward the surface. With Equations 5.1 to 5.3 describing the turbulence intensity in a circular channel and Equations 1.9 to 1.11 describing the turbulence intensity in a rectangular channel, a reasonable prediction could be made between the two for varying depths of gravel.

5.2 Two Dimensional Cross Sections

5.2.1 Equation Development

As outlined in Chapter 1, Ead *et al*. (2000) developed a set of equations that described the two dimensional velocity distributions within a circular culvert. Equations 1.12 and 1.13 modify the log law equation, enabling it to be representative of the entire flow depth. With the use of several modification equations that are a function of the spanwise distance away from the centerline, the modified log law equation can be applied over the entire cross section.

Although an extremely useful tool, the equations did not provide an acceptable fit to the data from this study. In particular, the profile described by Equations 1.12 and 1.13 do not have the distinctive velocity dip near the water surface. It is possible that because Ead *et al.* (2000) used much higher slopes for their tests, the resulting velocity profile had a substantially different shape. Since this is a large portion of the velocity profile it was decided that modification may be needed in order to produce a more desirable result.

Since the method to be developed is meant to be used as a tool for approximating the two dimensional velocity profiles at the design phase of a culvert installation, it is important that all parameters can be either assumed or calculated based on the available data. The first approximation to be used is the value of friction velocity. From Chapter 4 it was determined that the friction velocity at the culvert centerline can be approximated as 1.1

times the average friction velocity. This provided means to calculate the friction velocity from easily accessible geometric parameters. Only defining the friction velocity along the centerline is insufficient since it must be defined along the entire cross section. In order to achieve this, the shear stress distribution profiles from section 4.7 were superimposed and a best fit polynomial was fit to them. The data from the gravel embedment tests were not included in this since they had a very different distribution. Although not attempted here, it would be expected that similar work would lead to equivalent equations applicable to embedded culverts. In order to get these profiles to work well with our previous findings, the friction velocity along the centerline was set equal to 1.1 times the average friction velocity. Therefore the distribution of the shear stress normalized by average shear stress follows Equation 5.4 and can be seen in Figure 5.2.

$$\frac{\tau}{\tau_{av}} = \frac{U_*}{U_{*av}} = -1.39\left(\frac{d_p}{P}\right)^2 + 1.10 \tag{5.4}$$

where d_p is the distance along the wetted perimeter from the centerline towards the water surface.

The next parameter needed is the equivalent roughness height. Ead *et al*. (2000) found that this value should be equal to the actual height of the culvert corrugation. From averaging the fitted values of k for our data set, it was determined that, with variation, the average equivalent roughness height was 0.0123 m, roughly 0.95 times the corrugation height. It is therefore suggested that the equivalent roughness height should be defined according to Equation 5.5 for non embedded tests.

$$k = 0.95\ (corrugation\ height) \tag{5.5}$$

With the two calculated values, U_* and k, Equation 1.7 can be solved for the roughness shift ΔB. Lastly, the log law equation requires modification such that it is representative of the entire profile, not just the boundary layer. Similar to the process used by Ead *et al*. (2000), an additional term is added to the log law equation to reduce the velocity above the boundary region by a given amount, dependent on the height above the boundary region. The equations are stated as follows.

$$U^+ = \frac{1}{\kappa}\ln Y^+ + A_0 - \Delta B$$

$$Y^+ < 0.36\ H^+ \tag{5.6}$$

$$U^+ = \frac{1}{\kappa}\ln Y^+ + A_0 - \Delta B - 3.70\left(1 - 2\frac{d_p}{P}\right)\left[\frac{(Y^+ - 0.36H^+)}{(0.64\ H^+)}\right]^{1.38}$$

$$Y^+ \geq 0.36\ H^+ \tag{5.7}$$

where H^+ is the distance from the boundary to the water surface normalized by $\underline{\nu}/U_*$. It can also be seen in Equation 5.7 that the adjustment to the log law equation decreases along the wetted perimeter as well. It is adjusted such that the full velocity dip is felt along the centerline of the culvert, and at the water surface there is no adjustment to the log law.

5.2.2 Equation Application

The benefit of the equations developed by Ead *et al*. (2000) is that the calculations of the velocity at a point are a function of the vertical and horizontal position of that point. This makes the calculations simple by constructing a grid of points and performing a few quick calculations for each point. Although more simple to apply, the equations produced by Ead *et al*. (2000) were not able to adequately represent several key points of the cross sections, such as the velocity dip near the water surface, and varying shear stress along the culvert boundary. These key differences, potentially caused by the different slopes used in their experiments, lead to notably different results.

By using the above equations as they were developed, from the center to the radius of the culvert, it presents continuity problems when trying to model depths above the center of the culvert. In order to resolve this issue the cross section is modeled along radials from the center of the water surface to the culvert boundary. By using this technique to model the circular cross section it results in the calculated velocity profiles acting on an angle not always perpendicular to the culvert boundary. Since the angle of the profiles to the boundary is only extreme for very deep or shallow depths, it is assumed that the log law is adequately valid.

The steps used to model the various flow conditions used in the physical model study were as follows. First, an array of evenly distributed *x-y* point locations was created to provide enough data points to create a smooth contour. Then for each point location, the angle from vertical, about the center of the water surface was calculated using

trigonometry. Figure 5.3 shows an example of the orientation of the profiles and several of the respective parameters. Next, once again using trig and the angle already calculated, the relative distance along the wetted perimeter (d_p/P) that the profile starts from was calculated. This in turn was used to calculate the friction velocity (U_*) for the respective profile according to Equation 5.4. Since the equivalent roughness height (k) is already assumed to be equal to 0.95 times the corrugation height, a value of the roughness shift (ΔB) was added. Lastly, at each point, the distance from the boundary to the water surface (H^+) and the distance from the boundary to the point (Y^+) were calculated and normalized by ν/U_*. With this set of parameters there was enough information to begin calculating the point velocity.

This brings to light the increased complexity of this method when being compared to that of Ead *et al*. (2000). Ead's method required only the calculation of several parameters, all a function of the relative horizontal distance. Although the method proposed in this thesis is more complicated, it is still possible to model in EXCEL or in some other package such as MATLAB. For the results presented in this paper, the values were calculated in EXCEL and plotted in TecPlot, but a much faster method would have been to use MATLAB.

After having calculated all of the above mentioned parameters, the last step was to input the parameters at each x-y location into Equations 5.6 and 5.7. Then by multiplying by the friction velocity at the given point location, the resulting streamwise point velocity was obtained. This concluded the calculation process and the results can be used however

needed. The results of both the Ead *et al*. (2000) equations and the equations developed in this thesis can be seen in Figures 5.4 through 5.13 for several test conditions used in the physical modeling.

By visual comparison, the equations developed in this thesis provide a much more appropriate fit to the data. Of particular interest, the distribution of shear stress along the wetted perimeter, and the depressed maximum velocity are represented quite well. One interesting feature is the apparent notch in the contours along the centerline near the water surface. This was a result of all the profiles ending at one particular point and not all approaching the exact velocity. It should be considered numerical noise and since it is observed where the average velocity is greater than one, it is outside the area of primary interest. It is most important to note the quality in the area less than average velocity where fish passage is expected to occur. This area is very well represented and clearly shows proper application of the shear stress distribution and the velocity dip.

In order to determine if the equations in fact produce a good representation of the data, several values were extracted for comparison. The first comparison was to perform the exact same technique to determine the percentage of the area below average velocity and below 0.75 times average velocity. By performing this on both the cross sections produced from Equations 5.6 and 5.7, as well as those from Ead *et al*. (2000), comparisons could be made between both sets of equations and the data. The results are seen in Tables 5.1 and 5.2.

Table 5.1 – Area below average velocity

Test Name	Data	Proposed	Ead *et al*. (2000)
-	Area<U_{av}	Area<U_{av}	Area<U_{av}
-	%	%	%
S00028_Q086	46.1	40.6	12.4
S00110_Q086	38.5	45.8	10.7
S00110_Q175	48.3	40.4	12.7
S00270_Q086	44.6	47.0	10.8
S00270_Q175	49.5	44.2	10.0

From Table 5.1 it becomes apparent that the proposed equations are conservative of the amount of area below average velocity, while the equations of Ead *et al*. (2000) strongly underestimate this area. When looking at 0.75 times the average velocity seen in Table 5.2, the proposed equation once again slightly under predicts very consistently, while the equations of Ead *et al*. (2000) underestimate the area considerably.

Table 5.2 – Area below 0.75 times average velocity

Test Name	Data	Proposed	Ead *et al*. (2000)
-	Area<0.75U_{av}	Area<0.75U_{av}	Area<0.75U_{av}
-	%	%	%
S00028_Q086	19.1	15.2	5.1
S00110_Q086	20.1	17.3	2.4
S00110_Q175	19.8	15.1	5.5
S00270_Q086	25.4	18.2	2.6
S00270_Q175	19.5	16.7	2.5

In order to determine how the equations balance across the entire section, the point velocities were integrated to determine what the integrated discharge was. For the equations to properly balance over the entire section it should be expected that the integrated discharge be very close to the actual discharge that was used to produce the data set. In Table 5.3 it becomes clear that the proposed equations are balanced since the integrated discharge is within 5% for all tests except S00270_Q086 which was 8.1% off.

The Ead *et al*. (2000) equations result in a higher than expected integrated discharge where the results were consistently greater than 25% off.

After having reviewed both the relative areas and the integrated discharge values, there is a strong indication that the proposed equations appropriately represent the data. Coupled with the visual comparison between the predicted cross sectional velocity distribution and the actual data, it appears that the proposed equations work sufficiently well for modeling the two dimensional streamwise velocity distributions in the fully developed region of corrugated metal pipe culverts over the range of conditions tested in this study.

Table 5.3 – Cross section integrated discharge

Test Name	**Actual**	**Proposed**	**Ead *et al*. (2000)**
-	**Q**	**Q**	**Q**
-	**m^3/s**	**m^3/s**	**m^3/s**
S00028_Q086	0.086	0.086	0.109
S00110_Q086	0.086	0.082	0.109
S00110_Q175	0.175	0.176	0.221
S00270_Q086	0.086	0.079	0.108
S00270_Q175	0.175	0.168	0.223

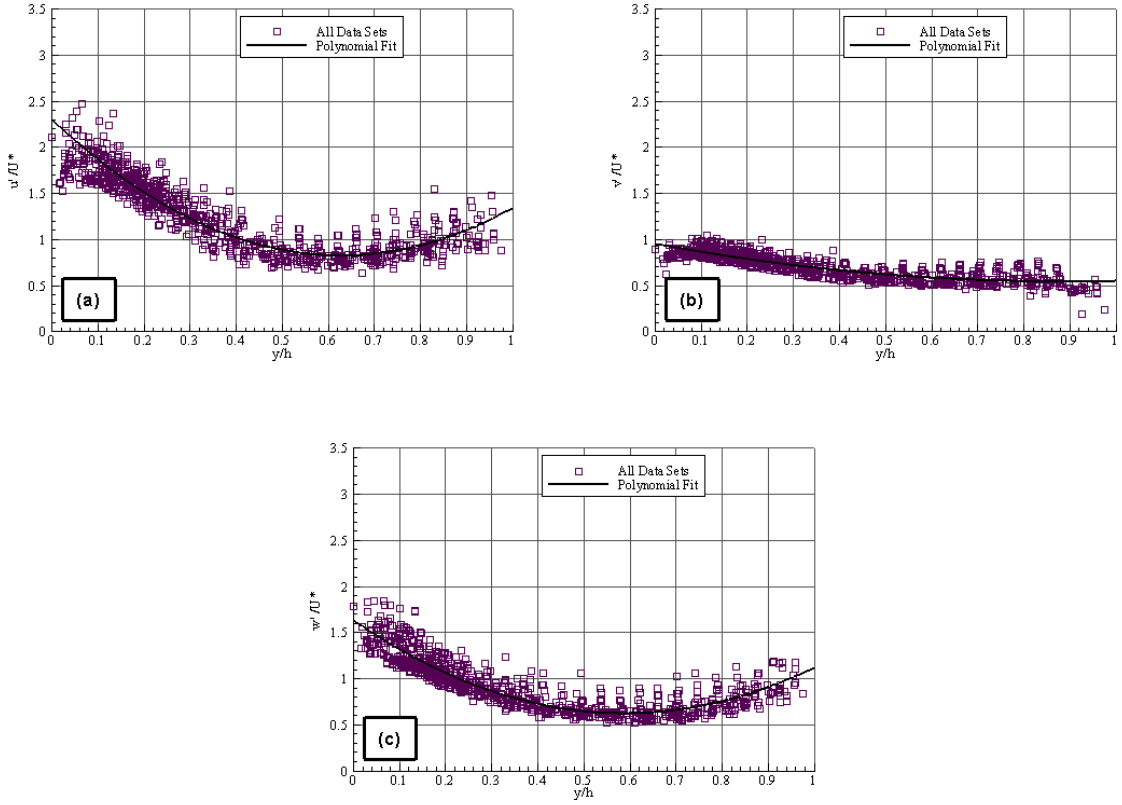

Figure 5.1 (a) Streamwise, (b) vertical and (c) spanwise turbulence intensities for developed sections of all non gravel embedment tests

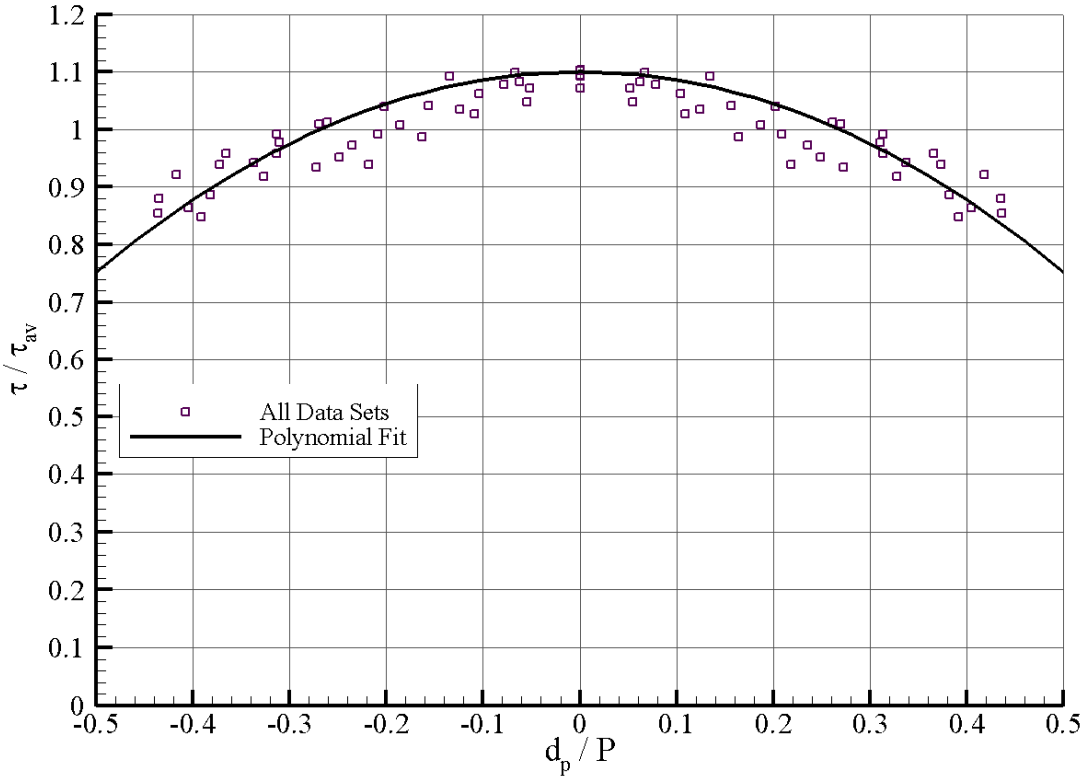

Figure 5.2 Shear distribution for all non gravel embedment tests and polynomial fit

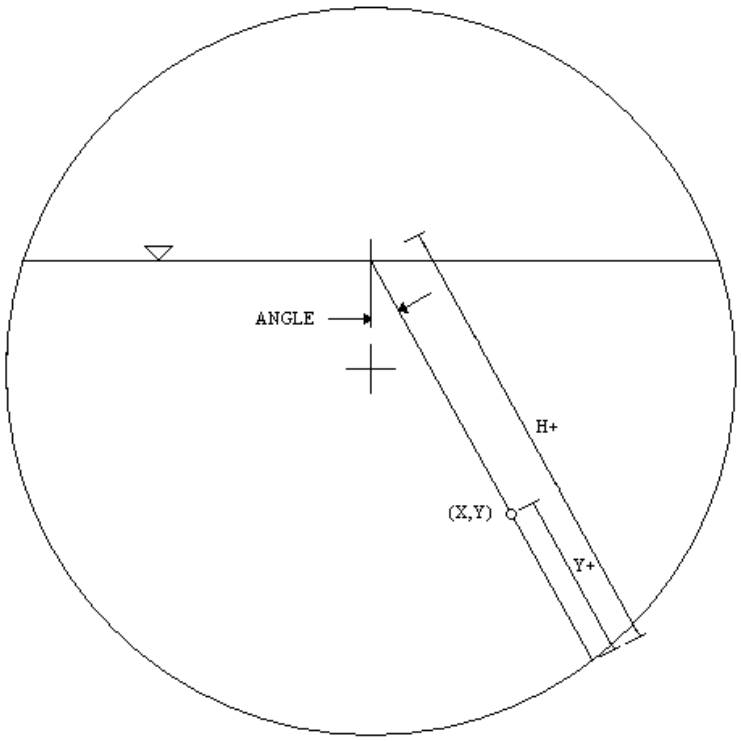

Figure 5.3 Orientation of the variation parameters for cross sectional modeling

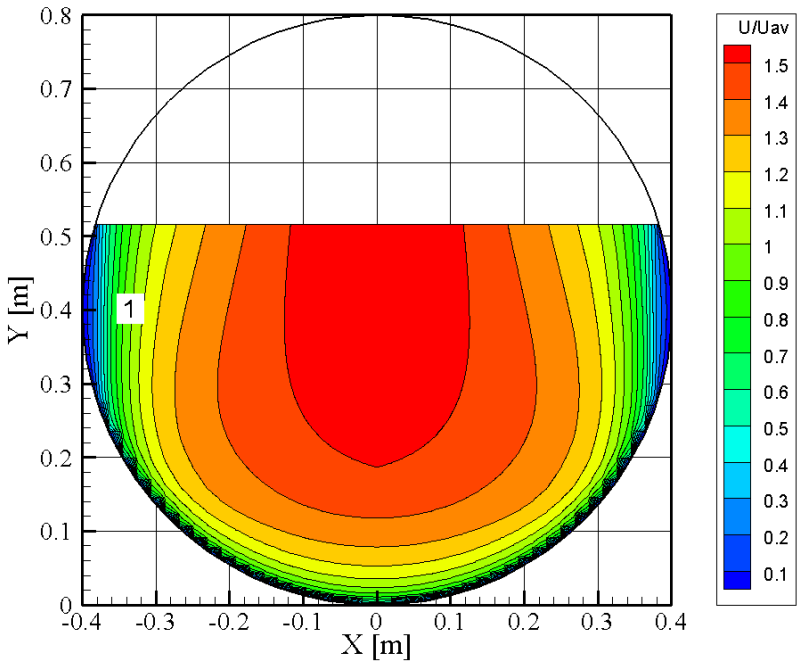

Figure 5.4 Normalized Ead *et al*. (2000) predicted 2D velocity distribution for test S00028_Q086

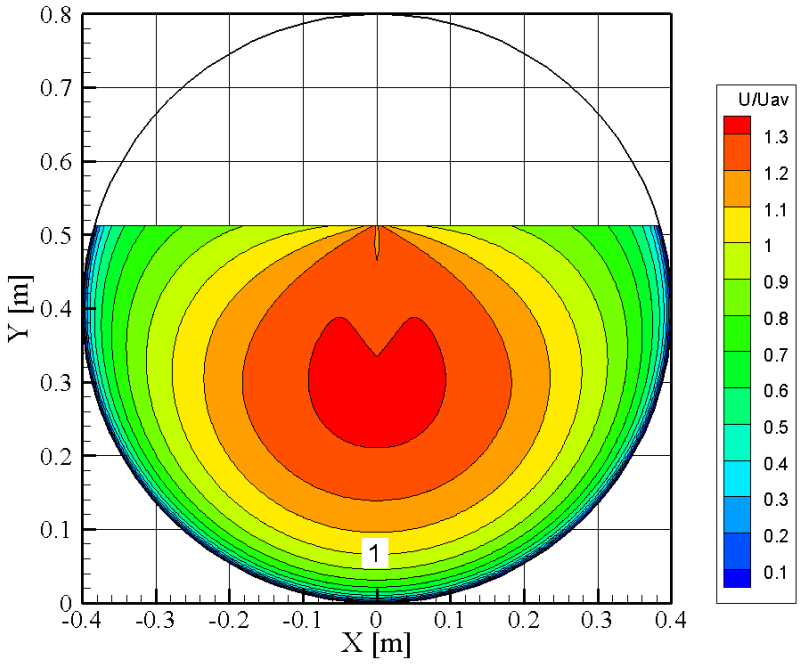

Figure 5.5 Normalized 2D predicted velocity distribution for test S00028_Q086

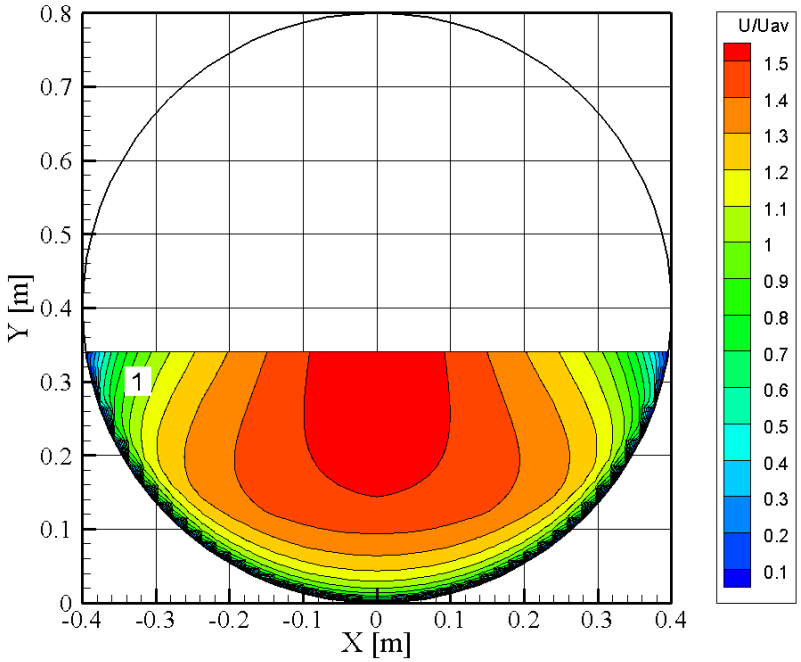

Figure 5.6 Normalized Ead *et al*. (2000) predicted 2D velocity distribution for test S00110_Q086

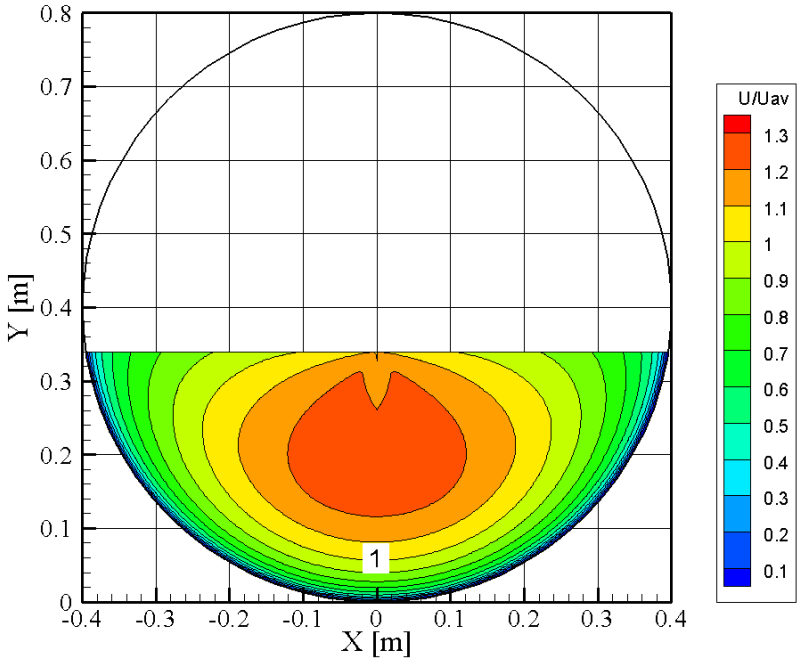

Figure 5.7 Normalized predicted 2D velocity distribution for test S00110_Q086

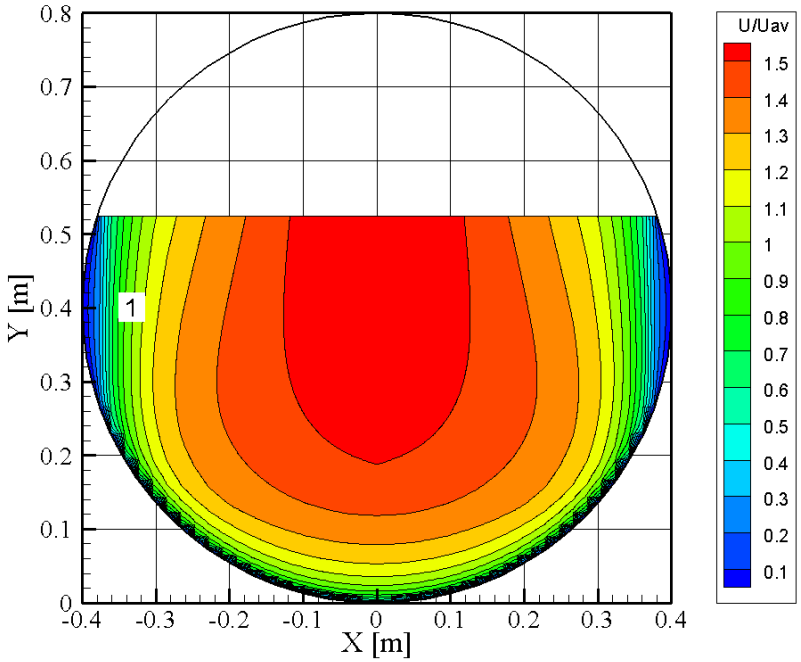

Figure 5.8 Normalized Ead *et al*. (2000) predicted 2D velocity distribution for test S00110_Q175

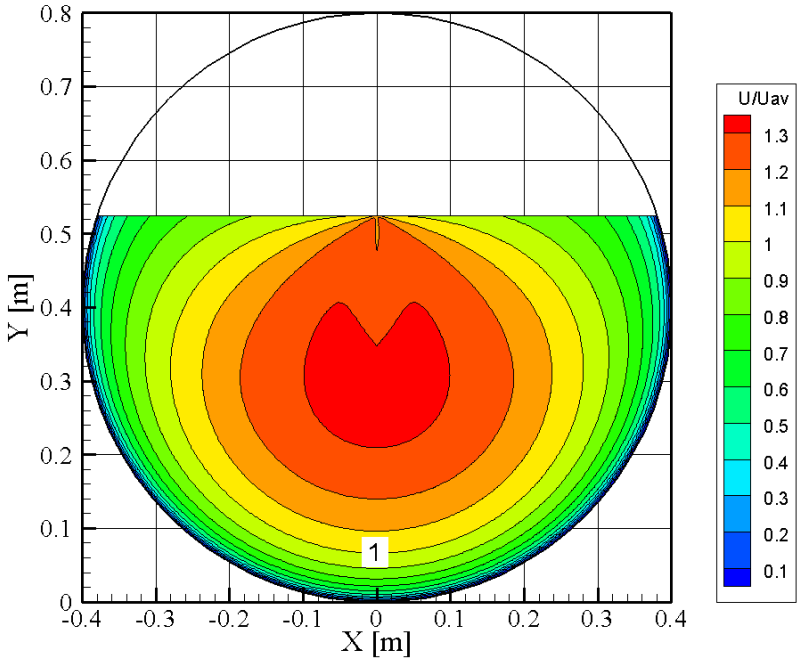

Figure 5.9 Normalized predicted 2D velocity distribution for test S00110_Q175

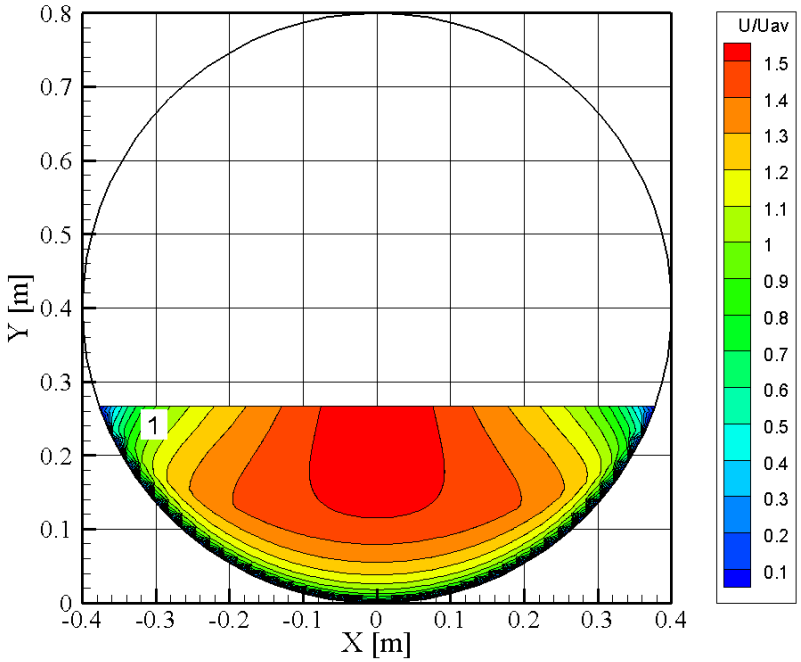

Figure 5.10 Normalized Ead *et al*. (2000) predicted 2D velocity distribution for test S00270_Q086

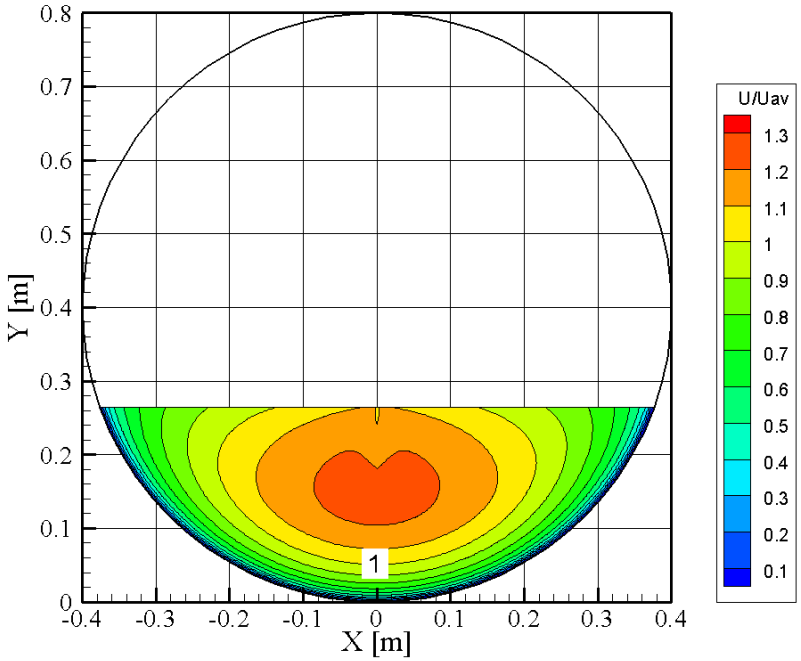

Figure 5.11 Normalized predicted 2D velocity distribution for test S00270_Q086

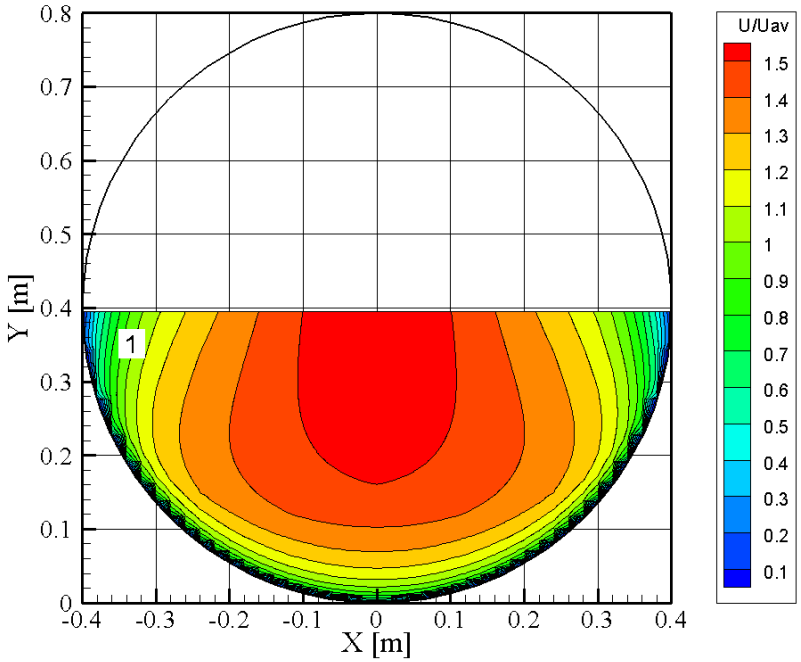

Figure 5.12 Normalized Ead *et al*. (2000) predicted 2D velocity distribution for test S00270_Q175

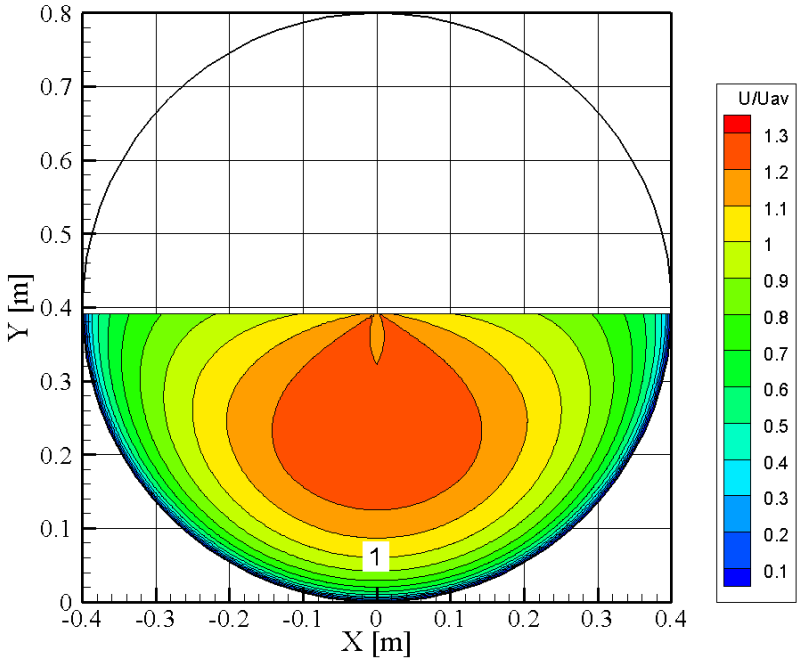

Figure 5.13 Normalized predicted 2D velocity distribution for test S00270_Q175

CHAPTER 6 *Conclusions and Future Work*

6.1 Summary

The typical design technique that is applied to the design of successful fish passage through a culvert consists of determining what the average velocity would be and ensuring that it is less than the prolonged swimming speed of the particular fish species found within the watercourse. As would be expected, the average velocity does not provide an adequate representation of the water velocity for all the various portions of the cross section, because it is merely an average. Therefore, by gaining a better understanding of the developed flow structure within a culvert, it could be possible that there are portions of the cross section that are better suited for fish passage. If these regions provide sufficient area of lower than average velocity, this may indicate that the current design technique is over conservative, from a hydraulics perspective.

Since a corrugated culvert presents a rough boundary surface, it was expected that there would be a region of lower velocity near the boundary, and a region of higher velocity concentrated near the center of the cross section. By determining how thick this boundary region is, it may allow for sufficient area to facilitate fish passage. If sufficient understanding of the flow patterns within circular CMP culvert can be made, it will lead to both better design and regulation techniques.

In addition to having a better understanding of the developed flow structure, it also became equally important to know the streamwise distance required for the flow to become fully developed. Since the developing region of the culvert will provide completely different conditions than the developed region, it may present a potential barrier for fish passage even if the rest of the culvert is acceptable.

In order to address the need for a better understanding of the aforementioned flow properties, a research project was proposed to conduct tests on a physical circular corrugated metal pipe culvert model over a variety of conditions. The conditions were chosen such that they would be representative of typical prairie culvert installations, with culvert slopes of 0.028%, 0.110%, 0.270%, and 0.488%. The model was designed, built, and tested at the Hydraulics Research and Testing facility at the University of Manitoba. Through analysis of the results as outlined throughout this document, the following conclusions have been drawn.

6.2 Conclusions

By acquiring vertical centerline velocity profiles at various locations along the length of the culvert it was seen that for tests without gravel embedment the development length appears to be longer for shallower slopes. This makes sense because the slower moving water of a shallow slope does not generate the turbulence intensity as quickly as the faster moving water of a steep slope. Therefore a culvert with a high slope will have a shorter development length than one with a nearly horizontal slope. For each test within this project the culvert was setup with an elevated projecting inlet. This means that as the water enters the culvert it will begin developing from a uniform profile. If a culvert was not elevated, so that its bottom was in line with the stream bed, the water would enter the culvert with some degree of boundary layer development. It can be expected that the development length would be shorter in this type of condition. It is also expected that the development length would be shorter with different inlet configurations, such as the inclusion of a headwall.

For tests with gravel embedment the development length was seen to take longer. Although, due to the variation in the gravel bed and the complexity of a portion of the water flowing through the bed, the centerline profiles tended to have some degree of fluctuation from one location to another. This fluctuation made choosing the development length difficult. Although not considered fully developed until the specified locations, the velocity profiles were similar much earlier in the culvert. It is important to note that two dimensional velocity measurements were taken well within the developed region.

The development length, although not greatly explored in this project, is an important portion of the flow structure within the culvert. Depending on the velocity distribution near the inlet and in the developing region there may be a velocity barrier that could be impassable even if the developed region is acceptable.

When analyzing the data from the vertical centerline profiles, each profile was individually fit to the log law equation in order to determine the friction velocity and the roughness shift. Through the equation fitting process it was determined that the friction velocity along the centerline of the culvert is typically equal to 1.1 times the average friction velocity of the channel. In addition, when using the fitted roughness shift to solve for the equivalent roughness height it was found to be equal to 0.0123 m, or 0.95 times the corrugation height. This was similar to the findings of Eat *et al.* (2000) where it was concluded that the equivalent roughness height was equal to the corrugation height.

When using the two dimensional cross section data, which was measured in radials perpendicular to the boundary, the friction velocity was found for multiple points along the wetted perimeter. By gathering the data together from each test it was found that the distribution of shear stress over the wetted perimeter is well described by Equation 5.4. The equation was valid for all non-gravel embedment depths. An important note for Equation 5.4 is that at the culvert centerline the friction velocity is still equal to 1.1 times the average friction velocity, as stated earlier.

In addition to analyzing the data for velocity distributions, the data were used to display the distribution of turbulence intensity along a centerline profile. The results were compared to a set of empirical equations that describe the distribution of turbulence intensity in a wide rectangular channel. The results were significantly different and consistent across each of the non-gravel embedment tests. Within the circular cross section of the culvert the turbulence intensity was seen to increase toward the surface, which is not seen within rectangular cross sections. Therefore, Equations 5.1 to 5.3 were fit to the data and do a reasonably good job of describing the turbulence intensity along the centerline profile of a circular cross section. When observing the turbulence intensity for the tests with increasing gravel embedment, it was seen that with more gravel embedment, the distribution of turbulence intensity approached the empirical equations previously developed for rectangular cross sections (Equations 1.9 to 1.11).

When working with the two dimensional cross sections several processes were done to quantify the results. First, by integrating the complete set of velocity points it was possible to calculate the integrated discharge of the section. For each test the integrated discharge was very similar to the actual discharge, indicating that the quality of the data is good. The exception was for the gravel embedment tests, where the two values of discharge were not equal, which indicated that there is a significant amount of flow through the gravel embedment.

In order to make the physical model testing results of this study usable in culvert design, a set of equations were created such that a two dimensional cross section of streamwise

velocity points can be derived. This was done with the use of the previously mentioned equations describing friction velocity and roughness shift. Using these developments and by modifying the log law equation to account for the entire height of a velocity profile, the technique was used to recreate the same situations that were tested in the physical model. The equations provided a good visual fit between the data and the model, and when calculating the percentage of area less than average velocity and less than 0.75 times average velocity, the model produced very comparable results and consistently under predicted the value. A slight under prediction was better to see since, for the model to be used as a resource in culvert design, it is better to be conservative.

As a general conclusion when discussing culvert design, the data from this project has shown that there is a significant amount of cross sectional area that contains velocity less than average velocity. This area could be utilized by fish when passing through a culvert and could require a prolonged swimming speed less than the average velocity in the culvert. At the same time, the area that is below average velocity is also the area that contains the highest velocity gradients and the highest turbulence intensity. The increased complexity of this region may have implications to the fish passing through the culvert and where they choose to swim. If the region becomes undesirable to the fish, because of the high gradient and increased turbulence intensity, then they would be forced to travel through the higher velocity water near the center of the culvert, or not be able to pass.

When comparing two dimensional cross sections of gravel embedment tests and those without gravel embedment, it was shown that there is a significant amount more area that

is below average velocity. The increased area occurs in the corners where the gravel bed meets the culvert wall. As well, the area is highly concentrated in the corners which results in a more prominent pathway potentially utilized by fish passage. Therefore it is recommended that for culverts were fish passage is required, gravel embedment should be used.

6.3 Future Work

Within the project there are several other potential points of research that should be pursued in the future to increase the understanding of culvert hydraulics. The following list provides an outline of potential topics that should be explored in order to fill in the gaps.

1) Different inlet configurations should be tested to determine their effect on the development length in the culvert. This should include a similar inlet as the elevated projecting inlet used in this study, but rather it should not be elevated to observe the significance.
2) Since the developed region is now well studied, a project should be run focused on the complex nature of the inlet and the developing region between the two. In addition, similar culvert configurations should be tested operating with an M1 or an M2 profile rather than at normal depth.
3) Collaboration should be done between hydraulics researchers and fish biology researchers. Although both are individually important, communication should

continue to be present to ensure that the more important portions of the culvert are being explored.

4) More work should be put into comparing the results of the physical model to that of various computational models, such as Flow3D, in order to identify shortcoming and to help make these models better at modeling culvert flow.
5) Lastly, at some point a site should be chosen to operate as a field based study to observe the hydraulic conditions of an operating culvert. The study could both collect velocity data and could study the operation of the culvert, and how well the current design techniques are working.

References

Abbs, T.J., Kells, J.A., and Katopodis, C., 2007. A Model Study of the Hydraulics Related to Fish Passage Through Backwatered Culverts, *Proceedings of the 18th CSCE Hydro Technical Conference*

Brederode, B., and Bradshaw, P., 1974. A Note on the Empirical Constants Appearing in the Logarithmic Law for Turbulent Wall Flows, *Aero Report* 74-03, Imperial College, UK

Chow, V.T., 1964. Open-Channel Hydraulics, *McGraw-Hill*, New York, N.Y., 680p

Coles, D., 1968. The Young Person's Guide to the Data, *Proceedings of AFOSR-IFP Stanford Conference on Computation of Turbulent Boundary Layers*, vol.2, 1-45

Corrugated Steel Pipe Institute, 2007. Handbook of Steel Drainage and Highway Construction Products, Cambridge, ON, 470p

Ead, S.A., Rajaratnam, N., Katopodis, C., and Ade, F., 2000. Turbulent Open-Channel Flow in Circular Corrugated Culverts, *Journal of Hydraulic Engineering*, 126(10), 750-757

Fisheries and Oceans Canada, 1996. Manitoba Stream Crossing Guidelines for the Protection of Fish and Fish Habitat, *Manitoba Natural Resources*, 48p + App

Katopodis, C., Robinson, P.R., and Sutherland, B.G., 1978. A Study of Model and Prototype Culvert Baffling for Fish Passage, *Canadian Fisheries and Marine Service*, Technical Report No. 828, 78p

Knight, D.W., and Sterling, M., 2000. Boundary Shear in Circular Pipes Running Partially Full, *Journal of Hydraulic Engineering*, 126(4), 263-275

Lotter, G.K., 1933. Considerations on Hydraulic Design of Channels with Different Roughness of Walls, *All-Union Scientific Research Institute of Hydraulic Engineering*, Leningrad, vol. 9, 238-241

Nezu, I., and Nakagawa, H., 1993. Turbulence in Open-Channel Flows, *A. A. Balkema*, Rotterdam, Netherlands, 281p

Nezu, I., and Rodi, W., 1986. Open-Channel Flow Measurements with a Laser Doppler Anemometer, *Journal of Hydraulic Engineering*, ASCE, 112, 335-355

Pope, S.B., 2000. Turbulent Flows, *Cambridge University Press*, Cambridge, UK, 770p

SonTek, 2001. SonTek ADVField Acoustic Doppler Velocimeter Technical Documentation, *SonTek*, San Diego, CA

Sterling, M., and Knight, D.W., 2000. Resistance and Boundary Shear in Circular Conduits with Flat Beds Running Part Full, *Proceedings of the Institution of Civil Engineers*, Water, Maritime and Energy, 142(4), 229-240

Strickler, A., 1923. Contributions to the Question of a Velocity Formula and Roughness Data for Streams Channels and Closed Pipelines, (Translated from German by Roesgan, T. and Brownlie, W.R.), Bern, Switzerland, 16

Sturm, T.W., 2001. Open Channel Hydraulics, *McGraw-Hill*, New York, N.Y., 493p

Appendix A – Velocity Plots

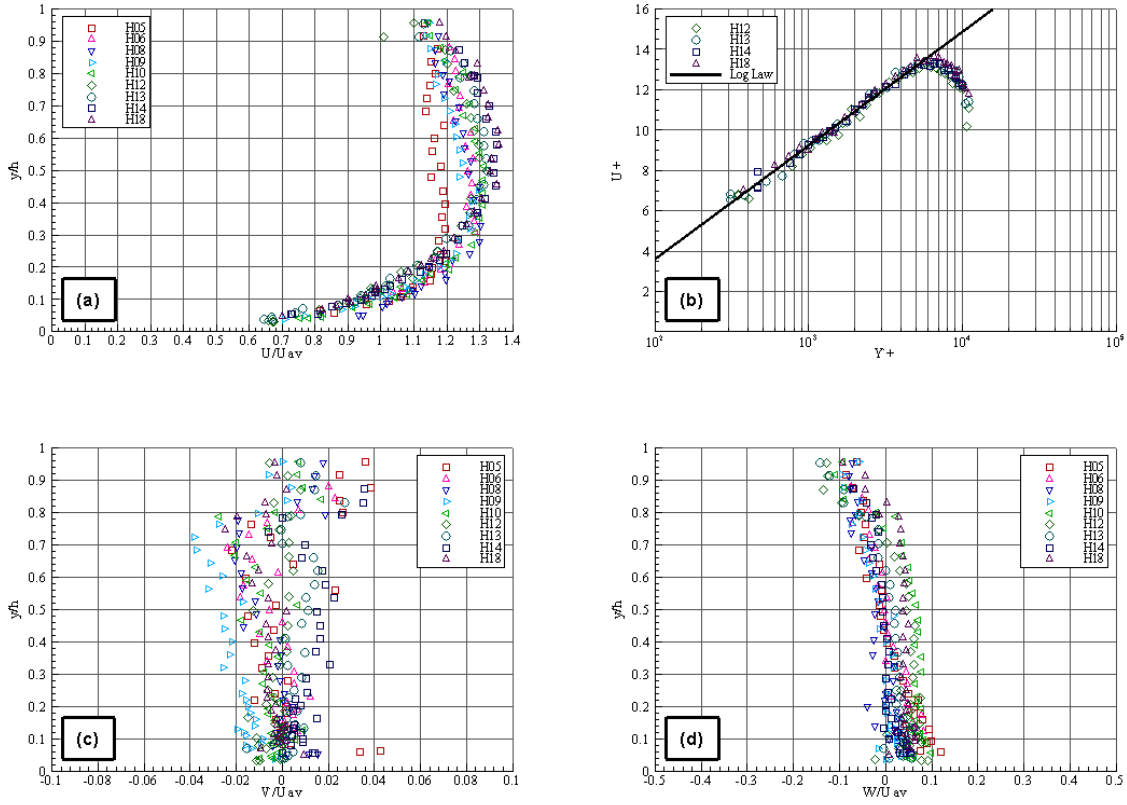

Figure A.1 (a) Streamwise velocity profiles, (b) logarithmic distribution, (c) vertical and (d) spanwise velocity profiles for test S00028_Q086

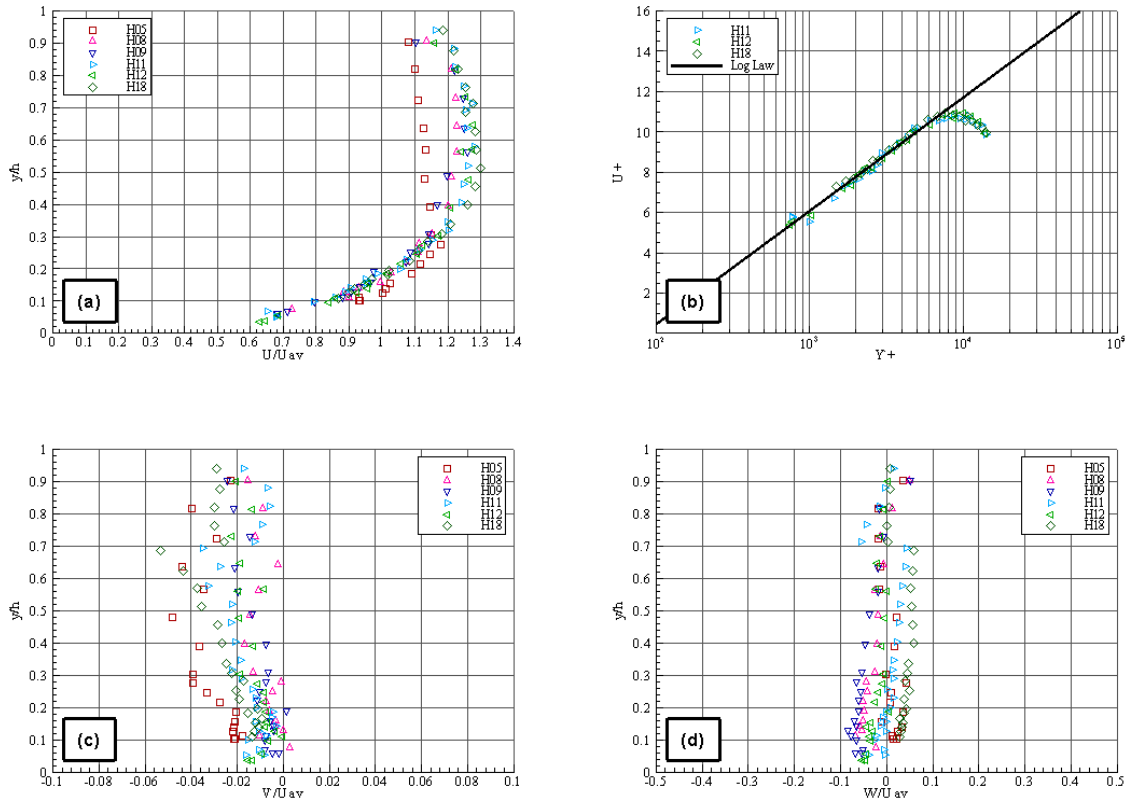

Figure A.2 (a) Streamwise velocity profiles, (b) logarithmic distribution, (c) vertical and (d) spanwise velocity profiles for test S00110_Q086

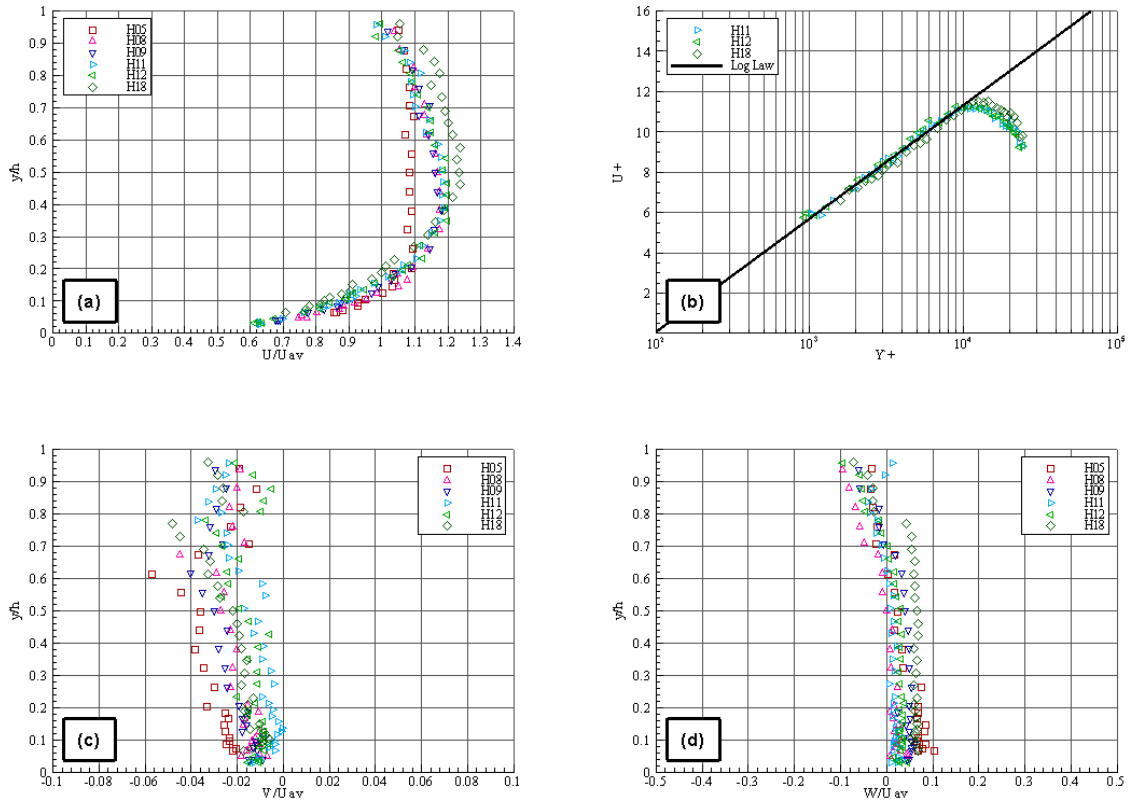

Figure A.3 (a) Streamwise velocity profiles, (b) logarithmic distribution, (c) vertical and (d) spanwise velocity profiles for test S00110_Q175

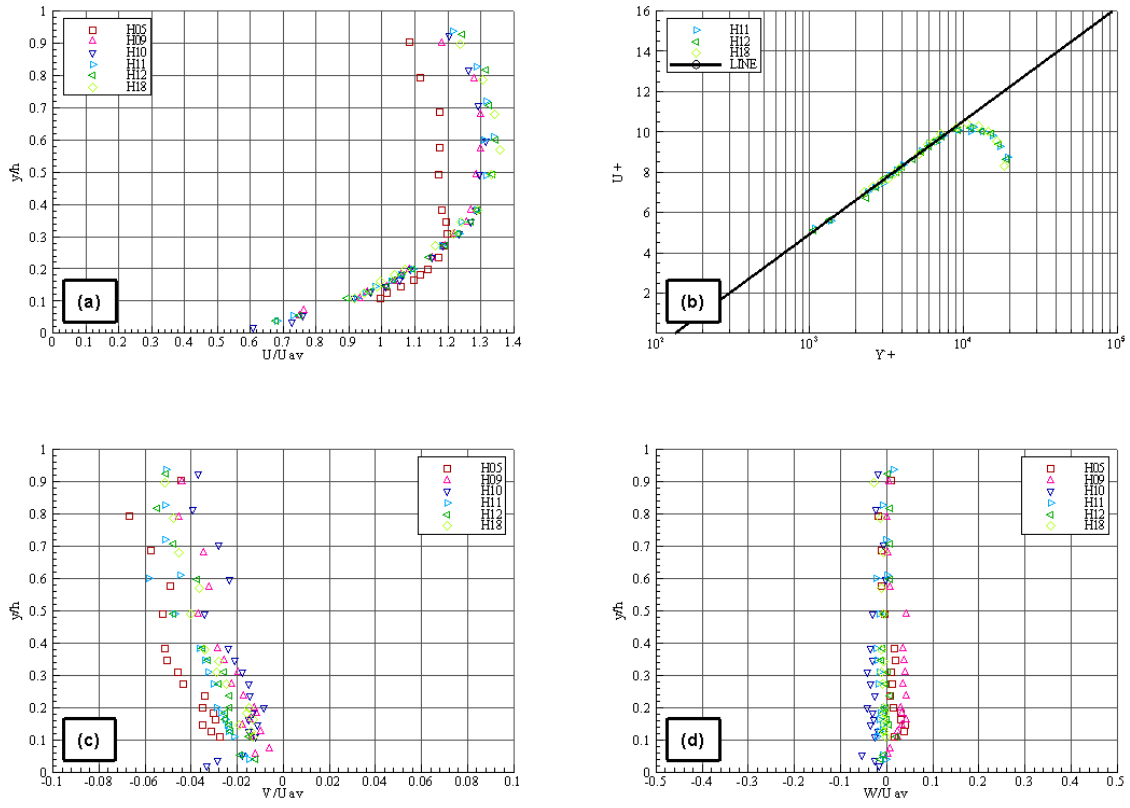

Figure A.4 (a) Streamwise velocity profiles, (b) logarithmic distribution, (c) vertical and (d) spanwise velocity profiles for test S00270_Q086

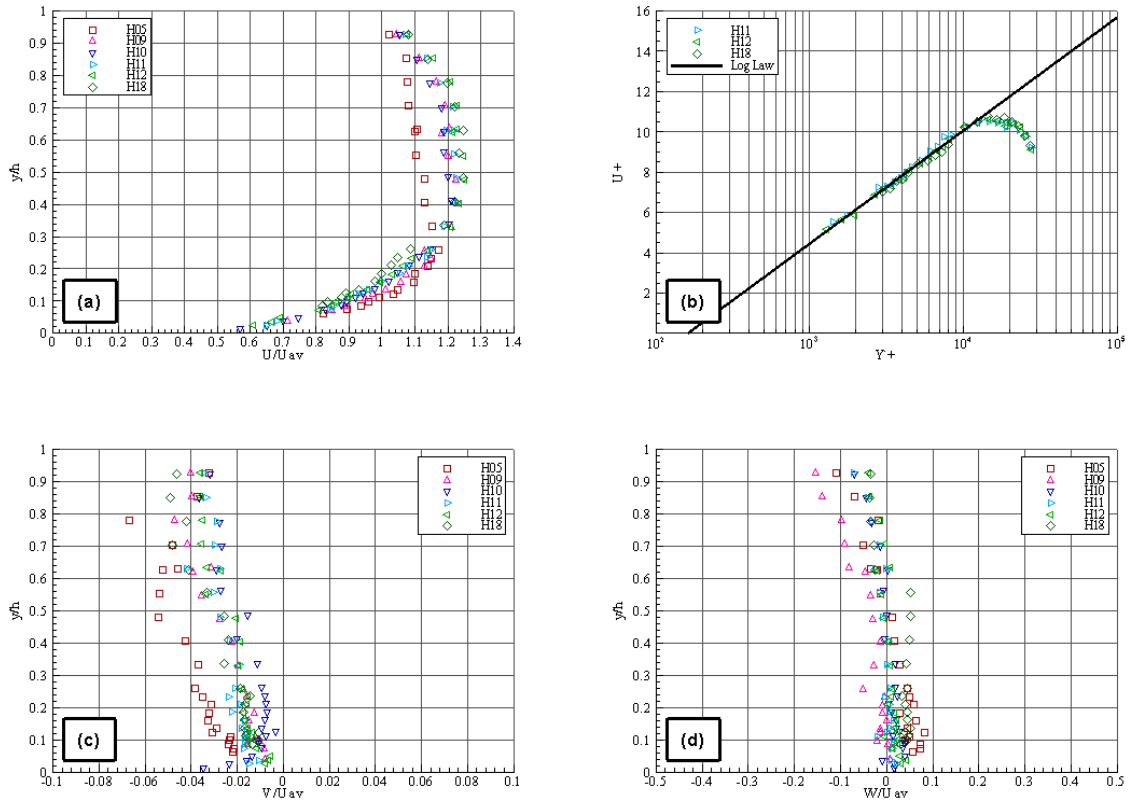

Figure A.5 (a) Streamwise velocity profiles, (b) logarithmic distribution, (c) vertical and (d) spanwise velocity profiles for test S00270_Q175

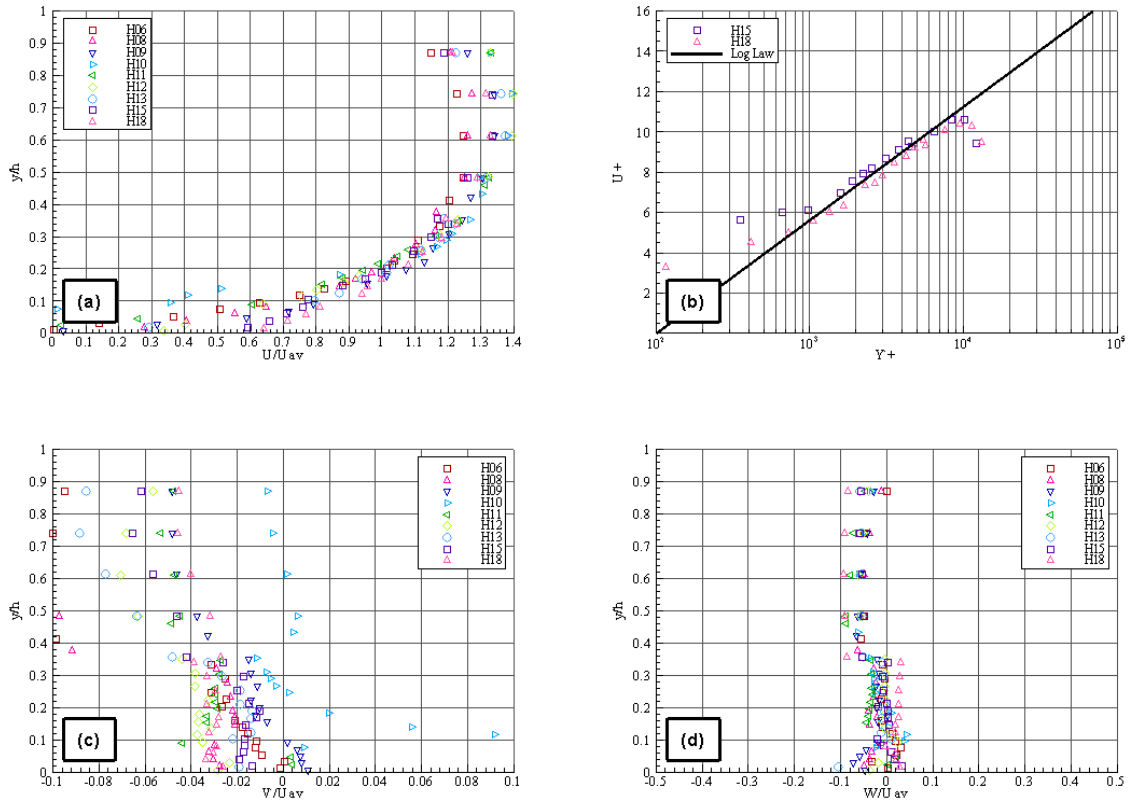

Figure A.6 (a) Streamwise velocity profiles, (b) logarithmic distribution, (c) vertical and (d) spanwise velocity profiles for test S00270_Q086_R10

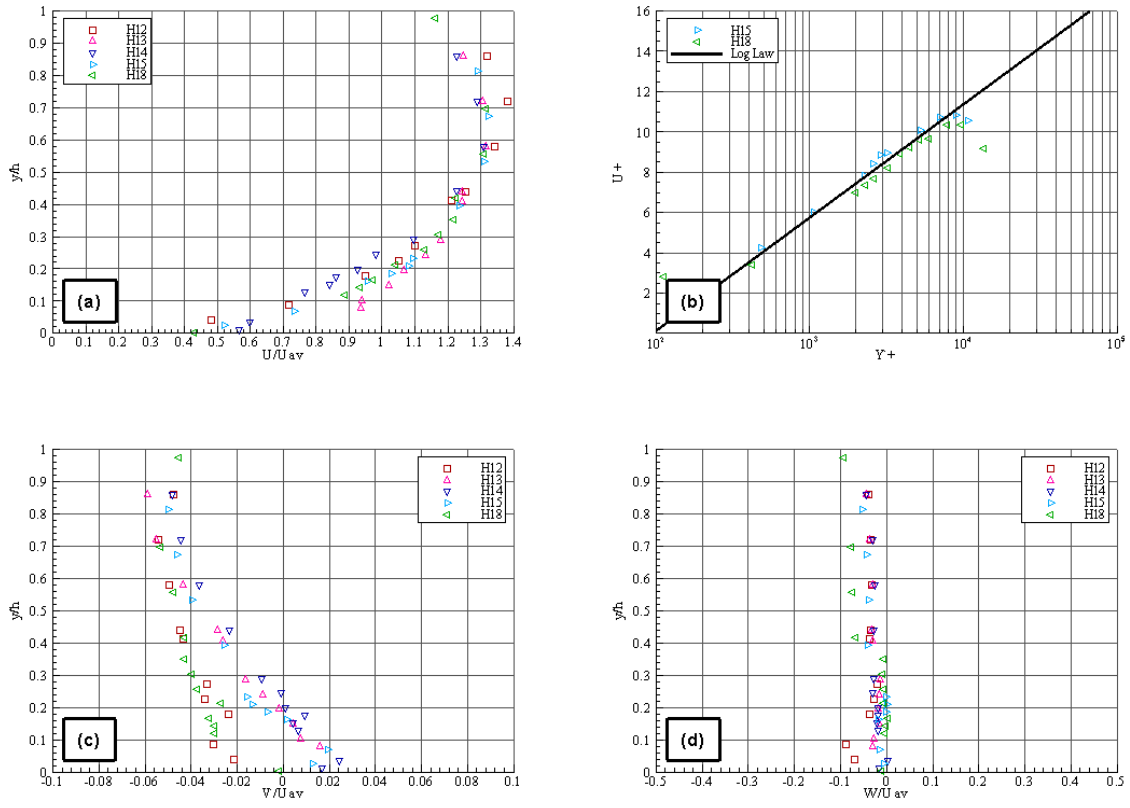

Figure A.7 (a) Streamwise velocity profiles, (b) logarithmic distribution, (c) vertical and (d) spanwise velocity profiles for test S00270_Q086_R18

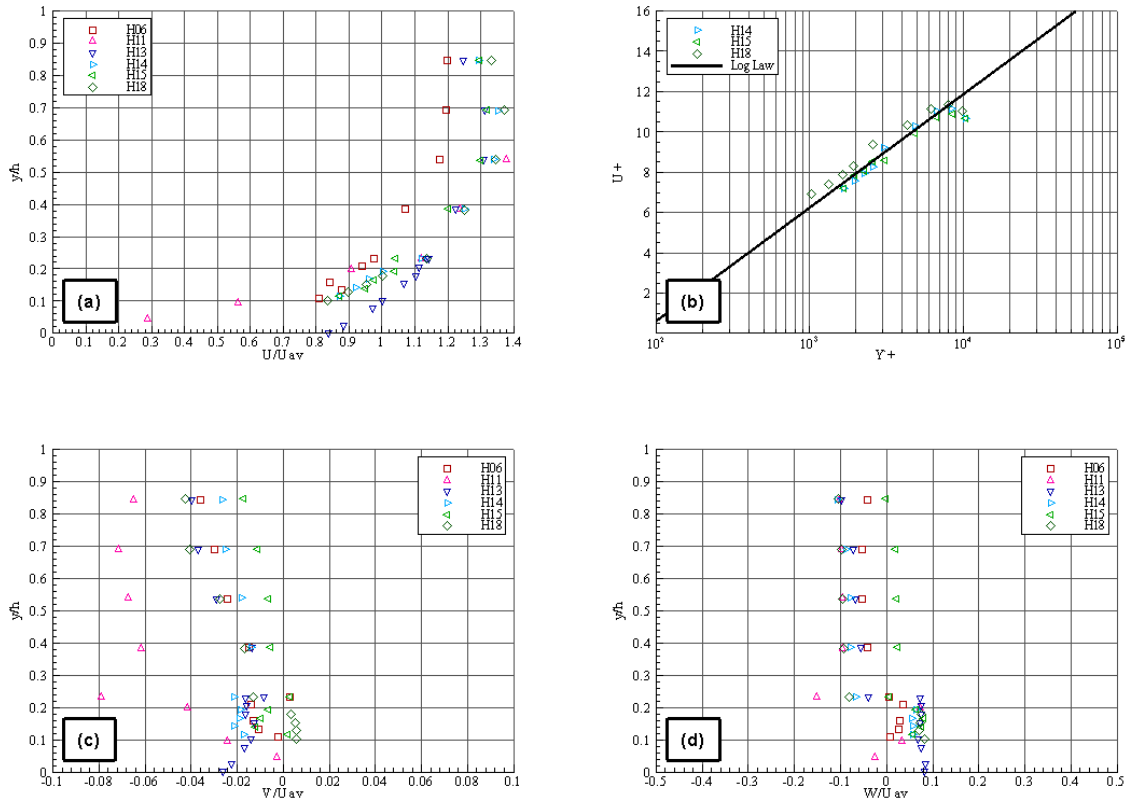

Figure A.8 (a) Streamwise velocity profiles, (b) logarithmic distribution, (c) vertical and (d) spanwise velocity profiles for test S00270_Q086_R28

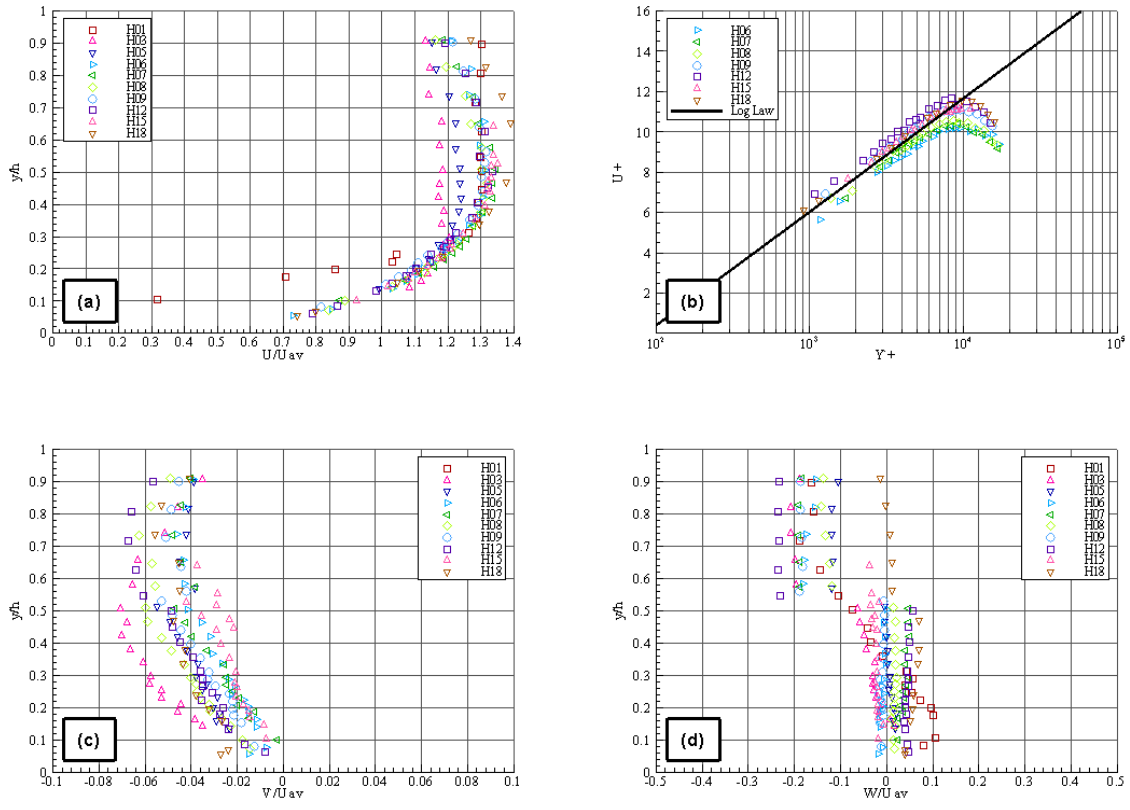

Figure A.9 (a) Streamwise velocity profiles, (b) logarithmic distribution, (c) vertical and (d) spanwise velocity profiles for test S00488_Q086

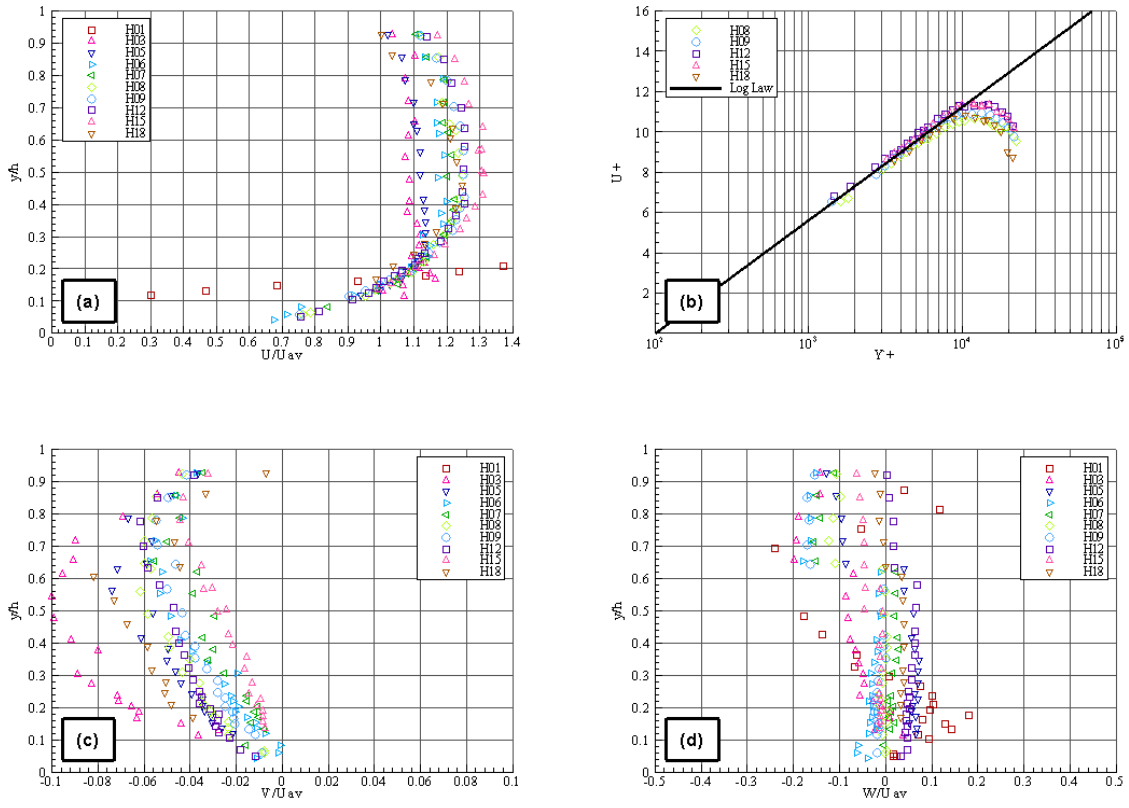

Figure A.10 (a) Streamwise velocity profiles, (b) logarithmic distribution, (c) vertical and (d) spanwise velocity profiles for test S00488_Q130

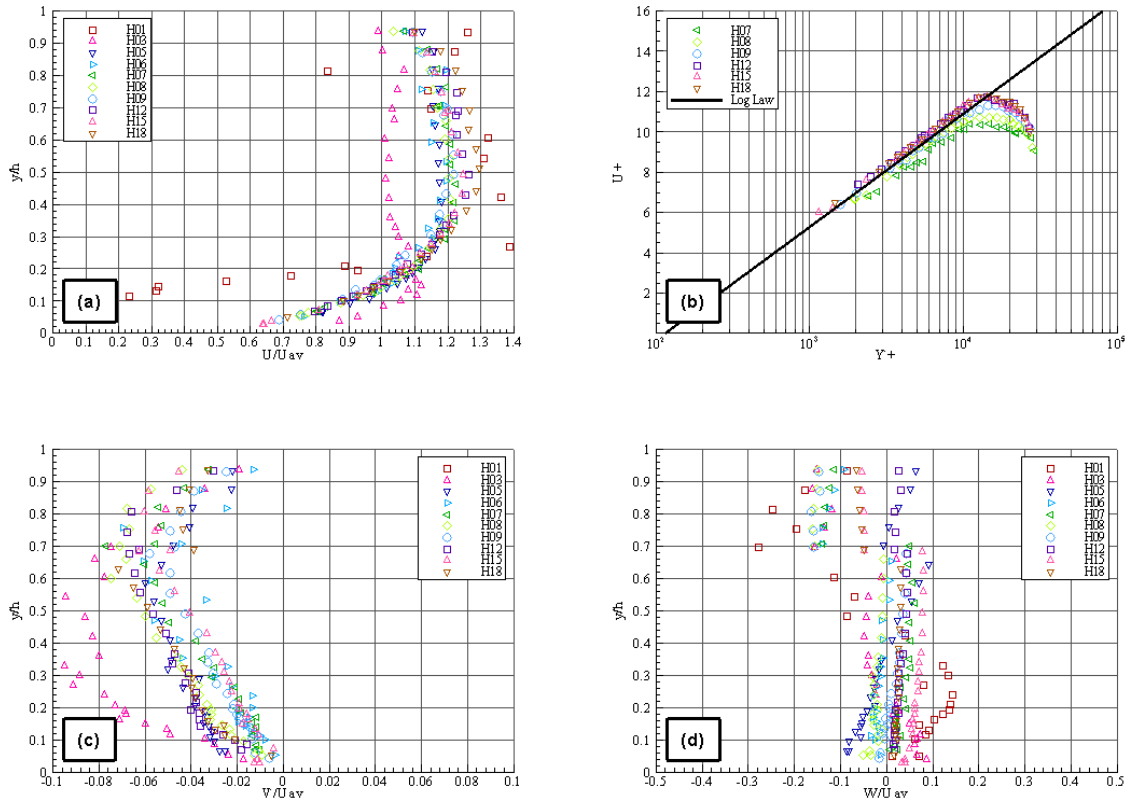

Figure A.11 (a) Streamwise velocity profiles, (b) logarithmic distribution, (c) vertical and (d) spanwise velocity profiles for test S00488_Q175

Appendix B – TKE and Reynolds Stress

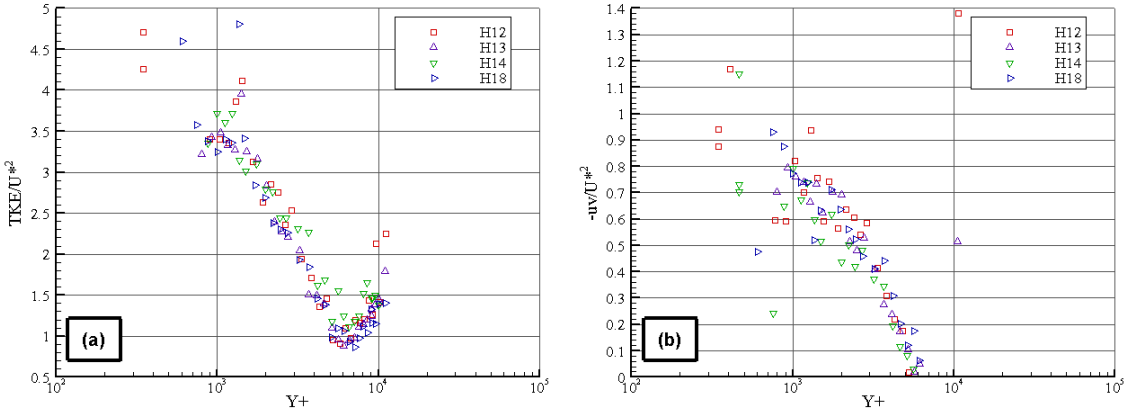

Figure B.1 - (a) Turbulent Kinetic Energy (TKE) and (b) Reynolds Stress (-uv) for test S00028_Q086

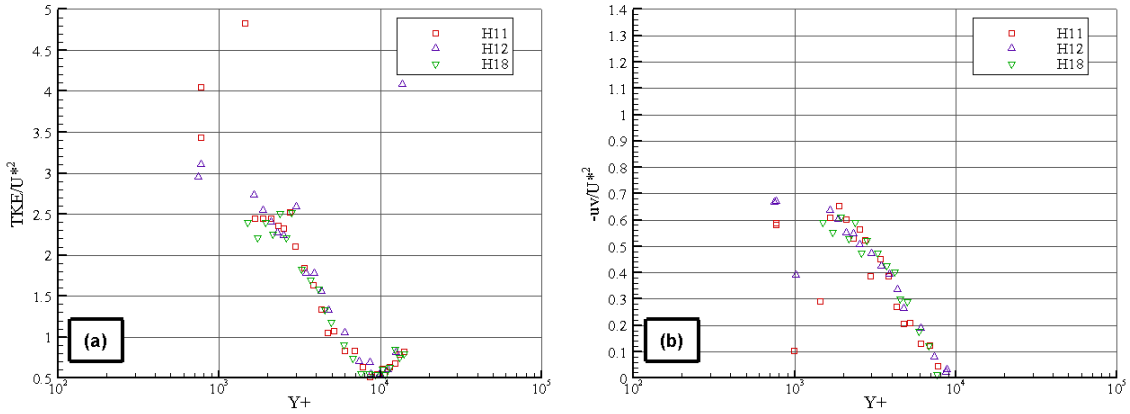

Figure B.2 - (a) Turbulent Kinetic Energy (TKE) and (b) Reynolds Stress (-uv) for test S00110_Q086

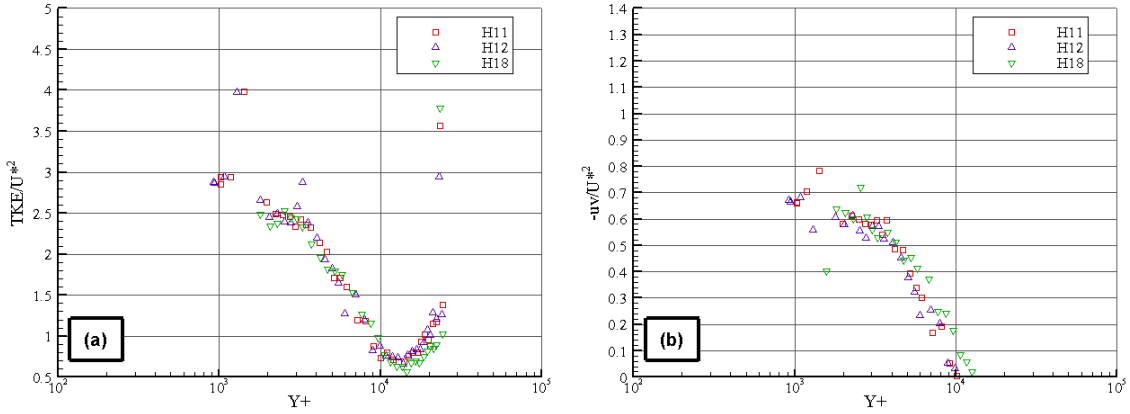

Figure B.3 - (a) Turbulent Kinetic Energy (TKE) and (b) Reynolds Stress (-uv) for test S00110_Q175

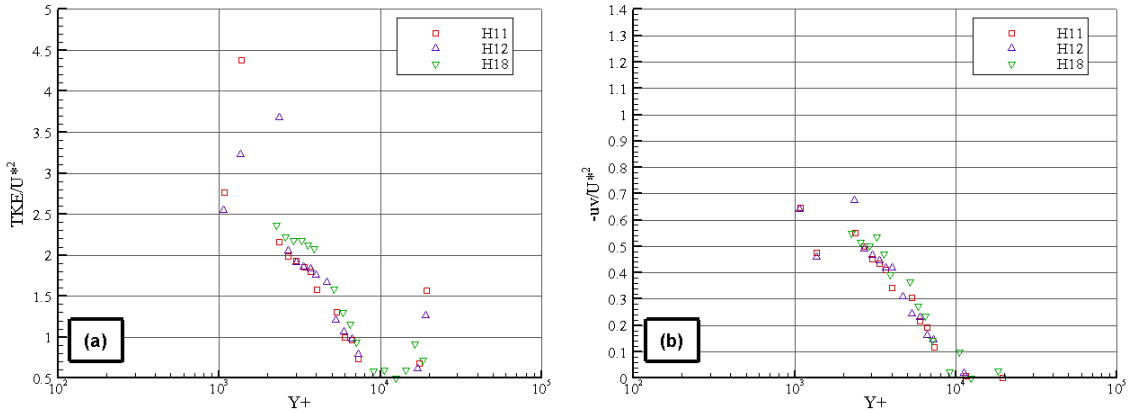

Figure B.4 - (a) Turbulent Kinetic Energy (TKE) and (b) Reynolds Stress (-uv) for test S00270_Q086

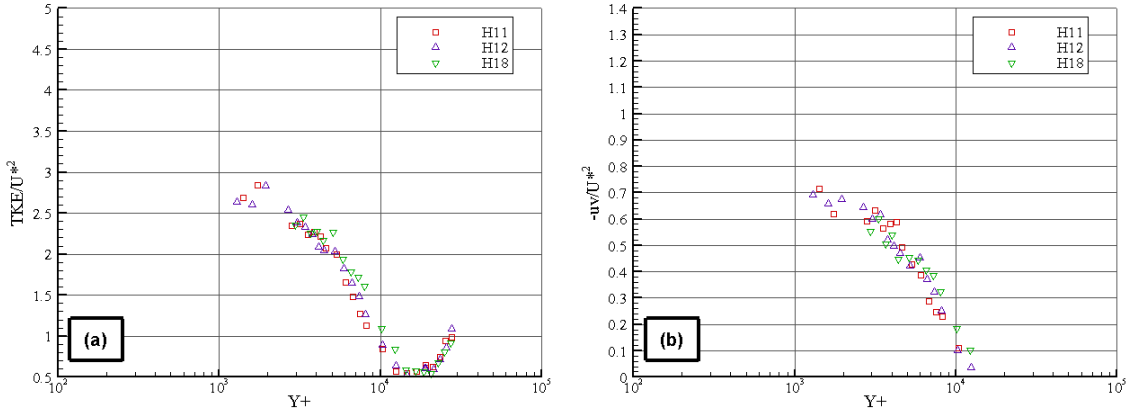

Figure B.5 - (a) Turbulent Kinetic Energy (TKE) and (b) Reynolds Stress (-uv) for test S00270_Q175

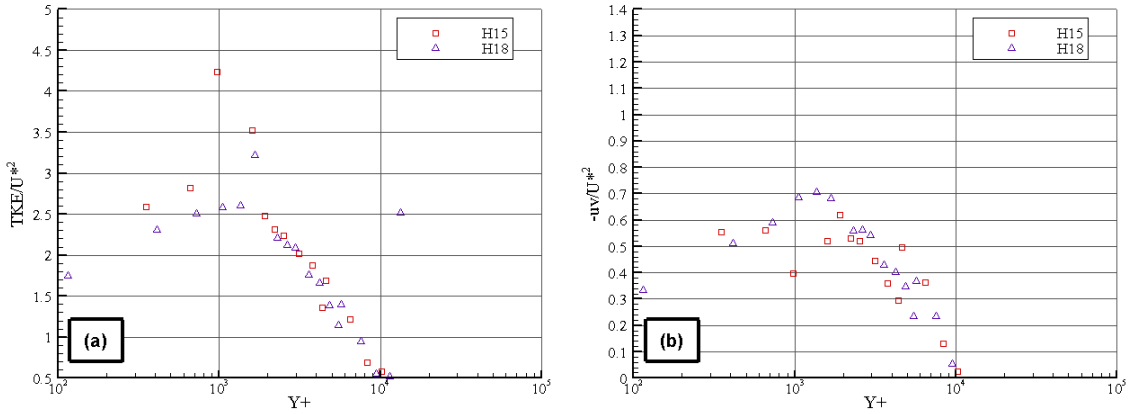

Figure B.6 - (a) Turbulent Kinetic Energy (TKE) and (b) Reynolds Stress (-uv) for test S00270_Q086_R10

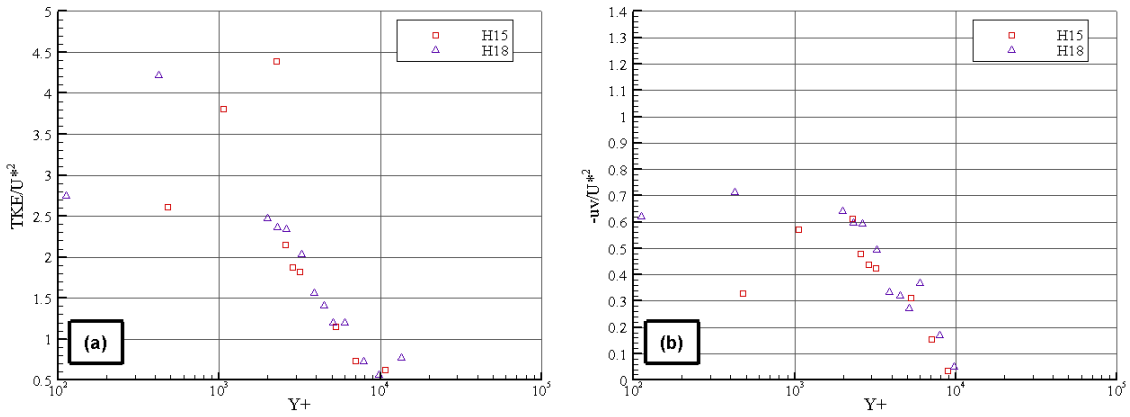

Figure B.7 - (a) Turbulent Kinetic Energy (TKE) and (b) Reynolds Stress (-uv) for test S00270_Q086_R18

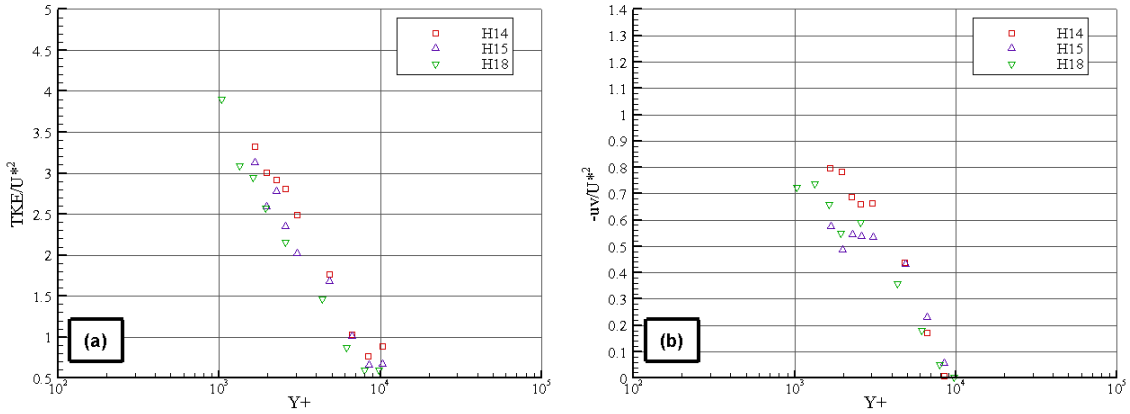

Figure B.8 - (a) Turbulent Kinetic Energy (TKE) and (b) Reynolds Stress (-uv) for test S00270_Q086_R28

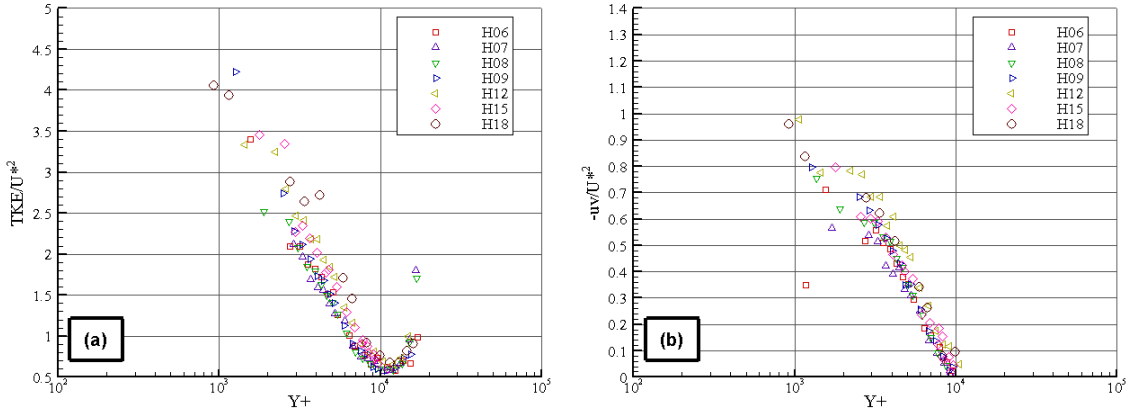

Figure B.9 - (a) Turbulent Kinetic Energy (TKE) and (b) Reynolds Stress (-uv) for test S00488_Q086

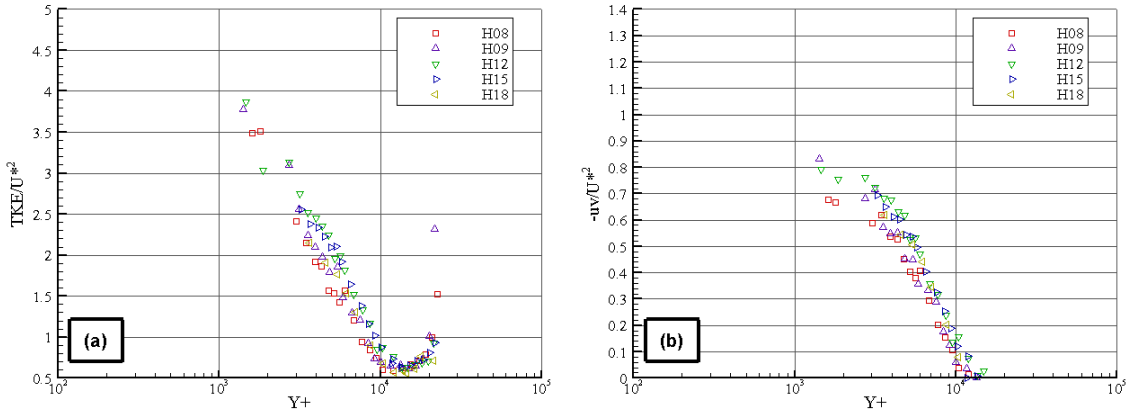

Figure B.10 - (a) Turbulent Kinetic Energy (TKE) and (b) Reynolds Stress (-uv) for test S00488_Q130

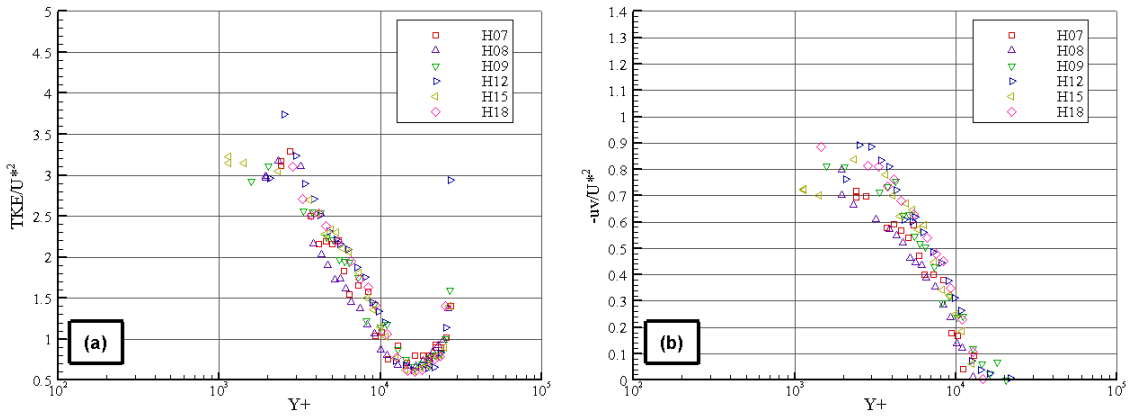

Figure B.11 - (a) Turbulent Kinetic Energy (TKE) and (b) Reynolds Stress (-uv) for test S00488_Q175

Appendix C – Survey Sheets

	Measured Value	Location	Water Surface Elevation
HW	1.122	-	**-0.7804**
P1	326.0	0.327	**-0.7952**
P2	328.0	0.600	**-0.7913**
P3	328.5	0.867	**-0.7904**
P4	328.5	1.207	**-0.7904**
P5	328.5	1.813	**-0.7904**
P6	328.0	2.756	**-0.7913**
P7	328.0	3.635	**-0.7913**
P8	328.0	4.578	**-0.7913**
P9	327.5	5.455	**-0.7923**
P10	327.5	6.401	**-0.7923**
P11	329.0	7.280	**-0.7925**
P12	329.0	8.226	**-0.7925**
P13	329.0	9.169	**-0.7925**
P14	329.0	10.046	**-0.7925**
P15	329.0	10.989	**-0.7925**
P16	328.5	11.868	**-0.7935**
P17	328.0	12.808	**-0.7945**
P18	328.0	13.754	**-0.7945**
P19	339.5	14.634	**-0.7946**
P20	339.0	15.577	**-0.7956**
P21	339.0	16.453	**-0.7956**
P22	338.5	17.396	**-0.7965**
P23	338.5	18.275	**-0.7965**
P24	338.5	19.221	**-0.7965**
P25	338.0	20.164	**-0.7975**
P26	338.0	20.771	**-0.7975**
P27	338.0	21.041	**-0.7975**
P28	337.0	21.380	**-0.7995**
TW	2.012	-	**-0.7964**

	Surveyed Value	Location	Culvert Bottom Elevation
BENCH	-0.64	-	**-**
HW	-	0.000	
S1	49.00	0.197	**-1.2839**
S2	49.10	0.800	**-1.2849**
S3	48.90	1.607	**-1.2829**
S4	48.70	3.226	**-1.2809**
S5	48.90	3.962	**-1.2829**
S6	48.95	4.769	**-1.2834**
S7	48.80	5.709	**-1.2819**
S8	49.00	6.452	**-1.2839**
S9	49.10	7.195	**-1.2849**
S10	48.75	8.141	**-1.2814**
S11	49.20	8.884	**-1.2859**
S12	48.70	9.690	**-1.2809**
S13	48.90	11.303	**-1.2829**
S14	48.95	12.109	**-1.2834**
S15	49.05	13.729	**-1.2844**
S16	49.30	14.535	**-1.2869**
S17	49.30	16.154	**-1.2869**
S18	49.25	16.897	**-1.2864**
S19	49.45	17.704	**-1.2884**
S20	49.25	18.644	**-1.2864**
S21	49.40	19.387	**-1.2879**
S22	49.60	20.130	**-1.2899**
TW		21.539	

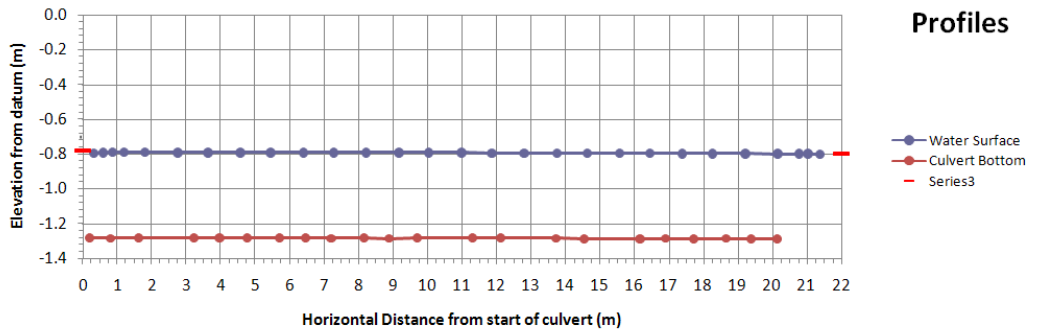

NOTES
-Measured values P1 - P28 are read off of the manometer boards
-Measured values HW and TW are read off of the depth guages
-Input all survey data in cm
-Surveyed values S1 - S22 are measured at the access holes
-BENCH is the survey level from the experiment datum
-All location data is in metres from the beginning of the culvert
-All elevation data is in inchs from the experiment datum

EXTRA INFORMATION		
Date	16-Oct-08	
Flow rate	0.086	m^3/s
Tail gate setting	33	-
Desired slope	0.025	%
Actual slope	0.028	%
Head Drop	0.016	m

Figure C.1 Survey sheet of test S00028_Q086

	Measured Value	Location	Water Surface Elevation
HW	0.713	-	**-0.9050**
P1	256.0	0.327	**-0.9316**
P2	260.0	0.600	**-0.9238**
P3	260.5	0.867	**-0.9228**
P4	260.0	1.207	**-0.9238**
P5	259.0	1.813	**-0.9257**
P6	258.0	2.756	**-0.9277**
P7	258.0	3.635	**-0.9277**
P8	257.0	4.578	**-0.9296**
P9	256.5	5.455	**-0.9306**
P10	256.0	6.401	**-0.9316**
P11	257.5	7.280	**-0.9318**
P12	256.5	8.226	**-0.9337**
P13	256.0	9.169	**-0.9347**
P14	255.5	10.046	**-0.9357**
P15	255.5	10.989	**-0.9357**
P16	255.0	11.868	**-0.9366**
P17	254.0	12.808	**-0.9386**
P18	253.5	13.754	**-0.9396**
P19	265.0	14.634	**-0.9397**
P20	264.5	15.577	**-0.9407**
P21	264.0	16.453	**-0.9416**
P22	263.5	17.396	**-0.9426**
P23	263.5	18.275	**-0.9426**
P24	263.0	19.221	**-0.9436**
P25	262.0	20.164	**-0.9455**
P26	261.5	20.771	**-0.9465**
P27	261.5	21.041	**-0.9465**
P28	261.0	21.380	**-0.9475**
TW	1.51	-	**-0.9495**

	Surveyed Value	Location	Culvert Bottom Elevation
BENCH	-8.57	-	**-**
HW	-	0.000	
S1	40.55	0.197	**-1.2787**
S2	40.50	0.800	**-1.2782**
S3	40.50	1.607	**-1.2782**
S4	40.65	3.226	**-1.2797**
S5	40.90	3.962	**-1.2822**
S6	41.30	4.769	**-1.2862**
S7	41.25	5.709	**-1.2857**
S8	41.35	6.452	**-1.2867**
S9	41.20	7.195	**-1.2852**
S10	41.10	8.141	**-1.2842**
S11	41.40	8.884	**-1.2872**
S12	41.50	9.690	**-1.2882**
S13	41.85	11.303	**-1.2917**
S14	42.00	12.109	**-1.2932**
S15	41.80	13.729	**-1.2912**
S16	42.10	14.535	**-1.2942**
S17	42.25	16.154	**-1.2957**
S18	42.30	16.897	**-1.2962**
S19	42.55	17.704	**-1.2987**
S20	42.50	18.644	**-1.2982**
S21	42.55	19.387	**-1.2987**
S22	42.60	20.130	**-1.2992**
TW		21.539	

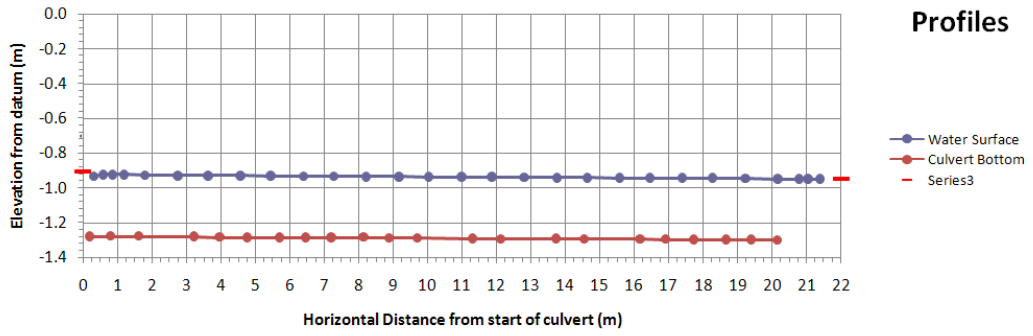

NOTES
-Measured values P1 - P28 are read off of the manometer boards
-Measured values HW and TW are read off of the depth guages
-Input all survey data in cm
-Surveyed values S1 - S22 are measured at the access holes
-BENCH is the survey level from the experiment datum
-All location data is in metres from the beginning of the culvert
-All elevation data is in inchs from the experiment datum

EXTRA INFORMATION		
Date	09-Dec-08	
Flow rate	0.086	m^3/s
Tail gate setting	5	-
Desired slope	0.100	%
Actual slope	0.110	%
Head Drop	0.044	m

Figure C.2 Survey sheet of test S00110_Q086

	Measured Value	Location	Water Surface Elevation
HW	1.324	-	**-0.7188**
P1	339.0	0.327	**-0.7699**
P2	344.0	0.600	**-0.7602**
P3	346.0	0.867	**-0.7563**
P4	346.0	1.207	**-0.7563**
P5	346.0	1.813	**-0.7563**
P6	345.0	2.756	**-0.7582**
P7	344.5	3.635	**-0.7592**
P8	344.0	4.578	**-0.7602**
P9	343.5	5.455	**-0.7612**
P10	342.5	6.401	**-0.7631**
P11	344.0	7.280	**-0.7633**
P12	343.0	8.226	**-0.7653**
P13	342.5	9.169	**-0.7662**
P14	342.0	10.046	**-0.7672**
P15	342.0	10.989	**-0.7672**
P16	341.5	11.868	**-0.7682**
P17	340.5	12.808	**-0.7701**
P18	340.0	13.754	**-0.7711**
P19	351.5	14.634	**-0.7712**
P20	351.0	15.577	**-0.7722**
P21	350.0	16.453	**-0.7741**
P22	349.5	17.396	**-0.7751**
P23	348.5	18.275	**-0.7771**
P24	348.0	19.221	**-0.7780**
P25	347.5	20.164	**-0.7790**
P26	347.0	20.771	**-0.7800**
P27	346.5	21.041	**-0.7810**
P28	346.5	21.380	**-0.7810**
TW	2.047	-	**-0.7858**

	Surveyed Value	Location	Culvert Bottom Elevation
BENCH	-8.57	-	**-**
HW	-	0.000	
S1	40.55	0.197	**-1.2787**
S2	40.50	0.800	**-1.2782**
S3	40.50	1.607	**-1.2782**
S4	40.65	3.226	**-1.2797**
S5	40.90	3.962	**-1.2822**
S6	41.30	4.769	**-1.2862**
S7	41.25	5.709	**-1.2857**
S8	41.35	6.452	**-1.2867**
S9	41.20	7.195	**-1.2852**
S10	41.10	8.141	**-1.2842**
S11	41.40	8.884	**-1.2872**
S12	41.50	9.690	**-1.2882**
S13	41.85	11.303	**-1.2917**
S14	42.00	12.109	**-1.2932**
S15	41.80	13.729	**-1.2912**
S16	42.10	14.535	**-1.2942**
S17	42.25	16.154	**-1.2957**
S18	42.30	16.897	**-1.2962**
S19	42.55	17.704	**-1.2987**
S20	42.50	18.644	**-1.2982**
S21	42.55	19.387	**-1.2987**
S22	42.60	20.130	**-1.2992**
TW		21.539	

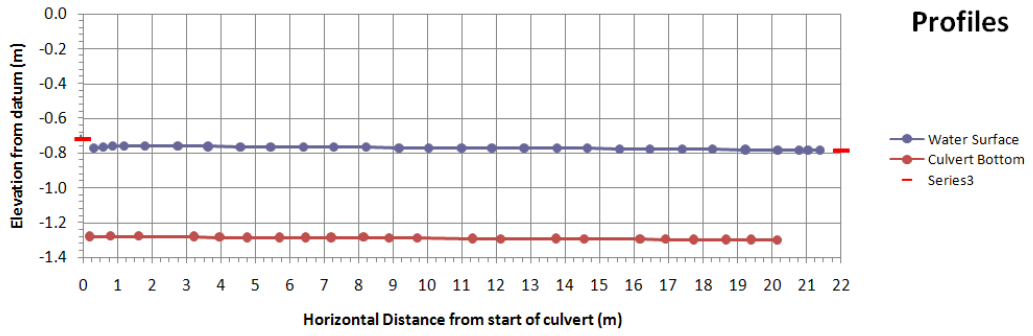

NOTES
-Measured values P1 - P28 are read off of the manometer boards
-Measured values HW and TW are read off of the depth guages
-Input all survey data in cm
-Surveyed values S1 - S22 are measured at the access holes
-BENCH is the survey level from the experiment datum
-All location data is in metres from the beginning of the culvert
-All elevation data is in inchs from the experiment datum

EXTRA INFORMATION		
Date	17-Dec-08	
Flow rate	0.176	m^3/s
Tail gate setting	25	-
Desired slope	0.100	%
Actual slope	0.110	%
Head Drop	0.067	m

Figure C.3 Survey sheet of test S00110_Q175

	Measured Value	Location	Water Surface Elevation
HW	0.562	-	**-0.9511**
P1	226.0	0.327	**-0.9900**
P2	230.0	0.600	**-0.9822**
P3	229.0	0.867	**-0.9842**
P4	231.0	1.207	**-0.9803**
P5	228.0	1.813	**-0.9861**
P6	227.0	2.756	**-0.9880**
P7	225.5	3.635	**-0.9910**
P8	224.5	4.578	**-0.9929**
P9	223.5	5.455	**-0.9949**
P10	222.0	6.401	**-0.9978**
P11	222.0	7.280	**-1.0009**
P12	220.5	8.226	**-1.0038**
P13	219.5	9.169	**-1.0058**
P14	217.5	10.046	**-1.0097**
P15	217.5	10.989	**-1.0097**
P16	215.0	11.868	**-1.0145**
P17	214.0	12.808	**-1.0165**
P18	213.0	13.754	**-1.0184**
P19	224.0	14.634	**-1.0195**
P20	222.5	15.577	**-1.0225**
P21	221.5	16.453	**-1.0244**
P22	220.0	17.396	**-1.0273**
P23	219.0	18.275	**-1.0293**
P24	218.0	19.221	**-1.0312**
P25	216.5	20.164	**-1.0341**
P26	215.0	20.771	**-1.0371**
P27	214.0	21.041	**-1.0390**
P28	213.5	21.380	**-1.0400**
TW	1.208	-	**-1.0415**

	Surveyed Value	Location	Culvert Bottom Elevation
BENCH	-9.35	-	**-**
HW	-	0.000	
S1	37.50	0.197	**-1.2560**
S2	37.60	0.800	**-1.2570**
S3	37.80	1.607	**-1.2590**
S4	38.00	3.226	**-1.2610**
S5	38.60	3.962	**-1.2670**
S6	39.20	4.769	**-1.2730**
S7	39.30	5.709	**-1.2740**
S8	39.40	6.452	**-1.2750**
S9	39.65	7.195	**-1.2775**
S10	39.25	8.141	**-1.2735**
S11	39.80	8.884	**-1.2790**
S12	40.00	9.690	**-1.2810**
S13	40.65	11.303	**-1.2875**
S14	41.00	12.109	**-1.2910**
S15	41.10	13.729	**-1.2920**
S16	41.35	14.535	**-1.2945**
S17	41.90	16.154	**-1.3000**
S18	42.15	16.897	**-1.3025**
S19	42.40	17.704	**-1.3050**
S20	42.30	18.644	**-1.3040**
S21	42.60	19.387	**-1.3070**
S22	42.90	20.130	**-1.3100**
TW		21.539	

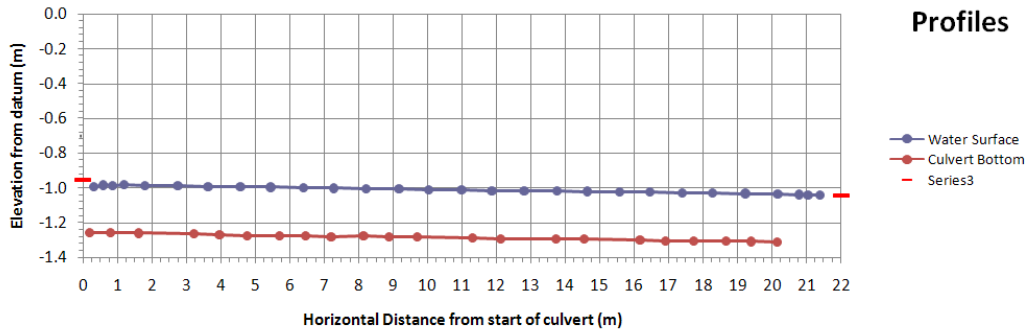

NOTES
-Measured values P1 - P28 are read off of the manometer boards
-Measured values HW and TW are read off of the depth guages
-Input all survey data in cm
-Surveyed values S1 - S22 are measured at the access holes
-BENCH is the survey level from the experiment datum
-All location data is in metres from the beginning of the culvert
-All elevation data is in inchs from the experiment datum

EXTRA INFORMATION		
Date	09-Jan-09	
Flow rate	0.085	m^3/s
Tail gate setting	22	-
Desired slope	0.250	%
Actual slope	0.270	%
Head Drop	0.090	m

Figure C.4 Survey sheet of test S00270_Q086

	Measured Value	Location	Water Surface Elevation
HW	1.064	-	**-0.7981**
P1	290.0	0.327	**-0.8653**
P2	295.0	0.600	**-0.8556**
P3	291.0	0.867	**-0.8634**
P4	296.0	1.207	**-0.8537**
P5	295.0	1.813	**-0.8556**
P6	293.0	2.756	**-0.8595**
P7	293.0	3.635	**-0.8595**
P8	289.0	4.578	**-0.8673**
P9	289.0	5.455	**-0.8673**
P10	287.0	6.401	**-0.8712**
P11	287.0	7.280	**-0.8743**
P12	286.0	8.226	**-0.8763**
P13	285.0	9.169	**-0.8782**
P14	284.0	10.046	**-0.8802**
P15	284.0	10.989	**-0.8802**
P16	281.0	11.868	**-0.8860**
P17	282.0	12.808	**-0.8841**
P18	279.0	13.754	**-0.8899**
P19	290.0	14.634	**-0.8910**
P20	287.0	15.577	**-0.8968**
P21	287.0	16.453	**-0.8968**
P22	286.0	17.396	**-0.8988**
P23	285.0	18.275	**-0.9007**
P24	284.0	19.221	**-0.9027**
P25	282.0	20.164	**-0.9066**
P26	283.0	20.771	**-0.9046**
P27	280.0	21.041	**-0.9105**
P28	281.0	21.380	**-0.9085**
TW	1.643	-	**-0.9089**

	Surveyed Value	Location	Culvert Bottom Elevation
BENCH	-9.35	-	**-**
HW	-	0.000	
S1	37.50	0.197	**-1.2560**
S2	37.60	0.800	**-1.2570**
S3	37.80	1.607	**-1.2590**
S4	38.00	3.226	**-1.2610**
S5	38.60	3.962	**-1.2670**
S6	39.20	4.769	**-1.2730**
S7	39.30	5.709	**-1.2740**
S8	39.40	6.452	**-1.2750**
S9	39.65	7.195	**-1.2775**
S10	39.25	8.141	**-1.2735**
S11	39.80	8.884	**-1.2790**
S12	40.00	9.690	**-1.2810**
S13	40.65	11.303	**-1.2875**
S14	41.00	12.109	**-1.2910**
S15	41.10	13.729	**-1.2920**
S16	41.35	14.535	**-1.2945**
S17	41.90	16.154	**-1.3000**
S18	42.15	16.897	**-1.3025**
S19	42.40	17.704	**-1.3050**
S20	42.30	18.644	**-1.3040**
S21	42.60	19.387	**-1.3070**
S22	42.90	20.130	**-1.3100**
TW		21.539	

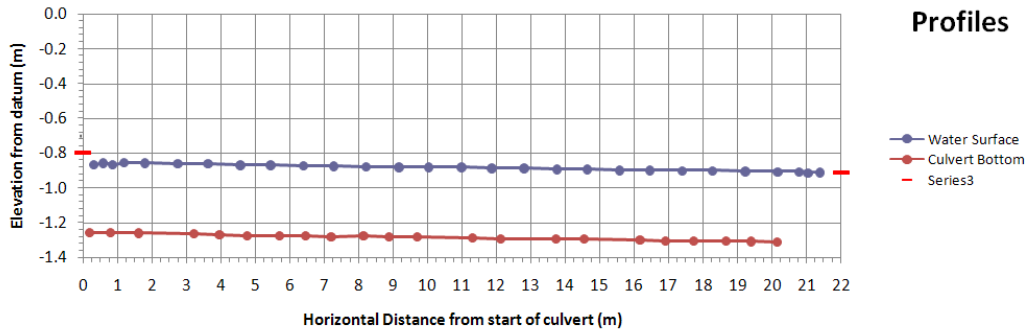

NOTES
-Measured values P1 - P28 are read off of the manometer boards
-Measured values HW and TW are read off of the depth guages
-Input all survey data in cm
-Surveyed values S1 - S22 are measured at the access holes
-BENCH is the survey level from the experiment datum
-All location data is in metres from the beginning of the culvert
-All elevation data is in inchs from the experiment datum

EXTRA INFORMATION		
Date	09-Jan-09	
Flow rate	0.176	m^3/s
Tail gate setting	33	-
Desired slope	0.250	%
Actual slope	0.270	%
Head Drop	0.111	m

Figure C.5 Survey sheet of test S00270_Q175

	Measured Value	Location	Water Surface Elevation
HW	0.67	-	-0.9181
P1	246.0	0.327	-0.9510
P2	247.0	0.600	-0.9491
P3	248.0	0.867	-0.9471
P4	248.5	1.207	-0.9462
P5	247.0	1.813	-0.9491
P6	246.0	2.756	-0.9510
P7	244.0	3.635	-0.9549
P8	242.5	4.578	-0.9579
P9	242.0	5.455	-0.9588
P10	240.5	6.401	-0.9618
P11	239.0	7.280	-0.9678
P12	237.5	8.226	-0.9707
P13	236.5	9.169	-0.9727
P14	236.0	10.046	-0.9736
P15	235.0	10.989	-0.9756
P16	234.0	11.868	-0.9775
P17	232.5	12.808	-0.9805
P18	231.5	13.754	-0.9824
P19	242.0	14.634	-0.9845
P20	241.0	15.577	-0.9864
P21	240.0	16.453	-0.9884
P22	238.5	17.396	-0.9913
P23	237.0	18.275	-0.9942
P24	235.5	19.221	-0.9971
P25	233.0	20.164	-1.0020
P26	232.5	20.771	-1.0030
P27	232.0	21.041	-1.0040
P28	231.5	21.380	-1.0049
TW	1.334	-	-1.0031

	Surveyed Values		Location	Culvert Elevation	Rock Elevation
BENCH	-9.35	-9.62	-	-	
HW	-		0.000		
S1	37.50	30.40	0.197	-1.2560	-1.1877
S2	37.60	29.80	0.800	-1.2570	-1.1817
S3	37.80	30.70	1.607	-1.2590	-1.1907
S4	38.00	31.10	3.226	-1.2610	-1.1947
S5	38.60	31.00	3.962	-1.2670	-1.1937
S6	39.20	31.30	4.769	-1.2730	-1.1967
S7	39.30	31.20	5.709	-1.2740	-1.1957
S8	39.40	30.70	6.452	-1.2750	-1.1907
S9	39.65	29.50	7.195	-1.2775	-1.1787
S10	39.25	29.50	8.141	-1.2735	-1.1787
S11	39.80	32.20	8.884	-1.2790	-1.2057
S12	40.00	33.40	9.690	-1.2810	-1.2177
S13	40.65	33.10	11.303	-1.2875	-1.2147
S14	41.00	33.60	12.109	-1.2910	-1.2197
S15	41.10	33.70	13.729	-1.2920	-1.2207
S16	41.35	34.10	14.535	-1.2945	-1.2247
S17	41.90	34.10	16.154	-1.3000	-1.2247
S18	42.15	34.10	16.897	-1.3025	-1.2247
S19	42.40	34.00	17.704	-1.3050	-1.2237
S20	42.30	33.90	18.644	-1.3040	-1.2227
S21	42.60	33.50	19.387	-1.3070	-1.2187
S22	42.90	32.70	20.130	-1.3100	-1.2107
TW			21.539		

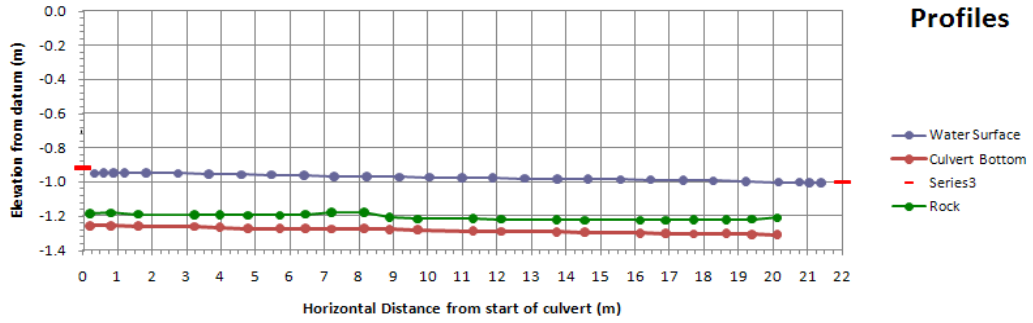

NOTES
-Measured values P1 - P28 are read off of the manometer boards
-Measured values HW and TW are read off of the depth guages
-Input all survey data in cm
-Surveyed values S1 - S22 are measured at the access holes
-BENCH is the survey level from the experiment datum
-All location data is in metres from the beginning of the culvert
-The second survey column is for rock elevations

EXTRA INFORMATION		
Date	16-Mar-09	
Flow rate	0.086	m^3/s
Tail gate setting	30	-
Desired slope	0.250	%
Actual slope	0.270	%
Head Drop	0.085	m
Desired rock depth	10.00	%
Actual rock depth	9.71	%

Figure C.6 Survey sheet of test S00270_Q086_R10

	Measured Value	Location	Water Surface Elevation
HW	0.823	-	-0.8715
P1	275.0	0.327	-0.8946
P2	275.0	0.600	-0.8946
P3	275.0	0.867	-0.8946
P4	274.0	1.207	-0.8965
P5	272.0	1.813	-0.9004
P6	272.0	2.756	-0.9004
P7	269.5	3.635	-0.9053
P8	269.0	4.578	-0.9062
P9	268.0	5.455	-0.9082
P10	265.5	6.401	-0.9131
P11	265.0	7.280	-0.9172
P12	264.0	8.226	-0.9191
P13	263.0	9.169	-0.9211
P14	262.5	10.046	-0.9220
P15	262.0	10.989	-0.9230
P16	260.5	11.868	-0.9259
P17	259.0	12.808	-0.9288
P18	258.0	13.754	-0.9308
P19	269.0	14.634	-0.9319
P20	268.0	15.577	-0.9338
P21	265.5	16.453	-0.9387
P22	265.0	17.396	-0.9397
P23	264.0	18.275	-0.9416
P24	262.0	19.221	-0.9455
P25	260.0	20.164	-0.9494
P26	258.5	20.771	-0.9523
P27	258.0	21.041	-0.9533
P28	259.0	21.380	-0.9514
TW	1.519	-	-0.9467

	Surveyed Values		Location	Culvert Elevation	Rock Elevation
BENCH	-9.35	-9.50	-	-	
HW	-		0.000		
S1	37.50	22.80	0.197	-1.2560	-1.1105
S2	37.60	23.00	0.800	-1.2570	-1.1125
S3	37.80	23.40	1.607	-1.2590	-1.1165
S4	38.00	22.80	3.226	-1.2610	-1.1105
S5	38.60	23.85	3.962	-1.2670	-1.1210
S6	39.20	23.30	4.769	-1.2730	-1.1155
S7	39.30	23.25	5.709	-1.2740	-1.1150
S8	39.40	22.90	6.452	-1.2750	-1.1115
S9	39.65	24.00	7.195	-1.2775	-1.1225
S10	39.25	23.70	8.141	-1.2735	-1.1195
S11	39.80	24.60	8.884	-1.2790	-1.1285
S12	40.00	28.20	9.690	-1.2810	-1.1645
S13	40.65	27.10	11.303	-1.2875	-1.1535
S14	41.00	25.75	12.109	-1.2910	-1.1400
S15	41.10	24.70	13.729	-1.2920	-1.1295
S16	41.35	28.50	14.535	-1.2945	-1.1675
S17	41.90	26.80	16.154	-1.3000	-1.1505
S18	42.15	27.90	16.897	-1.3025	-1.1615
S19	42.40	29.10	17.704	-1.3050	-1.1735
S20	42.30	26.80	18.644	-1.3040	-1.1505
S21	42.60	28.40	19.387	-1.3070	-1.1665
S22	42.90	26.90	20.130	-1.3100	-1.1515
TW			21.539		

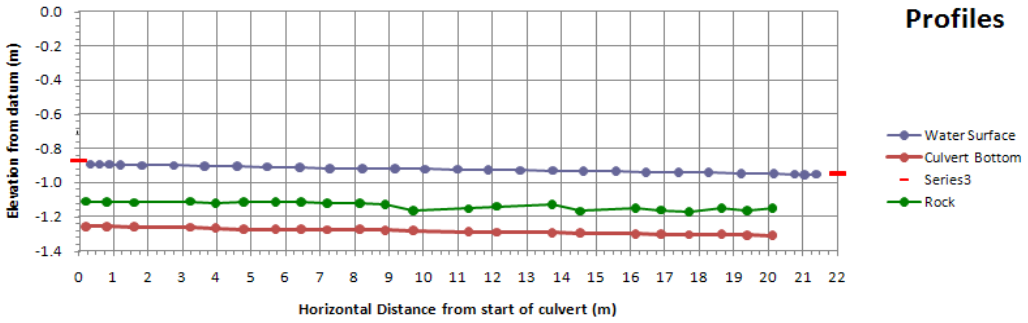

NOTES
-Measured values P1 - P28 are read off of the manometer boards
-Measured values HW and TW are read off of the depth guages
-Input all survey data in cm
-Surveyed values S1 - S22 are measured at the access holes
-BENCH is the survey level from the experiment datum
-All location data is in metres from the beginning of the culvert
-The second survey column is for rock elevations

EXTRA INFORMATION		
Date	9-Apr-09	
Flow rate	0.087	m^3/s
Tail gate setting	7	-
Desired slope	0.250	%
Actual slope	0.270	%
Head Drop	0.075	m
Desired rock depth	20.00	%
Actual rock depth	18.37	%

Figure C.7 Survey sheet of test S00270_Q086_R18

	Measured Value	Location	Water Surface Elevation
HW	1.018	-	-0.8121
P1	309.0	0.327	-0.8283
P2	310.0	0.600	-0.8264
P3	309.5	0.867	-0.8274
P4	308.5	1.207	-0.8293
P5	306.0	1.813	-0.8342
P6	306.0	2.756	-0.8342
P7	303.0	3.635	-0.8400
P8	301.0	4.578	-0.8439
P9	300.0	5.455	-0.8459
P10	294.0	6.401	-0.8576
P11	294.0	7.280	-0.8607
P12	293.0	8.226	-0.8626
P13	290.0	9.169	-0.8685
P14	291.5	10.046	-0.8656
P15	292.0	10.989	-0.8646
P16	289.5	11.868	-0.8694
P17	287.0	12.808	-0.8743
P18	285.0	13.754	-0.8782
P19	297.0	14.634	-0.8774
P20	294.5	15.577	-0.8822
P21	293.0	16.453	-0.8851
P22	291.0	17.396	-0.8890
P23	290.0	18.275	-0.8910
P24	287.0	19.221	-0.8968
P25	286.5	20.164	-0.8978
P26	287.0	20.771	-0.8968
P27	288.0	21.041	-0.8949
P28	289.5	21.380	-0.8920
TW	1.696	-	-0.8928

	Surveyed Values		Location	Culvert Elevation	Rock Elevation
BENCH	-9.35	-9.70	-	-	
HW	-		0.000		
S1	37.50	16.50	0.197	-1.2560	-1.0495
S2	37.60	17.00	0.800	-1.2570	-1.0545
S3	37.80	18.30	1.607	-1.2590	-1.0675
S4	38.00	15.95	3.226	-1.2610	-1.0440
S5	38.60	14.65	3.962	-1.2670	-1.0310
S6	39.20	16.55	4.769	-1.2730	-1.0500
S7	39.30	15.80	5.709	-1.2740	-1.0425
S8	39.40	13.90	6.452	-1.2750	-1.0235
S9	39.65	16.15	7.195	-1.2775	-1.0460
S10	39.25	15.10	8.141	-1.2735	-1.0355
S11	39.80	16.55	8.884	-1.2790	-1.0500
S12	40.00	19.70	9.690	-1.2810	-1.0815
S13	40.65	17.90	11.303	-1.2875	-1.0635
S14	41.00	18.65	12.109	-1.2910	-1.0710
S15	41.10	19.25	13.729	-1.2920	-1.0770
S16	41.35	18.30	14.535	-1.2945	-1.0675
S17	41.90	17.20	16.154	-1.3000	-1.0565
S18	42.15	18.75	16.897	-1.3025	-1.0720
S19	42.40	20.60	17.704	-1.3050	-1.0905
S20	42.30	20.10	18.644	-1.3040	-1.0855
S21	42.60	18.70	19.387	-1.3070	-1.0715
S22	42.90	21.00	20.130	-1.3100	-1.0945
TW			21.539		

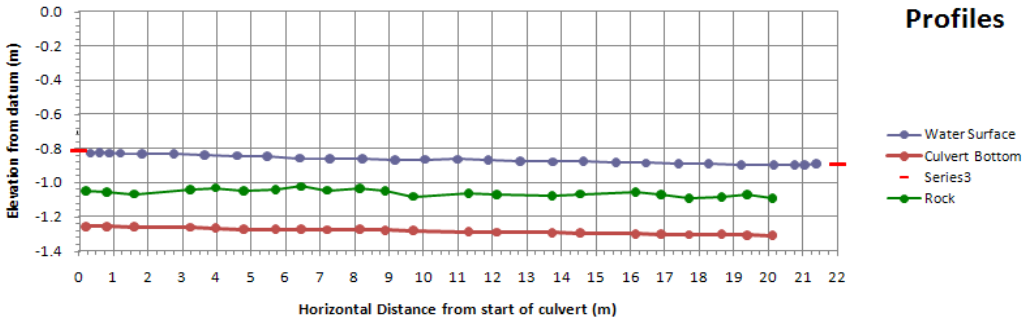

NOTES
-Measured values P1 - P28 are read off of the manometer boards
-Measured values HW and TW are read off of the depth guages
-Input all survey data in cm
-Surveyed values S1 - S22 are measured at the access holes
-BENCH is the survey level from the experiment datum
-All location data is in metres from the beginning of the culvert
-The second survey column is for rock elevations

EXTRA INFORMATION		
Date	27-Apr-09	
Flow rate	0.084	m^3/s
Tail gate setting	20	-
Desired slope	0.250	%
Actual slope	0.270	%
Head Drop	0.081	m
Desired rock depth	30.00	%
Actual rock depth	27.85	%

Figure C.8 Survey sheet of test S00270_Q086_R28

	Measured Value	Location	Water Surface Elevation
HW	0.534	-	**-0.9596**
P1	222.0	0.327	**-0.9978**
P2	223.0	0.600	**-0.9958**
P3	221.5	0.867	**-0.9988**
P4	222.5	1.207	**-0.9968**
P5	216.5	1.813	**-1.0085**
P6	215.5	2.756	**-1.0104**
P7	213.0	3.635	**-1.0153**
P8	210.0	4.578	**-1.0212**
P9	208.0	5.455	**-1.0251**
P10	204.0	6.401	**-1.0328**
P11	202.0	7.280	**-1.0399**
P12	197.5	8.226	**-1.0486**
P13	195.5	9.169	**-1.0525**
P14	193.0	10.046	**-1.0574**
P15	192.5	10.989	**-1.0584**
P16	188.5	11.868	**-1.0662**
P17	186.0	12.808	**-1.0710**
P18	183.0	13.754	**-1.0769**
P19	192.0	14.634	**-1.0819**
P20	189.0	15.577	**-1.0877**
P21	187.0	16.453	**-1.0916**
P22	183.5	17.396	**-1.0984**
P23	181.0	18.275	**-1.1033**
P24	178.0	19.221	**-1.1091**
P25	175.5	20.164	**-1.1140**
P26	174.0	20.771	**-1.1169**
P27	173.0	21.041	**-1.1189**
P28	172.0	21.380	**-1.1208**
TW	0.914	-	**-1.1311**

	Surveyed Value	Location	Culvert Bottom Elevation
BENCH	-0.95	-	**-**
HW	-	0.000	
S1	43.65	0.197	**-1.2335**
S2	43.90	0.800	**-1.2360**
S3	44.25	1.607	**-1.2395**
S4	44.80	3.226	**-1.2450**
S5	45.30	3.962	**-1.2500**
S6	45.90	4.769	**-1.2560**
S7	45.90	5.709	**-1.2560**
S8	46.10	6.452	**-1.2580**
S9	46.30	7.195	**-1.2600**
S10	46.25	8.141	**-1.2595**
S11	46.70	8.884	**-1.2640**
S12	47.65	9.690	**-1.2735**
S13	48.90	11.303	**-1.2860**
S14	49.40	12.109	**-1.2910**
S15	49.65	13.729	**-1.2935**
S16	50.20	14.535	**-1.2990**
S17	51.10	16.154	**-1.3080**
S18	51.50	16.897	**-1.3120**
S19	52.35	17.704	**-1.3205**
S20	52.50	18.644	**-1.3220**
S21	52.65	19.387	**-1.3235**
S22	53.10	20.130	**-1.3280**
TW		21.539	

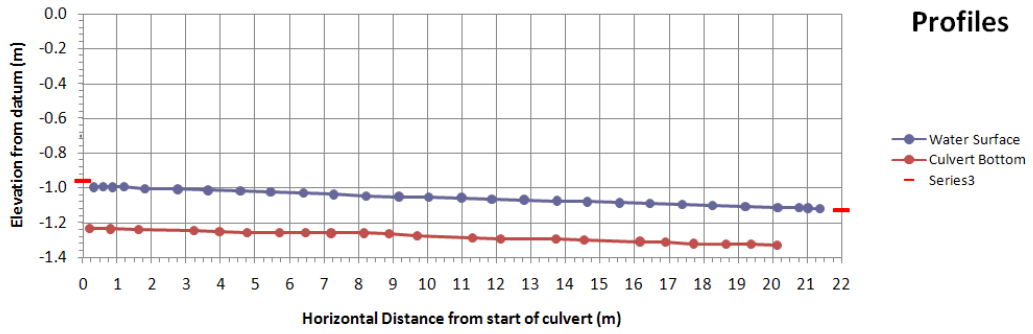

NOTES
-Measured values P1 - P28 are read off of the manometer boards
-Measured values HW and TW are read off of the depth guages
-Input all survey data in cm
-Surveyed values S1 - S22 are measured at the access holes
-BENCH is the survey level from the experiment datum
-All location data is in metres from the beginning of the culvert
-All elevation data is in inchs from the experiment datum

EXTRA INFORMATION		
Date	21-Aug-08	
Flow rate	0.086	m^3/s
Tail gate setting	?	-
Desired slope	0.500	%
Actual slope	0.488	%
Head Drop	0.172	m

Figure C.9 Survey sheet of test S00488_Q086

	Measured Value	Location	Water Surface Elevation
HW	0.762	-	**-0.8901**
P1	247.5	0.327	**-0.9481**
P2	253.0	0.600	**-0.9374**
P3	250.0	0.867	**-0.9433**
P4	250.5	1.207	**-0.9423**
P5	248.0	1.813	**-0.9471**
P6	245.0	2.756	**-0.9530**
P7	243.0	3.635	**-0.9569**
P8	240.0	4.578	**-0.9627**
P9	238.0	5.455	**-0.9666**
P10	234.0	6.401	**-0.9744**
P11	231.0	7.280	**-0.9834**
P12	226.5	8.226	**-0.9921**
P13	225.0	9.169	**-0.9951**
P14	222.0	10.046	**-1.0009**
P15	221.0	10.989	**-1.0029**
P16	216.5	11.868	**-1.0116**
P17	215.0	12.808	**-1.0145**
P18	212.0	13.754	**-1.0204**
P19	221.5	14.634	**-1.0244**
P20	218.0	15.577	**-1.0312**
P21	216.5	16.453	**-1.0341**
P22	213.5	17.396	**-1.0400**
P23	211.0	18.275	**-1.0449**
P24	207.0	19.221	**-1.0526**
P25	205.0	20.164	**-1.0565**
P26	201.0	20.771	**-1.0643**
P27	199.5	21.041	**-1.0672**
P28	199.0	21.380	**-1.0682**
TW	1.096	-	**-1.0756**

	Surveyed Value	Location	Culvert Bottom Elevation
BENCH	-0.95	-	**-**
HW	-	0.000	
S1	43.65	0.197	**-1.2335**
S2	43.90	0.800	**-1.2360**
S3	44.25	1.607	**-1.2395**
S4	44.80	3.226	**-1.2450**
S5	45.30	3.962	**-1.2500**
S6	45.90	4.769	**-1.2560**
S7	45.90	5.709	**-1.2560**
S8	46.10	6.452	**-1.2580**
S9	46.30	7.195	**-1.2600**
S10	46.25	8.141	**-1.2595**
S11	46.70	8.884	**-1.2640**
S12	47.65	9.690	**-1.2735**
S13	48.90	11.303	**-1.2860**
S14	49.40	12.109	**-1.2910**
S15	49.65	13.729	**-1.2935**
S16	50.20	14.535	**-1.2990**
S17	51.10	16.154	**-1.3080**
S18	51.50	16.897	**-1.3120**
S19	52.35	17.704	**-1.3205**
S20	52.50	18.644	**-1.3220**
S21	52.65	19.387	**-1.3235**
S22	53.10	20.130	**-1.3280**
TW		21.539	

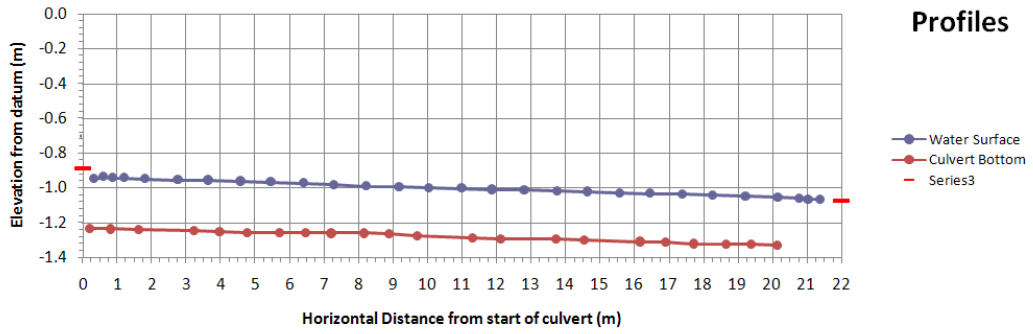

NOTES
-Measured values P1 - P28 are read off of the manometer boards
-Measured values HW and TW are read off of the depth guages
-Input all survey data in cm
-Surveyed values S1 - S22 are measured at the access holes
-BENCH is the survey level from the experiment datum
-All location data is in metres from the beginning of the culvert
-All elevation data is in inchs from the experiment datum

EXTRA INFORMATION		
Date	21-Aug-08	
Flow rate	0.129	m^3/s
Tail gate setting	?	-
Desired slope	0.500	%
Actual slope	0.488	%
Head Drop	0.186	m

Figure C.10 Survey sheet of test S00488_Q130

	Measured Value	Location	Water Surface Elevation
HW	0.995	-	**-0.8191**
P1	267.0	0.327	**-0.9101**
P2	279.0	0.600	**-0.8868**
P3	279.0	0.867	**-0.8868**
P4	277.0	1.207	**-0.8907**
P5	274.0	1.813	**-0.8965**
P6	271.0	2.756	**-0.9024**
P7	269.0	3.635	**-0.9062**
P8	265.0	4.578	**-0.9140**
P9	262.0	5.455	**-0.9199**
P10	259.0	6.401	**-0.9257**
P11	258.0	7.280	**-0.9308**
P12	252.0	8.226	**-0.9425**
P13	251.0	9.169	**-0.9444**
P14	247.0	10.046	**-0.9522**
P15	247.0	10.989	**-0.9522**
P16	242.0	11.868	**-0.9620**
P17	239.0	12.808	**-0.9678**
P18	235.0	13.754	**-0.9756**
P19	246.0	14.634	**-0.9767**
P20	241.0	15.577	**-0.9864**
P21	239.0	16.453	**-0.9903**
P22	236.0	17.396	**-0.9962**
P23	234.0	18.275	**-1.0001**
P24	230.0	19.221	**-1.0078**
P25	226.0	20.164	**-1.0156**
P26	224.0	20.771	**-1.0195**
P27	223.0	21.041	**-1.0215**
P28	222.0	21.380	**-1.0234**
TW	1.27	-	**-1.0226**

	Surveyed Value	Location	Culvert Bottom Elevation
BENCH	-0.95	-	**-**
HW	-	0.000	
S1	43.65	0.197	**-1.2335**
S2	43.90	0.800	**-1.2360**
S3	44.25	1.607	**-1.2395**
S4	44.80	3.226	**-1.2450**
S5	45.30	3.962	**-1.2500**
S6	45.90	4.769	**-1.2560**
S7	45.90	5.709	**-1.2560**
S8	46.10	6.452	**-1.2580**
S9	46.30	7.195	**-1.2600**
S10	46.25	8.141	**-1.2595**
S11	46.70	8.884	**-1.2640**
S12	47.65	9.690	**-1.2735**
S13	48.90	11.303	**-1.2860**
S14	49.40	12.109	**-1.2910**
S15	49.65	13.729	**-1.2935**
S16	50.20	14.535	**-1.2990**
S17	51.10	16.154	**-1.3080**
S18	51.50	16.897	**-1.3120**
S19	52.35	17.704	**-1.3205**
S20	52.50	18.644	**-1.3220**
S21	52.65	19.387	**-1.3235**
S22	53.10	20.130	**-1.3280**
TW		21.539	

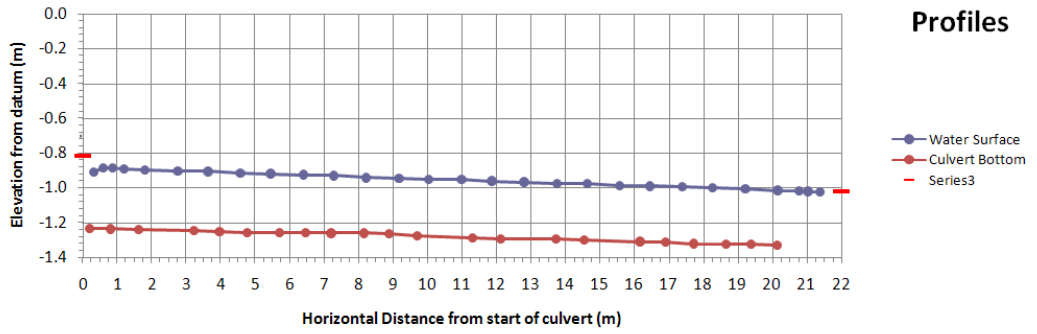

NOTES
-Measured values P1 - P28 are read off of the manometer boards
-Measured values HW and TW are read off of the depth guages
-Input all survey data in cm
-Surveyed values S1 - S22 are measured at the access holes
-BENCH is the survey level from the experiment datum
-All location data is in metres from the beginning of the culvert
-All elevation data is in inchs from the experiment datum

EXTRA INFORMATION		
Date	22-Aug-08	
Flow rate	0.175	m^3/s
Tail gate setting	?	-
Desired slope	0.500	%
Actual slope	0.488	%
Head Drop	0.204	m

Figure C.11 Survey sheet of test S00488_Q175